BSPE 00352-539-5

포항분지의 선상지-삼각주 퇴적층의 퇴적기구 및 진화

Depositional Mechanism and Evolution of the Fan-delta sequences developed on the Margin of the Pohang Basin

1993. 3.

한 국 해 양 연 구 소

제 출 문

한국해양연구소장 귀하

본 보고서를 "포항분지의 선상지-삼각주 퇴적층의 퇴적기구 및 진화"

연구의 최종보고서로 제출합니다.

1993년 3월

연구책임자: 박 병 권 (한국해양연구소)
전 승 수 (한국해양연구소)
정 갑 식 (한국해양연구소)
이 희 준 (한국해양연구소)
연 구 원: 황 인 걸 (서울대해양학과)
이 철 우 (서울대해양학과)

요약문

I. 제목

마이오세 포항분지의 분지해석연구: 말골 선상지 삼각주의 퇴적기구및 퇴적사

II. 연구내용및 결과

마이오세 포항분지는 수 개의 교호하는 선상지 삼각주 (말골, 도음산, 매산, 덕성, 고현 및 유계 선상지 삼각주 등)로 구성되어있다. 그 중 말골 선상지 삼각주는 사면 사태에 의한 퇴적물이 특징으로, 각력암, 역암, 사암 및 이암으로 구성되어있다. 말골 선상지 삼각주의 퇴적층은 입도와 일차 퇴적구조에 의해 15개의 퇴적상으로 분류되어 퇴적상의 특징 기술 및 퇴적기구 해석이 수행되었다. 이 선상지 삼각주 퇴적층은 우세한 퇴적상 및 퇴적작용에 의해 육상 선상지 (alluvial fan), 수중 사태 사면 (submarine scree apron), 삼각주 사면 (slope apron) 및 분지 평원 (basin plain)의 특징적인 퇴적환경을 갖는 4개의 상조합으로 분류된다.

상조합 I은 괴상 및 희미한 층리의 각력암, 괴상, 희미한 층리와 사층리를 보이는 역암으로 주로 구성되어 있으며, 괴상의 사암 및 이암이 협재한다. 각력암층은 쇄설류 (debris flow), 고응축류 (hyperconcentrated flow) 또는 판류 (sheetflood)에 의해 퇴적된 것이며, 역암은 망상 하천 (braided stream) 환경에서 역암사주 (gravel bar)의 이동과 2차 하도 충전 (secondary channel fill)에

의해 형성된 것으로 해석된다. 괴상의 이암은 하도사이 지역 (interchannel area)에서 뜬짐의 침강으로 퇴적되었으며, 괴상의 사암은 천해환경에서 급격한 뜬짐의 침강으로 퇴적되었다.

상조합 II는 급경사 (> 20°)를 이루는 괴상 및 희미한 층리의 역암으로 구성되며, 판상의 층형을 보인다. 이 역암은 단층애 주변의 급경사면에서 쇄설낙하 (debris fall) 및 쇄설류에 의해 퇴적된 것이다. 이 상조합은 분지 주변부를 따라 좁고 긴 대상으로 분포하며 (넓이: < 300 m), 역의 조성은 인근 기반암의 조성에 따라 변한다. 상조합의 분포 특성과 역의 조성은, 퇴적물이 단층애를 따라 분포하는 수 개의 급류에 의해 공급된 것임을 지시한다.

상조합 III은 두꺼운 괴상의 이암으로 구성되며, 괴상, 점이층리, 역점이층리를 보이는 역암및 사암이 협재한다. 괴상의 이암은 세립질 퇴적물의 느린 침강으로 형성된 것이며, 역암 및 사암은 저탁류 또는 쇄설류에 의해 퇴적된 것이다. 상조합 IV는 두꺼운 담회색의 이암으로 구성되며, 이는 세립질 쇄설성 퇴적물 및 생물 기원 퇴적물의 침강에 의한 반원양성 퇴적(hemipelagic settling)에 의해 형성되었다.

퇴적상, 상조합의 분포, 입도, 역의 조성 등의 급격한 공간적 변화에 따라 말골 선상지 삼각주 퇴적층은 3 개의 퇴적 단위로 구분되며, 이는 3 단계의 선상지 삼각주 진화를 지시한다. 분지형성 초기 (Stage M-1)에 형성된 최하부층은 백악기 및 에오세의 기반암 상부에 분포하는 육상 선상지 퇴적물로 구성되어 있다. 그러나, 육상 선상지 말단부에서 일부 역암 및 사암은 상향 조립화 경향 (coarsening-pward trend)을 보이며, 천해성 미화석도 분포한다. 따라서, 이 시

기 동안은 삼각주가 천해환경으로 전진하는 천해성 선상지 삼각주가 발달하였음을 알수있다. 분지 형성 두번째 시기 (Stage M-2)의 퇴적물은 사면 사태형 선상지 삼각주 (scree-apron-type fan delta)의 특징을 보이며, 육상 및 수중 사태 사면, 삼각주 사면 환경에서 퇴적 되었다. 하부 경계면은 역의 조성, 퇴적상 및 상조합, 주향 및 경사의 급격한 변화가 특징이며, 이는 퇴적 동시성 지구조운동에 기인한것으로 해석된다. 분지 주변부에 분포하는 트러스트 단층 (thrust fault)과 역전된 하부층도 퇴적 동시성 지구조 운동을 지시한다. 분지 형성 말기 (Stage M-3) 퇴적층은 반원양성 퇴적으로 형성된 두꺼운 담회색 이암이 특징이다. 하부 경계면은 이암 내에서 쇄설성 퇴적물의 급격한 감소와 생물 기원 퇴적물의 증가로 특징 지워진다. 이는 퇴적 동시성 지구조 운동에 의해 하천 유역에서 공급되는 퇴적물이 급격히 감소 하였음을 지시한다.

SUMMARY

I. Title of Study

Basin Analysis of the Miocene Pohang Basin: Depositional Processes and Depositional History of the Malgol Fan-delta System

II. Abstract

The Yeonil Group Sequence in the Miocene Pohang Basin is represented by several coalescing fan deltas including Malgol, Doumsan, Maesan, Duksung, Gohyun and Yugye systems. Among the fan delta systems, the Malgol fan delta is characterized by scree-apron-type deposits. The sequence comprises breccia, gravelstone, sandstone and mudstone units which can be classified into 15 sedimentary facies, based on grain size, primary sedimentary structure and bed geometry. The entire sequence can be organized into four facies organizations (or facies associations), representing deposition in alluvial fan, submarine scree apron, slope apron and basin plain environments.

The Facies Association I consist of disorganized breccias, crudely-stratified breccia, disorganized gravelstone, crudely-stratified gravelstone and cross-bedded gravelstone with thin layers of homogeneous muddy sandstone and massive sandstone. The breccia units were deposited either by subaerial debris flows, hyperconcentrated flows or sheetfloods. The gravelstone units may represent deposition from migration of gravel bars and secondary channel fills in braided streams. The muddy sandstone units represent deposition in interchannel areas,

whereas the sandstone units were deposited by rapid suspension settling in shallow marine environment.

The Facies Association II is characterized by steeply-inclined beds (> 25°) of disorganized gravelstone and crudely-stratified gravelstone with sheet-like bed geometry. The gravelstone units were deposited by debris fall (or grain fall, gravity slide) and cohesive or cohesionless debris flows (or density-modified grain flows) on a steeply-inclined slope (submarine scree apron) environments. The occurrence of this association as a long, narrow (< 300 m) belt along the basin margin and the regional variation in clast composition depending on the adjacent basement rocks suggest that most sediments were derived from a line source (or multi-point sources).

The Facies Association III comprises thick homogeneous muddy sandstone in which thin units of disorganized gravelstone, graded gravelstone, inverse-to-normally graded gravelstone, massive sandstone and graded sandstone are partly intercalated. The thick homogeneous muddy sandstones were deposited by slow suspension settling of fine-grained materials, whereas the gravelstone and sandstone units represent intermittent sediment gravity flows such as high- or low-density turbidity currents and cohesive or cohesionless debris flows.

The Facies Association IV is characterized by thick, light yellowish gray mudstone, deposited by particle-by-particle settling of fine-grained clastic sediments and biogenic grains.

Based on facies distribution, architecture, grain size and clast composition, the

sedimentary sequence in the Malgol system can be grouped into three units, representing three stages of fan-delta evolution: 1) deposition of coastal alluvial fan (Stage M-1), 2) deposition of scree-apron-type fan delta (Stage M-2), and 3) deposition of hemipelagic muds (Stage M-3).

The sequence deposited during the early stage (Stage M-1) is represented by alluvial fan deposits (Facies Association I) which unconformably overlie the Cretaceous and Eocene basement rocks (sedimentary, granitic, felsite and volcanic rocks). The coarsening-upward trend of the gravelstone and sandstone units suggests that the alluvial fan may have prograded to the shallow marine environment, forming a coastal alluvial fan.

The Stage M-2 sequence is represented by scree-apron-type fan-delta system, containing alluvial fan (or subaerial scree apron; Facies Association I), submarine scree apron (Facies Association II) and slope apron (Facies Association III) deposits. The lower boundary of the sequence is represented by an abrupt vertical change in clast composition, sedimentary facies and bed attitude. The variations may largely be due to the syndepositional tectonic movement of the basement, probably related to thrust faults in the basin margin. The sequence generally shows an upward fining trend, suggesting that sediment supply rate from the adjacent fault-bounded drainage basin gradually decreased.

The sequence deposited during the last stage (Stage M-3) is represented by thick light yellowish gray mudstone, deposited by particle-by-particle settling of fine-grained clastic sediments and biogenic grains (hemipelagic settling). The

sequence boundary between the Stage M-2 and Stage M-3 is represented by an abrupt vertical decrease in clastic grains, in which the overlying sequence contains abundant biogenic grains. It may indicate that the sediment supply from the alluvial feeder system terminated abruptly during the last stage of the fan-delta progradation.

BASIN ANALYSIS OF THE MIOCENE POHANG BASIN: DEPOSITIONAL PROCESSES AND DEPOSITIONAL HISTORY OF MALGOL FAN-DELTA SYSTEM

Contents

List of Figures

List of Tables

Chapter 1. INTRODUCTION

Fan deltas occur in various tectonic and geologic settings including rift (Leeder & Gawthorpe, 1987; Leeder et al., 1988; Gawthorpe et al., 1990), pull-apart (Crowell, 1975; Link & Osbourne, 1978; Gloppen & Steel, 1981; Dunne & Hempton, 1984), foreland (Surlyk, 1978) and back-arc (Ineson, 1989; Choe, 1990; Chough et al., 1990; Hwang & Chough, 1990) basins as well as fjords (Prior & Bornhold, 1988, 1989, 1990). As the fan deltas occur along the basin margins, they commonly act as recorders of tectonic movement during the deposition. Tectonism affects fan-delta systems on a variety of scale (Alexander & Leeder, 1987; Leeder & Gawthorpe, 1987; Leeder et al., 1988; Gawthorpe & Colella, 1990). Basin-wide scale tectonic movement such as footwall uplift and subsidence of the hangingwall determine the sediment source areas and depocenters. Fault geometry along the footwall determines the location, scale and gradient of the drainage system which are responsible for the dimension of depositional systems in the hangingwall depocenter (e.g. Leeder et al., 1988). Forms and depositional systems and progradational patterns as well as internal geometry of the depositional systems are also related to the timing, style and magnitude of the tectonic movement (e.g. Gawthorpe & Colella, 1990).

As the fan deltas occur near the interface between the subaerial and subaqueous parts, slight variation in base-level changes induced either by

tectonic movement or eustatic/climatic changes can give rise to significant variation in sedimentary facies and architectures as well as progradational pattern of the fan-delta systems (e.g. Postma & Cruickshank, 1988; Colella, 1988b). The progradation pattern at the delta front is also controlled by the sediment supply rate from the alluvial feeder system. In a natural basin, one variable may dominate. However, dynamic interplay of the two or even all of these variables commonly create complex overlapping patterns of sedimentary facies and facies associations with various scale cyclic trends. These variables also resulted in the progradation of various types of fan delta systems including Gilbert-type, shoal-water-type, slope-type, scree-apron-type fan delta systems along the faulted basin margin.

The Miocene Pohang Basin provides an unusual opportunity to study sedimentary facies and depositional processes of fan deltas containing six fan-delta systems: Doumsan, Maesan, Duksung, Gohyun, Malgol and Yugye systems (Fig. 1-1). These fan deltas are represented by deep-water-type systems including large-scale Gilbert-type (Doumsan, Duksung and Gohyun systems), steep slope-type (Maesan and part of Doumsan systems) and scree apron-type (Malgol and Yugye systems) fan deltas. Individual fan deltas evolved differently according to the timing, style and magnitude of the tectonic movement and resultant variation in sediment supply rate from the alluvial feeder system. These factors also resulted in the overlapping of

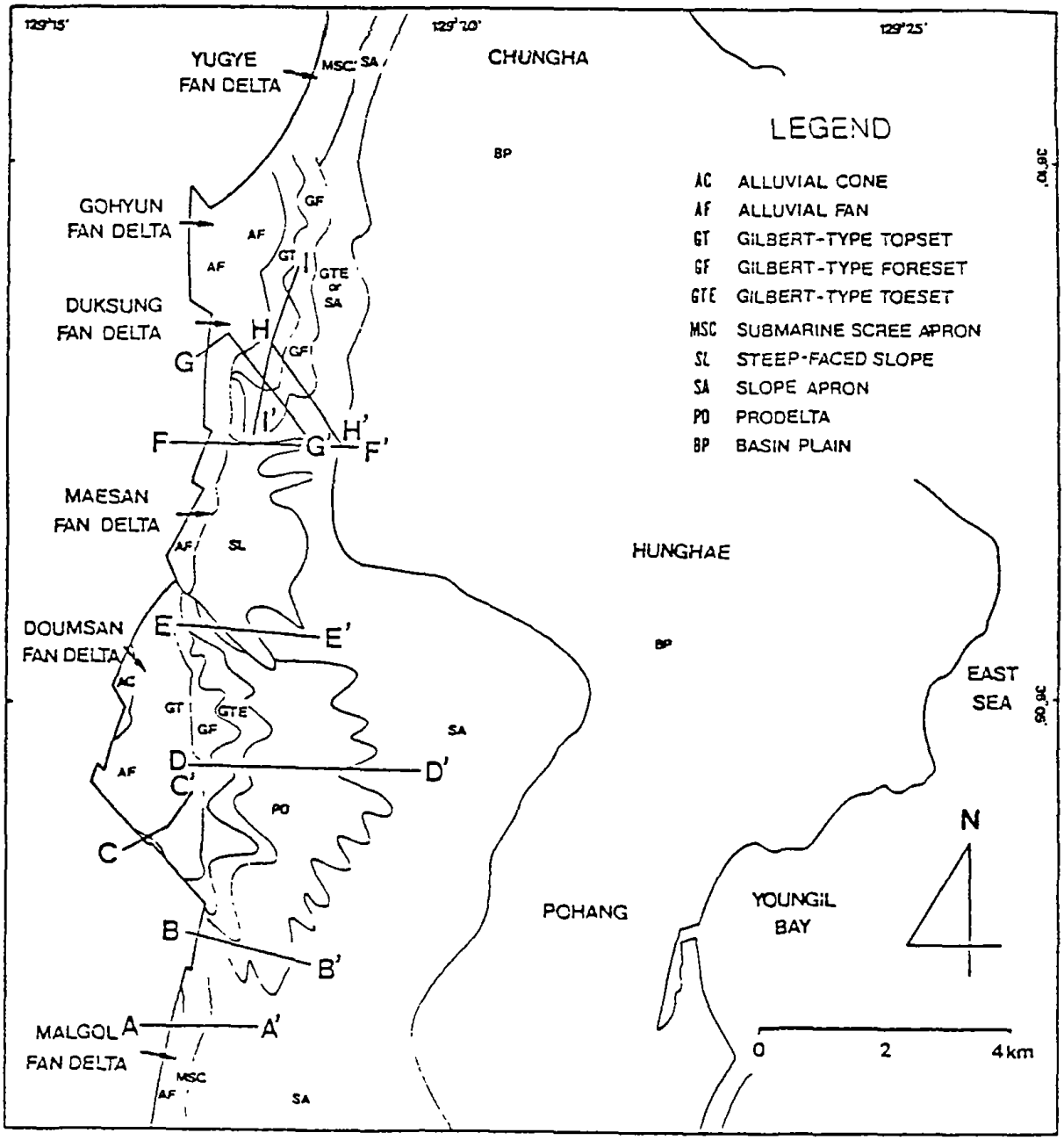

Fig. 1-1. Simplified distribution map of fan-delta systems in the Pohang Basin.

adjacent fan-delta systems with different sediment source areas. Unravelling of the various factors, thus, will present some ideas on the development various types of fan-delta systems and their evolutionary patterns as well as overlapping of adjacent depositional systems, largely controlled by tectonic subsidence and uplift, base-level changes and variation in sediment supply rate. In addition, it will serve as a clue to understand the tectonic evolution and basin-fill history of the Pohang Basin.

Among the six fan deltas in the western margin of Pohang Basin, the Malgol system mimics a scree-apron-type (or slope-type) fan delta, deposited in alluvial fan (or subaerial scree apron), submarine scree apron, slope apron and basin plain environments. This system occurs as a long, narrow belt (< 500 m in width) along the fault-bounded basin margin. This fan delta provides an excellent example to study the syndepositional tectonic movement of the basin margin and resultant variation in depositional systems, as the sedimentary sequence commonly shows abrupt vertical variation in clast composition, shape, sedimentary facies and architectures.

Chapter 2. PREVIOUS WORK

During the last three decades, the Pohang Basin (Miocene) has received much attention for its hydrocarbon potential and other economic minerals (benthonites and kaoline deposits). Most of the studies were, however, concentrated on stratigraphy and paleontology (e.g. Um et al., 1964; Kim, 1965). Sedimentological studies were carried out only recently (Chang, 1984; You, 1985; Choe, 1986; Choe & Chough, 1988; Chough et al., 1989, 1990; Chough et al., 1993; Hwang, 1989, 1993; Hwang & Chough, 1990).

2.1. STRATIGRAPHY

Early stratigraphic studies on the Yeonil Group were made by Tateiwa (1924) and Kanehara (1935, 1936a, b). They divided the group into the Chunbuk Conglomerate and Yeonil Shale in ascending order (Table 2-1). Um et al. (1964) mapped the Pohang sheet (1:50,000) and subdivided the Yeonil Group into six formations based on plant fossils and lithology (Table 2-1). Kim (1965) carried out foraminiferal studies in which the lithostratigraphic scheme is similar to that of Um et al. (1964) with different formation names and boundaries. Later, Yoon (1975) made a similar approach based on the occurrence of bivalves and divided the group into the lower Danguri Conglomerate and the upper Euichang Group (Table 2-1). Based on lithology and stratigraphic position, he subdivided the Chungogsa Formation into three

Table 2-1. Miocene stratigraphy of Yeonil Group.

	Tateiwa (1924)	Kanehara (1936b)	Um et al. (1964)	Kim (1965)	Yoon (1975)	Yun (1986)	Choe & Chough (1988)	This study
Yeonil Group	Ennichi Shale	Ennichi Shale	Yonam F.	Oomockdong F.	Yonghan F.	Duho F.	Duho & Idong F.	Duho F. (150-200 m)
			Duho F.	Pohang F.	Duho F.			
			Idong F.	Eedong F.	Idong F.	Hagjeon F.	Hunghae F.	Hunghae F. (180-200 m)
			Heunghae F.	Daegock F.	Heunghae F.			
			Hakrim F.	Songhacdong F.	Hagjeon F.		Hakrim F.	Hakrim F. (100-180 m)
	Senpoku Conglo.	Senpoku Conglo.	Chunbuk Conglo.	Seoam Conglo.	Euichang Group / Chungogsa F.: Daljeon Alt. Mem. / Doeumsan Alt. Mem. Bomunji Alt. Mem.	Chunbuk Conglo. F.	Chunbuk F.	Chunbuk F. (150-600 m)
					Danguri Conglo.			

members (Table 2-1). Yun (1986) suggested a somewhat different scheme, dividing the Yeonil Group into three formations (Table 2-1).

In spite of these efforts, it was still difficult to identify each formation in the field. The confusion was largely due to the failure in recognizing lateral and vertical facies changes of individual lithologic units. In this study, the Yeonil Group sequence was divided into four formations based on lithofacies associations: Chunbuk Fm. (gravelstone), Hakrim Fm. (sandstone), Hunghae Fm. (sandstone/mudstone) and Duho Fm (mudstone) (Choe & Chough, 1988) (Table 2-1). These formation names are identical with those of Um et al. (1964), but the lithologic boundaries are different (see Chapter 3).

2.2. PALEONTOLOGY

Paleontological studies were carried out by many geologists on various microfossils including foraminifers (Kim, 1965; Yoo, 1969; Kim & Choi, 1977a, 1977b; Shin, 1981; Lee, 1982; Choi, 1983; Kim, 1990), silicoflagellates and ebridians (Lee, 1978b, 1979; You, 1983; You & Goh, 1984), diatoms (Lee, 1975, 1978a, 1983, 1984, 1986), palynomorphs and dinoflagellates (Takahashi & Kim, 1979; Yun, 1981; Bong, 1982, 1985; Chun et al., 1983; Kim, 1987) as well as macrofossils such as plant debris, bivalves and scapods (Yoon, 1975, 1976a, 1976b, 1978, 1979; Chun, 1982) (Table 2-2). Various biostratigraphic zonations based on foraminifers, molluscs, diatoms and nannofossils were

Table 2-2. Summary of paleontological studies (modified after Choe, 1990)

Author	Fossil	Biozone	Climate	Seawater	Age
Tateiwa (1924)	plant mollusca		warm		Miocene
Kanehara (1935, 1936a, 1936b)	plant bivalve scaphopod gastropod coral		warm	cold	Middle to Upper Miocene
Kim (1965)	foramini-fera	2 zonules & 3 subzonules		cold	Miocene
Yoo (1969)	foramini-fera	3 faunal breaks		cold	upper Middle Miocene
Yoon (1975, 1976a, b 1978, 1979)	bivalve scaphopod gastropod	7 zones			late Early to Middle Miocene
Kim & Choi (1977a, b)	foramini-fera	4 biozones			Miocene
Takahashi & Kim(1979)	palynomorph				Late Miocene
Lee (1975, 1978a 1983 1984)	diatom	2 zones & 4 subzones		cold	early Middle to late Middle Miocene
Lee (1978b, 1979)	silicofla-gellate ebridian	1 zone & 4 subzones		cold	Miocene
Yun (1981)	dinofla-gellate				
Shin (1981)	foramini-fera			cold & warm	Middle to Late Miocene
Lee (1982)	foramini-fera		temperate	cold	Middle to Late Miocene
Choi (1983)	foramini-fera				Middle to Late Miocene
Chun (1982)	plant		temperate		Early to Middle Miocene
Chun et al (1983)	palynomorph dinocyst tasmanitid	6 stages	warm to temperate		Middle to Late Miocene
Ling & Kim (1983)	archaeo-monad				late Early Miocene

Table 2-2 (continued)

Author	Fossil	Biozone	Climate	Seawater	Age
You (1983)	silicoflagellate ebridian nannoplankton	2 zonules		cold	middle to early Late Miocene
You & Koh (1984)	silicoflagellate ebridian			cold	Middle Miocene
Bong (1982, 1984, 1985)	palynomorph	6 stages	warm to temperate		Middle Miocene
Choi, Kim & Bong (1984)	tasmanitid				
Lee (1986)	diatom	1 zone & 4 subzones		cold & warm	Middle to early Late Miocene
You, Koh & Kim(1986)	nanno-	2 zonules & 2 subzonules		cold & warm	early Middle to Late Miocene
Kim (1987)	palynomorph		warm to temperate		Early to Middle Miocene
Kim (1990)	foraminifera			cold & warm	late Early to Late Miocene
Yun et al (1990)	dinoflagellate ostracoda foraminifera			cold & warm	late Early Miocene
Huh (1991)	ostracoda				Miocene

made in outcrop and well sections (Kim, 1965; Yoon, 1975, 1978; You, 1983; Lee, 1984). These studies revealed that the Yeonil Group was deposited in Miocene Epoch under mixed conditions of warm and cold waters (Kim, 1965; Yoo, 1969; Shin, 1981; Lee, 1982; You, 1983; You & Koh, 1984; Lee, 1986; You et al., 1986). Climate of the adjacent terrestrial area was warm to temperate (Chun, 1982; Bong, 1982, 1985; Chun et al., 1983; Lee, 1984; Kim, 1987). Benthic foraminiferal assemblage indicates that the sequence was deposited in the upper to middle bathyal (Hakrim Fm.) and middle to lower bathyal (Hunghae and Duho fms.) environments (Kim, 1965; Kim & Choi, 1977a, 1977b; Shin, 1981; Choi, 1983), whereas the lower part of the sequence (Chunbuk Fm.) was deposited in subaerial and shallow water environments as suggested by bivalves (Yoon, 1975, 1976a, 1976b). Studies of well sections on foraminiferal assemblage indicate progressive deepening environment from shelf to middle to lower bathyal depth (Kim & Choi, 1977a, 1977b; Kim, 1990). These are generally in good agreement with the result of geohistory analysis in the adjacent continental margin (Barg, 1986; Chough & Barg, 1986, 1987), in that the basin was subsided abruptly (ca. 700 m/my) during the Miocene.

2.3. SEDIMENTOLOGY

In spite of the extensive studies on stratigraphy and paleontology,

sedimentological studies were carried out only recently. Chang (1984) and You (1985) studied grain size and clast composition in the Yeonil Group, and suggested that the group was deposited in various environments including coastal alluvial fan (Chunbuk Fm.), shelf-slope (Hakrim Fm.), submarine fan (Hunghae Fm.) and basin plain (Duho and Idong fms.). According to Choe (1986) and Choe & Chough (1988), sedimentary facies of the Hunghae Formation are represented by 1) sand and mudstone (low-density turbidity current), 2) coarse sand (high-density turbidity current), 3) homogeneous mudstone (hemipelagic settling), 4) chaotic deposits (rockfall and slide/-slump), and 5) gravelstone (debris flow). Based on facies associations, they suggested that the Hunghae Formation was deposited in coalescing debris (slope) aprons off fan deltas (Choe & Chough, 1988).

A continued study on the Chunbuk Formation made it possible to identify a fan-delta system near the Doumsan Mountain and named 'Doumsan fan delta' (Hwang, 1989; Chough et al, 1989, 1990; Hwang & Chough, 1990). The Doumsan fan delta is represented by composite fan-delta system with both Gilbert- and slope-type fan deltas. The system was deposited in various depositional environments, including: 1) subaerial fan (massive and stratified breccias with sheet geometry), 2) braided stream (massive, stratified and cross-bedded gravelstones with channel geometry), 3) Gilbert-type topset (massive, laminated sandstone and massive, crudely-stratified and cross-

bedded gravelstone with coarsening upward trends), 4) Gilbert-type foreset (steeply inclined stratified gravelstone), and 5) Gilbert-type toeset (deformed units of crudely stratified and graded gravelstone, and massive muddy sandstone) environments (Hwang, 1989; Chough et al, 1990; Hwang & Chough, 1990). The sequence shows a radial, lateral facies transition, progressively fining and thinning away from the point of sediment origin, west of the Doumsan mountain (Hwang, 1989). Choe (1990) further carried out detailed analyses of sedimentary facies for the submarine Doumsan fan delta (Hakrim Fm.). He identified 22 sedimentary facies which can be organized into 4 facies associations deposited in distinct depositional environments such as 1) submarine channels (chutes), 2) lobes, 3) sheet sandstone bodies, and 4) interchannels and interlobes. The study revealed that the submarine Doumsan fan delta is dominated by mass-flows, and the distribution of facies associations indicates downslope decelerating sediment gravity flows which may have initiated from the resedimentation of the steeply-inclined foreset and nearshore sediments (Choe, 1990).

3. GEOLOGIC SETTING AND LITHOLOGY

The Yeonil Group sequence unconformably overlies the Cretaceous and Eocene sedimentary and igneous rocks (Fig. 3-1). The sedimentary rocks include brownish and dark gray gravelstone, sandstone and shale of Silla Series (Cretaceous), which are intruded by granitic and volcanic rocks (Eocene). The former are exposed in the western part of the Pohang Basin, whereas the latter are widely distributed in the western and northeastern parts of the basin (Fig. 3-1). The volcanic rocks include agglomerate, rhyodacite and rhyolite tuff. Biotite granite and andesite also occur. The basement is faulted and tilted and largely composed of sedimentary (Cretaceous) and volcanic (Eocene) rocks (Kim & Yoon, 1982; Han et al., 1986; Kim, 1990).

The Yeonil Group sequence occurs on the eastern part of the Yangsan fault (Fig. 3-2). Previous studies based on regional geologic mapping, measurement of paleomagnetism and seismological survey revealed that the Yangsan Fault experienced right-lateral strike-slip movement (Reedman & Um, 1975; Kim, 1985a, 1985b; Lee et al., 1986). Lee (1974), Choi & Park (1985), Yoon (1986) and Kim (1988), however, conceived that dip-slip movement was dominated. Recently, Lee (1989), Woo (1989) and Chang et al. (1990) carried out detailed geologic mapping along the Yangsan Fault. Based on pre-fault reconstruction of the Cretaceous sedimentary sequence, they suggested that the Yangsan fault experienced 35 km of right-lateral

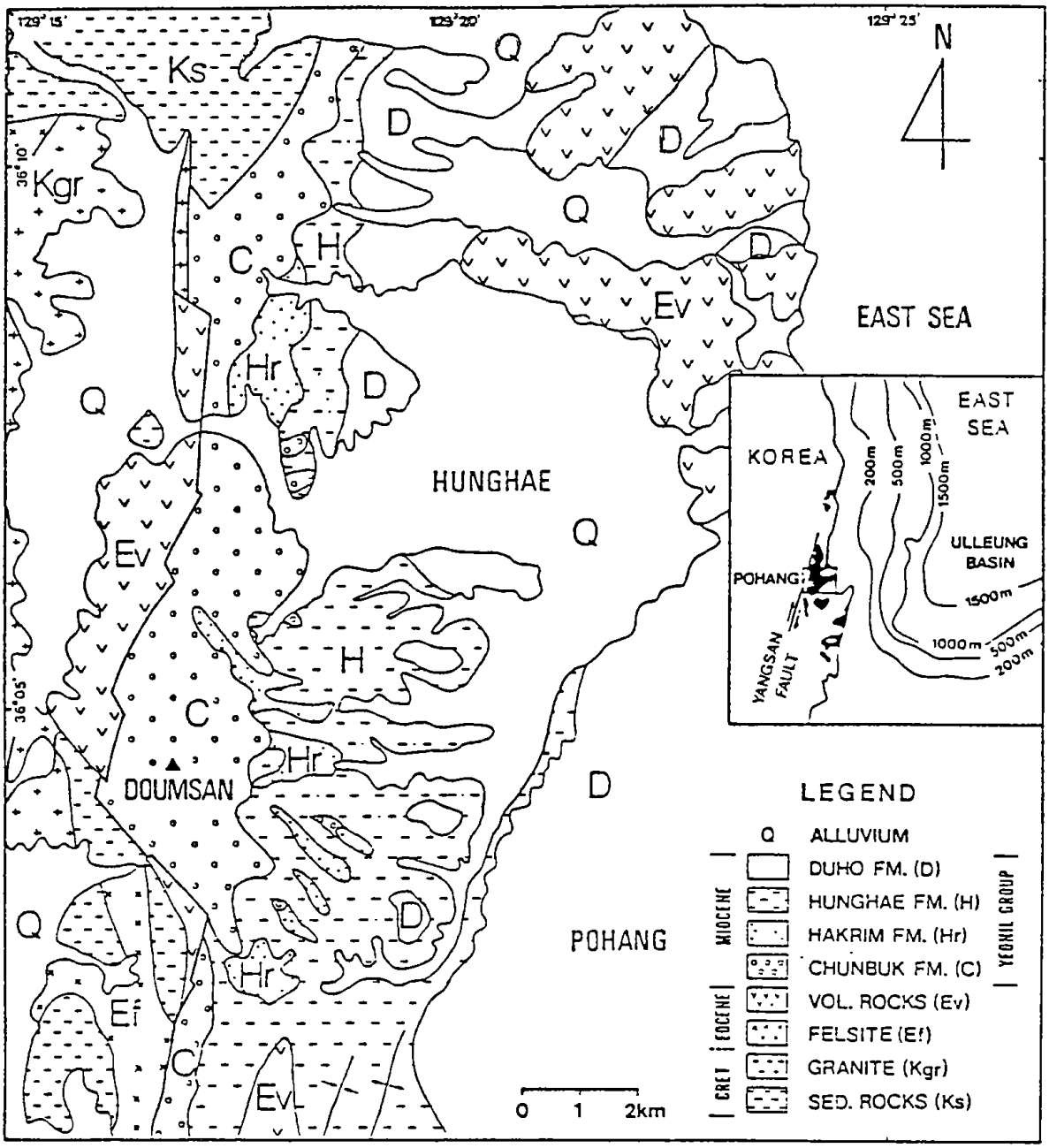

Fig. 3-1. Simplified geologic (lithofacies distribution) map of Pohang Basin (modified after Chough et al., 1990).

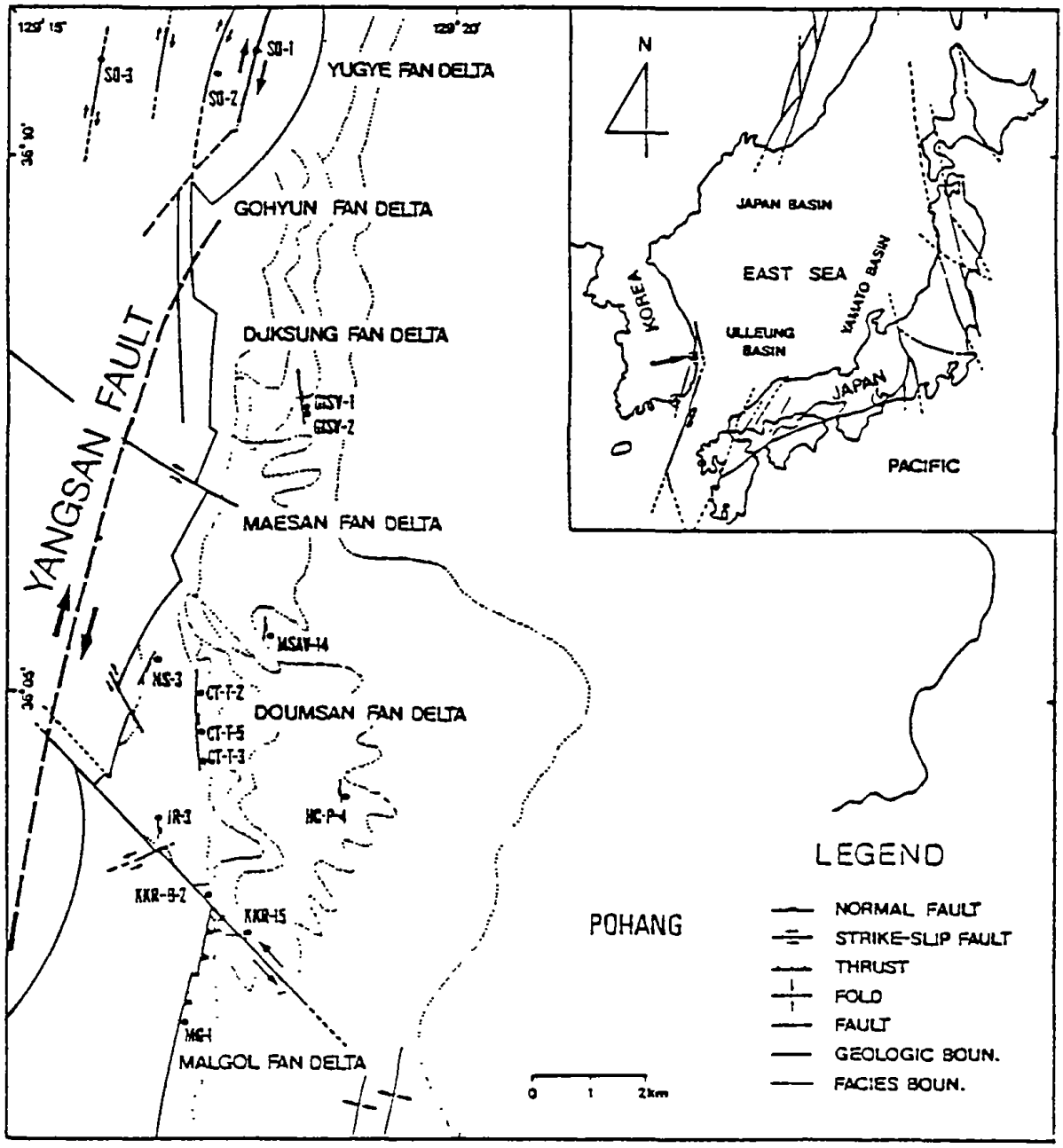

Fig 3-2. Simplified structural map in the western part of the Pohang Basin

strike-slip movement in which the movement postdates middle Eocene and predates middle Miocene.

The Yeonil Group sequence generally trends north-south with a dip of 5°-30°E. The entire sequence is more than 1 km thick and comprises various lithologic units of gravelstone, sandstone and mudstone (Um et al., 1964). In spite of the extensive geologic mapping based on litho- and bio-stratigraphy during the last three decades (Um et al., 1964; Kim, 1965; Yoon, 1975; Yun, 1986), it was difficult to identify each formation in the field. The confusion was largely due to the failure of recognizing lateral and vertical facies changes of individual lithologic units. As the previous schemes were established partly based on paleontological evidence, identification of individual formation was further complicated, warranting a definitive and quantitative study of lithologic and facies units.

In this study, the Yeonil Group was divided into four formations, based on lithologic units. The lithologic units are based on quantitative measurement of grain size (Fig. 3-3A): gravelstone (> 20% gravels); gravelly sandstone (5-20% gravels, 80% < sands < 95%); gravelly mudstone (5-20% gravels, 80% < muds < 95%); sandstone (> 80% sands, < 15% muds, < 5% gravels); mudstone (> 80% muds, < 15% sands, < 5% gravels); muddy sandstone (< 5% gravels, 50% < sands <70%, 30% < muds <50%); sandy mudstone (< 5% gravels, 50% < muds <70%, 30% < sands <50%). This

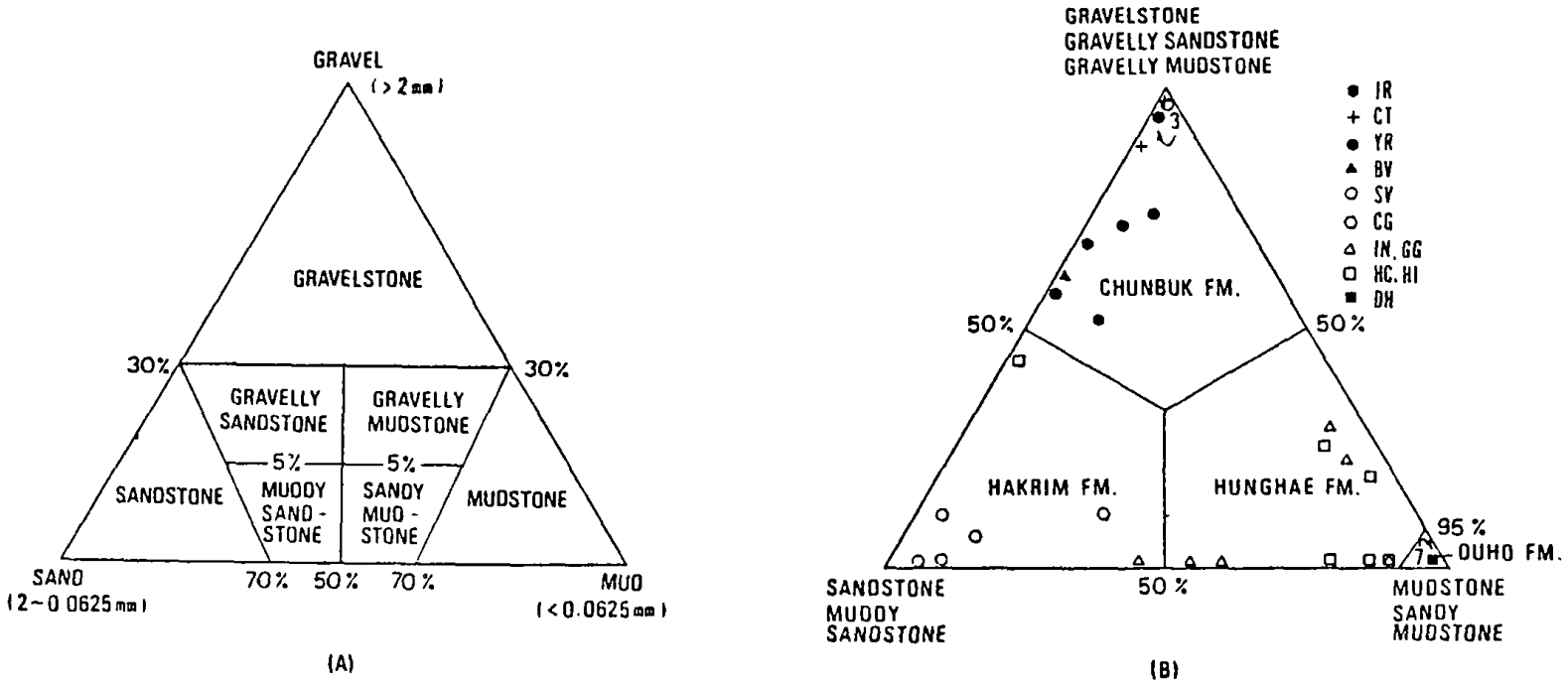

Fig. 3-3. Triangular plots of lithofacies for Yeonil Group: A) lithofacies defined by volume (percentage) of gravel, sand and mud beds, B) lithofacies association of each formation. JR = Jungok Reservoir, CT = Chungoksa Temple, YR = Yongyun Reservoir, BV = Bumchon Valley, SV = Songhak Valley, CG = Chogok Village, IN = Iin Village, HC = Hakchun Village, HI = Hail Village, DH = Duho Village.

scheme is similar to that commonly used by sedimentologists, but its application to the Yeonil Group sequence proved to be useful in defining individual formations whose formation boundaries have been disputed for the last three decades.

In outcrop sections, bed thickness of each lithologic unit was estimated quantitatively to classify the facies units (formations). In counting bed thickness, laterally discontinuous slide blocks and gravelstone wedges were not considered for further estimation. It turned out that the deposits can be divided into four formations (Fig. 3-3B). The Chunbuk Formation comprises more than 50% of gravelstone, gravelly sandstone and gravelly mudstone whereas the Hakrim Formation consists of more than 50% of sandstone and muddy sandstone (Fig. 3-3B). The Hunghae Formation is represented by interlayered sandstone and mudstone (more than 50% of mudstone and sandy mudstone) (Fig. 3-3B). The Duho Formation is dominated by thick mudstone (> 95% mudstone) (Fig. 3-3B). Using this scheme, the formation boundaries were redefined.

This scheme is useful in defining each formation in the field, which is bounded by lateral lithofacies change. Furthermore, the geologic map based on this scheme proved to be very useful to identify depositional systems (fan-delta systems) in which the gravelstone (Chunbuk Fm.) and sandstone (Hakrim Fm.) show radial distributional patterns (i.e. Doumsan fan delta;

Hwang, 1989; Chough et al., 1989, 1990; Hwang & Chough, 1990). Further detailed study revealed that the distribution of lithofacies shows not only lateral variation but also vertical and spatial transition depending on the variation in sediment supply rate from the various alluvial feeder systems and tectonic history of the basin. Neither the litho- and bio-stratigraphy, nor the chronostratigraphy can exactly explain the complex distribution of lithofacies in the Pohang Basin, which warrants a more detailed analysis of genetic sequence stratigraphy (Sloss, 1988; Galloway, 1989a, b). In the following section, distinctive features and stratigraphic position of each formation largely based on quantitative lithologic units are briefly described.

3.1. CHUNBUK FORMATION

The Chunbuk Formation occurs as a narrow belt along the western boundary of the Yeonil Group with variable thickness (150 - 600 m) (Fig. 3-1). It is composed of more than 50% of gravelstone, gravelly sandstone and gravelly mudstone in which sandstone and mudstone layers are partly intercalated (Fig. 3-3B). It occurs on the lowest part of the Yeonil Group sequence and unconformably overlies the Cretaceous sedimentary rocks and Eocene granitic and volcanic rocks (Fig. 3-1). The sequence laterally grades into and is partly overlain by the Hakrim Formation. In topographically high areas, this formation is in direct contact with the Hunghae Formation. In

some regions, it overlies the Hakrim and Hunghae formations (for summary, refer to Hwang, 1993).

Clasts of the Chunbuk Formation vary from granule to megaclasts (several meters in diameter), and are mainly composed of sedimentary (Cretaceous), granitic and volcanic (Eocene) rocks, derived from the basement rocks in the western part. The lowest part of the formation is composed of breccias where the clast composition varies according to the directly underlying basement rocks. The middle and upper parts consist of subangular to rounded clasts which show a systematic variation in clast composition according to the major sediment source (fan apex). The matrix varies from muddy sands to sands; some mudstone and sandstone beds contain thin lignite fragments. Microfossils are rare, but some beds contain abundant mollusc fossil fragments of brackish to shallow marine types (Yoon, 1975, 1976a, b).

3.2. HAKRIM FORMATION

The Chunbuk Formation laterally grades into and is partly overlain by the Hakrim Formation (Fig. 3-1). In some regions (i.e. Maesan), the Hakrim Formation is overlain by the Chunbuk Formation (for summary, refer to Hwang, 1993). The Hakrim Formation is well exposed along the valleys which run radially from the Doumsan mountain to the villages of Kukurim,

Songhak, Hail, Iin, Hakchun, Chogok and Maesan (for summary, refer to Choe, 1990). Near the Doumsan mountain, the topographically high areas are occupied by the Hunghae Formation and the Chunbuk Formation is in direct contact with the Hunghae Formation. Therefore, the Hakrim Formation occurs only along the valleys and shows patchy distribution (Fig. 3-1). Near the Doumsan mountain, the formation is well exposed with thickness for more than 150 m (max. 180 m), whereas the southern and northern parts of the basin contain thin units of this formation (< 10 m in thickness). Thus, this formation shows a radial distributional pattern from the point of sediment origin, west of the Doumsan mountain (Fig. 3-1).

The Hakrim Formation comprises more than 50% of sandstone and muddy sandstone with intercalating gravelstone and mudstone (Fig. 3-3B). In the field, the muddy sandstones are commonly mistaken for mudstone or sandy mudstone, but detailed analyses of grain size revealed that sand components are more abundant (> 50% sands) (Fig. 3-3A). The sandstones are light brown to greenish gray in color and are commonly massive, graded and laminated with channel or sheet geometry (Choe, 1990). Outsized gravels are common, forming pockets and lenses of gravels. Rip-up mud clasts, lignite fragments and plant debris are commonly contained. The sandstone unit is variable in thickness from a few centimeters up to 15 m. The gravelstone layers are commonly wedged (channel or lobe geometry) and the

clasts are more rounded than those of the Chunbuk Formation. The mudstone and muddy sandstone is dark gray in color and occur as thick homogeneous units. Microfossils are common; some beds contain broken mollusc fossil fragments. Armored mudstone balls and chaotic units also occur.

3.3. HUNGHAE FORMATION

The Hakrim Formation laterally grades into and partly overlain by the Hunghae Formation (Fig. 3-1). In topographically high areas and in the northern and southern parts of the Doumsan mountain, this formation is in direct contact with the Chunbuk Formation (Fig. 3-1). Partly, this formation intercalates with the Chunbuk Formation (i.e. Maesan section; for detailed spatial distribution, refer to Hwang, 1993). This formation is, in turn, overlain by the Duho Formation (Fig. 3-1). It is well exposed in Gigok, Iin, Hail, Hakchun and Chogok villages (for summary, see Choe, 1986; Choe & Chough, 1988). This formation is largely composed of alternating units of sandstone and mudstone (50% < mudstone and sandy mudstone < 95%). The mudstones are generally homogeneous and are dark gray in color, whereas the sandstones consist of massive, graded and laminated, fine to coarse sands. The gravelstone units are generally wedged (channel or lobe geometry) (Choe, 1986; Choe & Chough, 1988). Chaotic units such as

slide/slump, armored mudstone balls and isolated calcite-cemented slide blocks are common. Microfossils such as foraminifers, diatoms, silico-flagellates, ebridians, nannofossils and palynomorphs are abundant (Kim, 1965; Lee, 1975, 1984; You, 1983; Bong, 1985; Koh, 1986).

3.4. DUHO FORMATION

The Duho Formation conformably overlies the Hunghae Formation and is well exposed in the vicinity of Pohang City (Fig. 3-1). It is characterized by thick, olive gray, homogeneous mudstone (> 95% mudstone) with thin interlayers of sandstone. Some mudstone units are thinly laminated. According to Garrison et al. (1979), the mudstone resembles 'porcelanites' of the Monterey Formation in California. Macrofossils such as mollusc fragments and plant debris as well as microfossils are abundant. Calcite-cemented mudstone blocks (several meters in diameter) are also present.

Chapter 4. DESCRIPTION OF MEASURED SECTIONS

The Malgol fan-delta sequence is well exposed along the gullies which run through the villages of Kukurim, Malgol, Dalbat and Gwangbang as well as Ankye and Daljun reservoirs (Fig. 4-1). In this fan delta, four sections were measured in detail: Malgol (MG), Gwangbang (GB), Maebong (MB) and Daljun Reservoir (DR) sections (Fig. 4-1). In each section, sedimentary characteristics such as grain size, clast composition, sedimentary structures and fabrics are described in detail. Data on paleocurrent patterns, bed attitudes and fault patterns are also given in the following section.

4.1. Malgol Section (MG)

This section lies along the valley which runs from the villages of Malgol to Dalbat (Fig. 4-1). The sequence is more than 500 m thick, in which 5 subsections (about 60 m thick) were measured. According to Hwang (1989, 1993), the sequence was deposited in three depositional environments: alluvial fan (subsection MG-1), submarine scree apron (subsections MG-2 and -3) and slope apron (subsections MG-4, and -5) environments (Fig. 4-2).

Subsection MG-1

This section lies along the valley near the Malgol village (Fig. 4-1), and occupies the lowermost part of the Malgol fan-delta system (Fig. 4-2). This

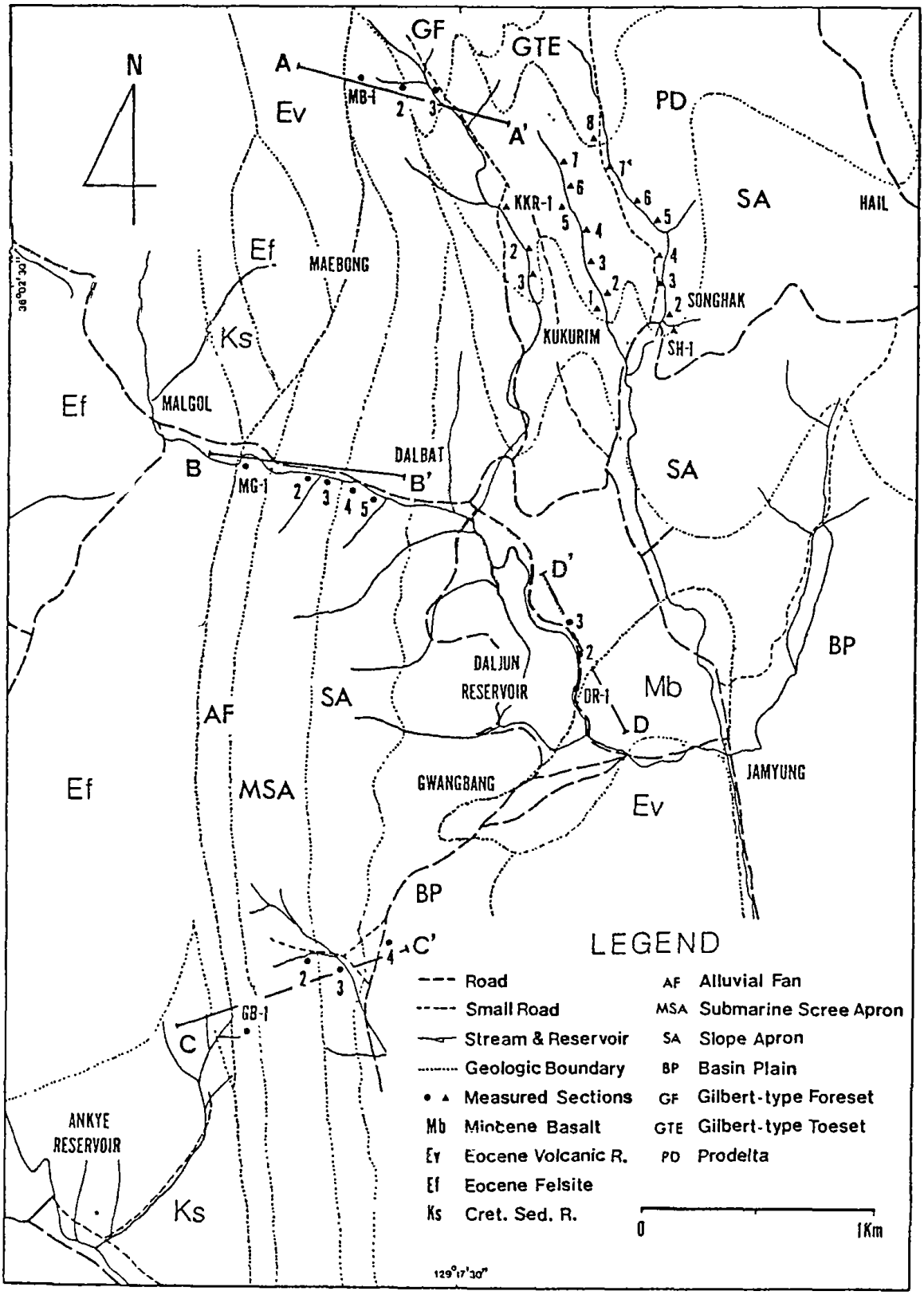

Fig. 4-1. Location map of measured sections; Malgol fan-delta area.

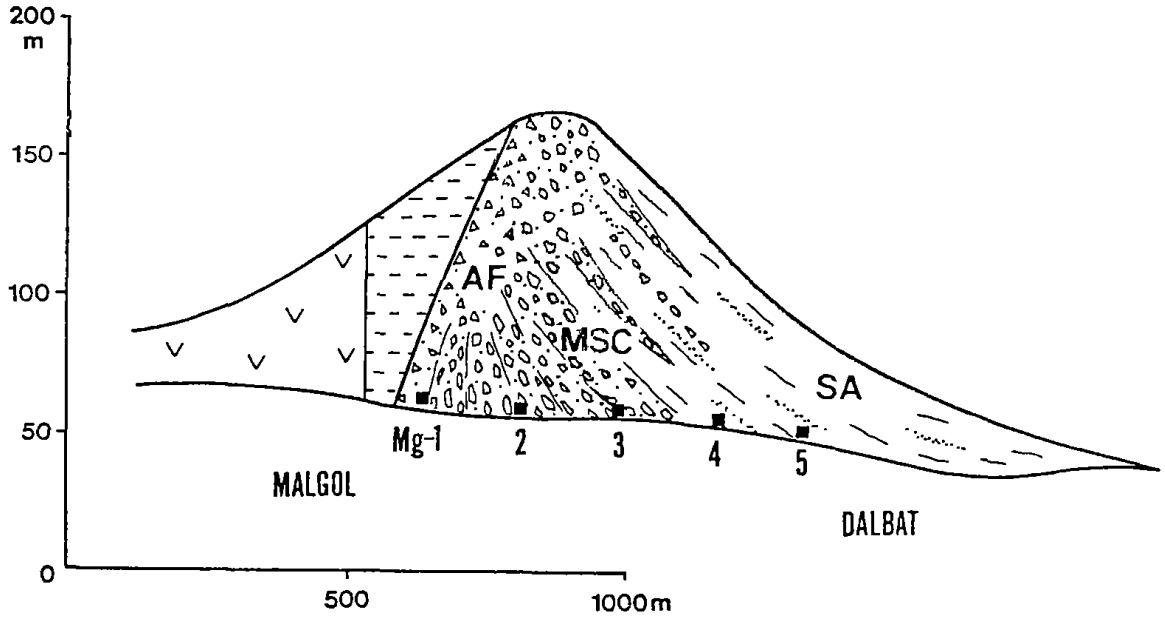

Fig. 4-2. Simplified cross-section of the Malgol section. Note stratigraphic positions of measured sections. For location, see Fig. 4-1.

section is bounded by volcanic rocks (Eocene) and sedimentary rocks (Cretaceous), approximately 20 m west of the outcrop (Fig. 4-2). In this section, parts of the Cretaceous and Eocene basement rocks overlie the Miocene sedimentary sequence, representing a thrust fault (Fig. 4-2). In the lower part, the Miocene sedimentary sequence is overturned with a general trend of N18°E/75°NW, probably related to the thrust fault (Fig. 4-2).

The lower part of the sequence is represented by alternating units of disorganized breccias (Facies B1-a and B1-b) and crudely-stratified breccia (Facies B2) with sheet-like bed geometry (Fig. 4-3). Clasts of the breccias are angular to subangular and are largely composed of felsite (Eocene) (upto 80%) with small amounts of sedimentary rocks (Cretaceous) and granitic

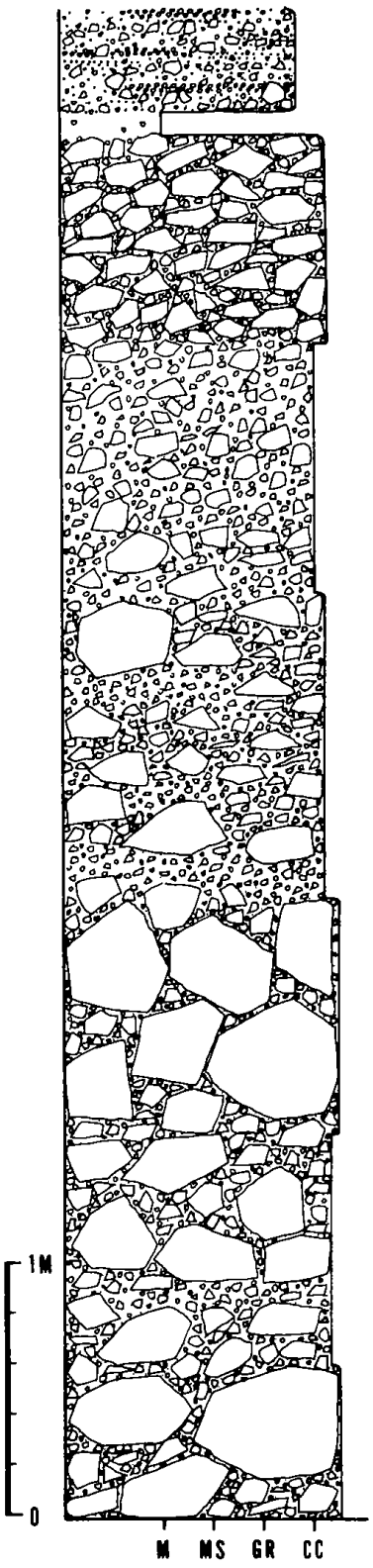

Crudely-stratified gravelstone (G2-a); angular brownish shale and sandstone clasts; brownish sand matrix.

Homogeneous muddy sandstone (M1-a); widely dispersed granule-size gravels.

Disorganized breccia (B1-a); parallel oriented clasts; clast-supported; brownish muddy sand matrix.

Disorganized breccia (B1-b); matrix-supported; brownish muddy sand matrix; clasts oriented parallel to bedding plane.

Crudely-stratified breccia (B2); matrix- or clast-supported; clasts oriented parallel to bedding plane; brownish muddy sand matrix.

Disorganized breccia (B1-a); clast-supported; brownish muddy sand matrix.

Crudely-stratified breccia (B2); matrix- or clast-supported; brownish muddy sand matrix.

Disorganized breccia (B1-a); clast-supported; brownish muddy sand matrix; 22 m east of the sequence boundary with Eocene felsite.

Fig. 4-3. Columnar section and description of subsection MG-1. For location, see Fig. 4-1.

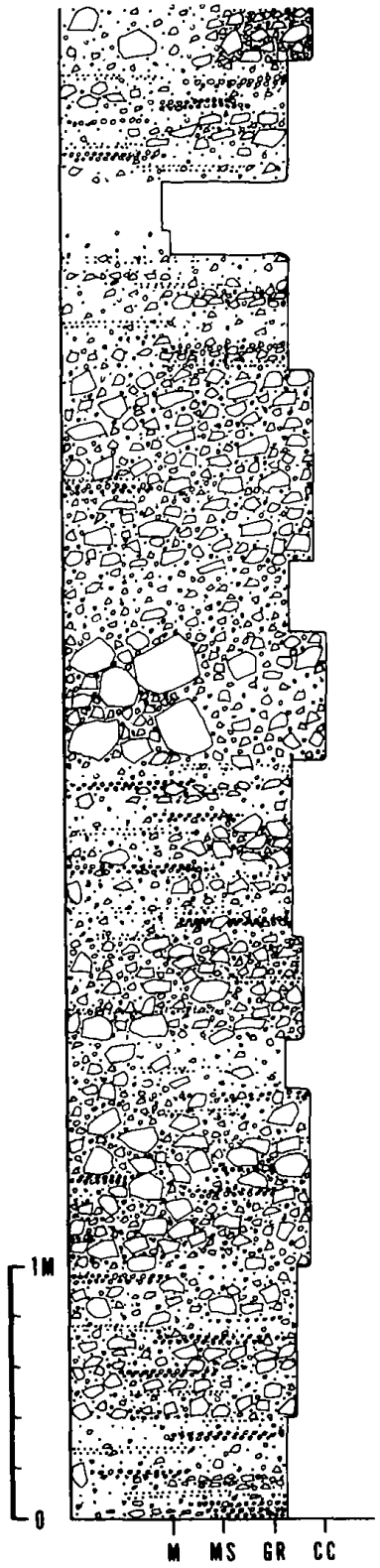

Laterally discontinuous disorganized gravelstone (G1-a); matrix- or clast-supported; brownish sand matrix.

Crudely-stratified gravelstone (G2-a); laterally discontinuous sandstone, gravelstone and gravelly sandstone layers; brownish sand matrix.

Homogeneous muddy sandstone (M1-a).

Homogeneous muddy sandstone (M1-a); small amounts of gravels.

Crudely-stratified gravelstone (G2-a); laterally discontinuous sandstone, gravelly sandstone and gravelstone layers.

Crudely-stratified gravelstone (G2-a); parallel oriented clasts; matrix- or clast-supported; brownish sand matrix; diffuse lower and upper boundaries.

Disorganized gravelstone (G1-a); matrix-supported.

Laterally discontinuous crudely-stratified gravelstone (G2-a).

Crudely-stratified gravelstone (G2-a); laterally discontinuous gravelstone, gravelly sandstone and sandstone layers.

Crudely-stratified gravelstone (G2-a); brownish sand matrix; matrix- or clast-supported.

Crudely-stratified gravelstone (G2-a); matrix-supported.

Crudely-stratified gravelstone (G2-a); brownish sand matrix; matrix- or clast-supported.

Crudely-stratified gravelstone (G2-a); laterally discontinuous gravelstone, gravelly sandstone and sandstone layers.

Crudely-stratified gravelstone (G2-a); laterally discontinuous gravelstone, gravelly sandstone and sandstone layers.

Fig. 4-3 (continued)

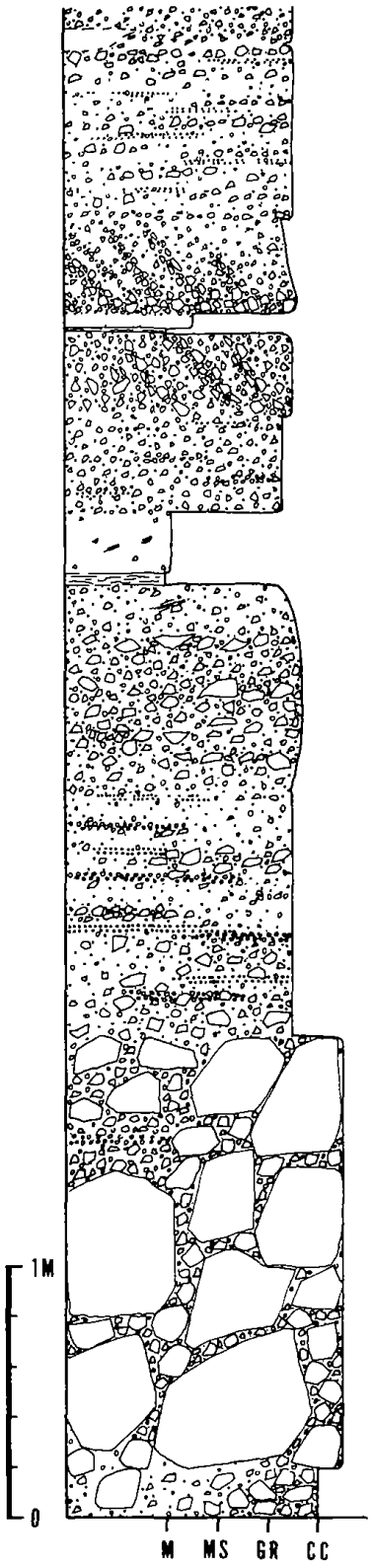

Laterally discontinuous muddy sandstone layer.

Crudely-stratified gravelly sandstone (G2-a); laterally discontinuous sandstone, gravelly sandstone layers; upward increase in mud matrix.
Cross-bedded gravelstone (G6); upward decrease in gravel content; foreset units are partly openwork.
Massive sandstone layer (S1-a); sharp lower and upper boundaries.
Thin mudstone layer; lignite laminae; sharp lower and upper boundaries.
Cross-bedded gravelstone (G6).
Crudely-stratified gravelstone (G2-a).
Homogeneous muddy sandstone (M1-a); lignite fragments; widely dispersed gravels.
Thinly laminated muddy sandstone; lignite laminae.

Crudely-stratified gravelstone (G2-a); lignite fragments.

Crudely-stratified gravelstone (G2-a); laterally discontinuous gravelstone, gravelly sandstone and sandstone layers.

Disorganized boulder-size breccia (B1-a); partly crudely-stratified; clast-supported; brownish muddy sand matrix.

Fig. 4-3 (continued)

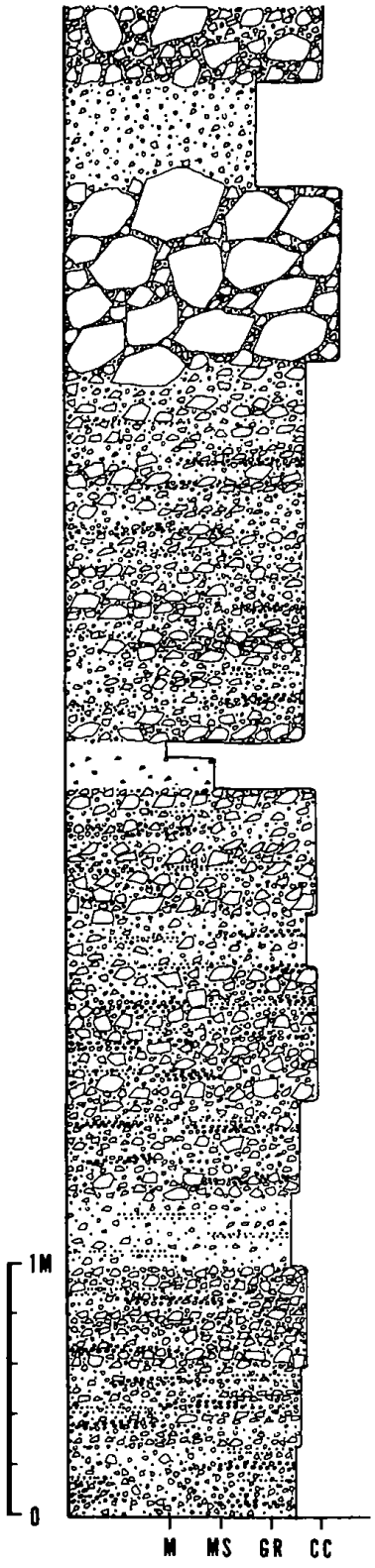

Disorganized gravelly sandstone (G1-a); matrix-supported; brownish sand matrix.

Disorganized boulder-size gravelstone (G1-a); clast-supported; brownish sand matrix.

Crudely-stratified gravelstone (G2-a); laterally discontinuous sandstone, gravelly sandstone and gravelstone layers; partly openwork; brownish sand matrix with small amounts of brownish mud.

Homogeneous muddy sandstone (M1-a); sharp lower and upper boundaries.
Homogeneous muddy sandstone (M1-a); widely dispersed granule-size gravels.

Crudely-stratified gravelstones (G2-a); laterally discontinuous sandstone, gravelly sandstone and gravelstone layers; partly openwork; brownish sand matrix with small amounts of mud.

Fig. 4-3 (continued)

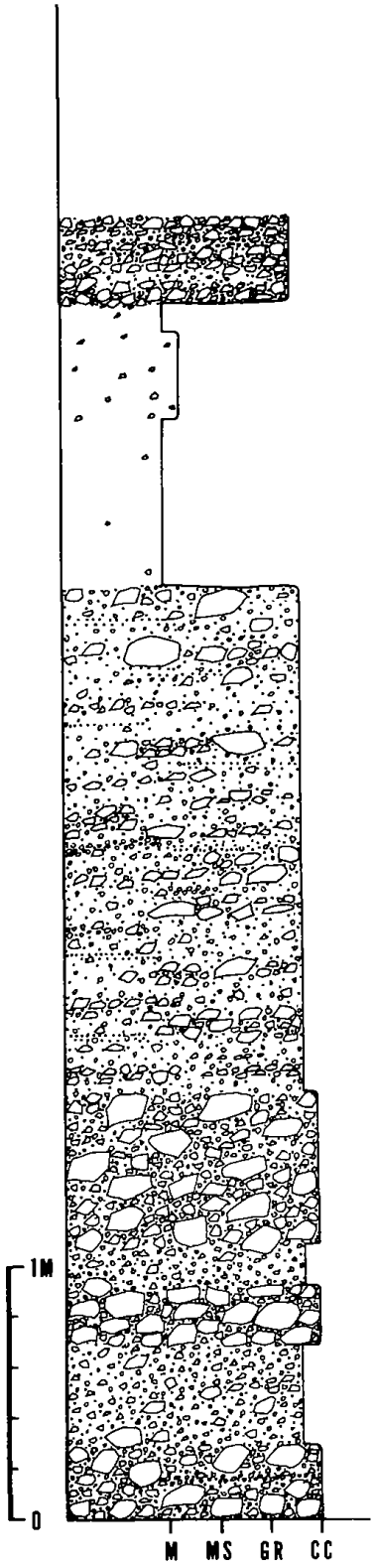

Crudely-stratified gravelstone (G2-a); laterally discontinuous sandstone, gravelly sandstone and gravelstone layers; partly openwork; sand matrix.
Homogeneous muddy sandstone (M1-a).

Homogeneous muddy sandstone (M1-a); small amounts of gravels.

Homogeneous muddy sandstone (M1-a).

Crudely-stratified gravelstones (G2-a); laterally discontinuous sandstone, gravelly sandstone and gravelstone layers; clasts oriented parallel to bedding plane; imbricated [a(t), b(i)]; partly openwork; brownish sand matrix.

Disorganized gravelstone (G1-a); clasts oriented parallel to bedding plane; imbricated [a(t), b(i)]; clast-supported; brownish sand matrix; diffuse lower and upper boundaries.

Disorganized gravelstone (G1-a); matrix-supported.
Disorganized gravelstone (G1-a); clast-supported; clasts oriented parallel to bedding plane; partly imbricated [a(t), b(i)].

Disorganized gravelstone (G1-a); matrix-supported.

Fig. 4-3 (continued)

rocks (Eocene) and volcanic rocks (Eocene); some units are entirely composed of angular clasts of felsite (100%). The matrix is represented by brownish muddy sands. Most clasts are aligned parallel to bedding plane (Fig. 4-3).

The number of the breccia unit gradually decreases vertically, whereas that of the gravelstone unit gradually increases (Fig. 4-3). In the middle and upper parts of the exposure, the sequence is represented by disorganized gravelstone (Facies G1-a), crudely-stratified gravelstone (Facies G2-a) and cross-bedded gravelstone (Facies G6) in which thin layers of homogeneous muddy sandstone (Facies M1-a) are partly intercalated (Fig. 4-3). The gravels are largely composed of subangular to subrounded clasts of sedimentary rocks (Cretaceous) (65%) and felsite (Eocene) (25%). The matrix is represented by poorly-sorted brownish sands which are largely composed of rock fragments of sedimentary rock (Cretaceous). The homogeneous muddy sandstones (Facies M1-a) are generally thin and commonly scoured by gravelstone units. In this unit, color varies from light brown to dark gray according to organic content. In this part, the sequence shows a generally trend of N18°E/85°SE.

Subsection MG-2

This section lies along the valley approximately 100 m east of subsection

MG-1 (Fig. 4-1). Stratigraphically, this section overlies subsection MG-1 (Fig. 4-2). The sequence is characterized by steeply-inclined (> 40°) beds of disorganized gravelstone (Facies G1-b) and crudely-stratified gravelstone (Facies G2-b) (Figs. 4-4 and -5). The stratification is represented by thin (one or two clasts thick), laterally discontinuous large clast layers, or parallel oriented large clast trains with diffuse lower and upper boundaries. Most clasts are aligned parallel to bedding plane; some are imbricated [a(p), a(i)]. Clasts are largely composed of felsite (Eocene) (52%) and sedimentary rocks (Cretaceous) (38%) with small amounts of granitic and volcanic rocks (Eocene) (10%). The clast composition differs from that of the underlying sequence (subsection MG-1) in which the clasts are largely composed of sedimentary rocks (Cretaceous) (65%) and felsite (Eocene) (25%). In this section, most clasts are angular to subangular and are either matrix- or clast-supported in poorly-sorted sand matrix. Detailed measurement of clast orientation (measuring about 70 grains) indicates an eastward paleocurrent direction (95°).

Subsection MG-3

This section lies along the valley approximately 50 m east of subsection MG-2 (Fig. 4-1). Stratigraphically, this section overlies subsection MG-2 (Fig. 4-2). The sequence is characterized by steeply-inclined (25°) beds of disorga-

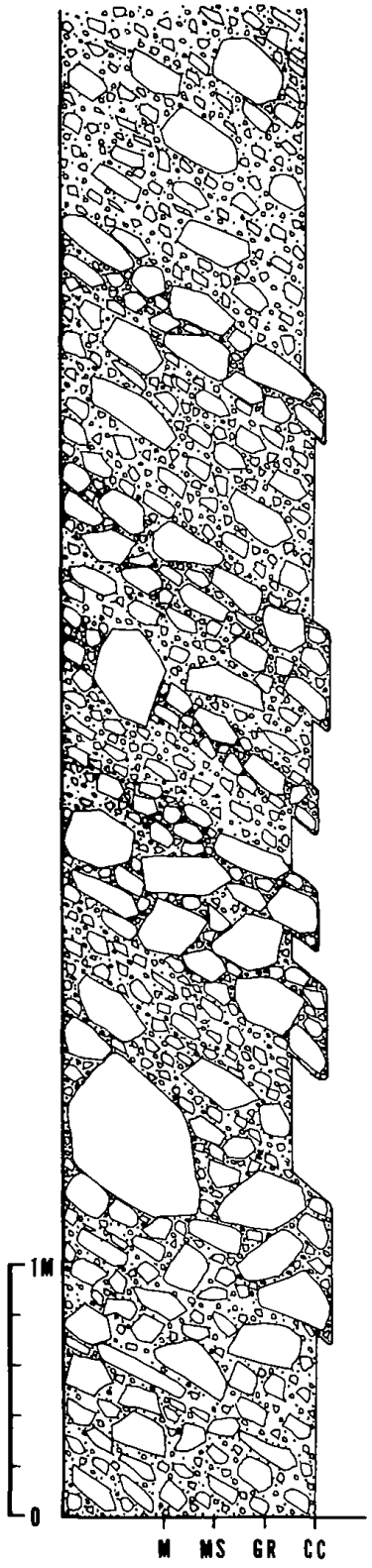

Disorganized gravelstone (G1-b); matrix-supported; poorly-sorted sand matrix; clasts oriented parallel to bedding plane; partly imbricated [a(p), a(i)].

Disorganized gravelstone (G1-b); clast-supported; poorly-sorted sand matrix; clasts oriented parallel to bedding plane; partly imbricated [a(p), a(i)]; downslope decrease in bed thickness.

Disorganized gravelstone (G1-b); matrix-supported; poorly-sorted sand matrix; clasts oriented parallel to bedding plane; partly imbricated [a(p), a(i)].

Crudely-stratified gravelstone (G2-b); clast- or matrix-supported; poorly-sorted sand matrix; laterally discontinuous large clast layers; clasts oriented parallel to bedding plane; imbricated [a(p), a(i)].

Disorganized gravelstone (G1-b); matrix-supported; poorly-sorted sand matrix; clasts oriented parallel to bedding plane; imbricated [a(p), a(i)].

Disorganized gravelstone (G1-b); outsized gravels; matrix- or clast-supported; clasts oriented parallel to bedding plane; imbricated [a(p), a(i)].

Disorganized gravelstone (G1-b); matrix-supported; poorly-sorted sand matrix; clasts oriented parallel to bedding plane; imbricated [a(p), a(i)].

Fig. 4-4. Columnar section and description of subsection MG-2. For location, see Fig. 4-1.

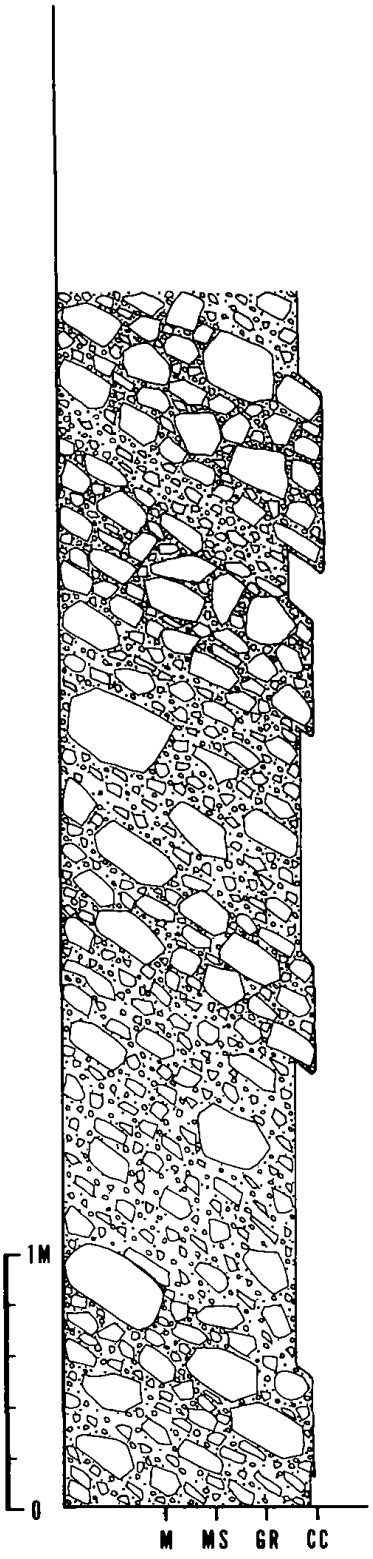

Disorganized gravelstone (G1-b); clast-supported; poorly-sorted sand matrix; clasts oriented parallel to bedding plane; partly imbricated [a(p), a(i)].

Disorganized gravelstone (G1-b); matrix-supported; poorly-sorted sand matrix; clasts oriented parallel to bedding plane; partly imbricated [a(p), a(i)].

Disorganized gravelstone (G1-b); clast-supported; poorly-sorted sand matrix; clasts oriented parallel to bedding plane; partly imbricated [a(p), a(i)].

Crudely-stratified gravelstone (G2-b); matrix-supported; poorly-sorted sand matrix; laterally discontinuous large clast trains; clasts oriented parallel to bedding plane; imbricated [a(p), a(i)].

Disorganized gravelstone (G1-b); clast- or matrix-supported; poorly-sorted sand matrix; clasts oriented parallel to bedding plane; imbricated [a(p), a(i)].

Disorganized gravelstone (G1-b); matrix-supported; poorly-sorted sand matrix; clasts oriented parallel to bedding plane; imbricated [a(p), a(i)].

Fig. 4-4 (continued)

Fig. 4-5. Photograph of subsection MG-2. Note steeply-inclined beds (> 40°) of disorganized gravelstone (Facies G1-b) and crudely-stratified gravelstone (Facies G2-b). Measuring bar is 2 m long.

nized gravelstone (Facies G1-b) and crudely-stratified gravelstone (Facies G2-b), largely similar to those of subsection MG-2 (Fig. 4-6). The stratification is represented by thin (one or two clasts thick), laterally discontinuous large clast trains with diffuse lower and upper boundaries (Fig. 4-6). Most clasts are aligned parallel to bedding plane; some are imbricated [a(p), a(i)] (Fig. 4-6).

Subsection MG-4

This section lies along the valley which runs from Malgol to Dalbat

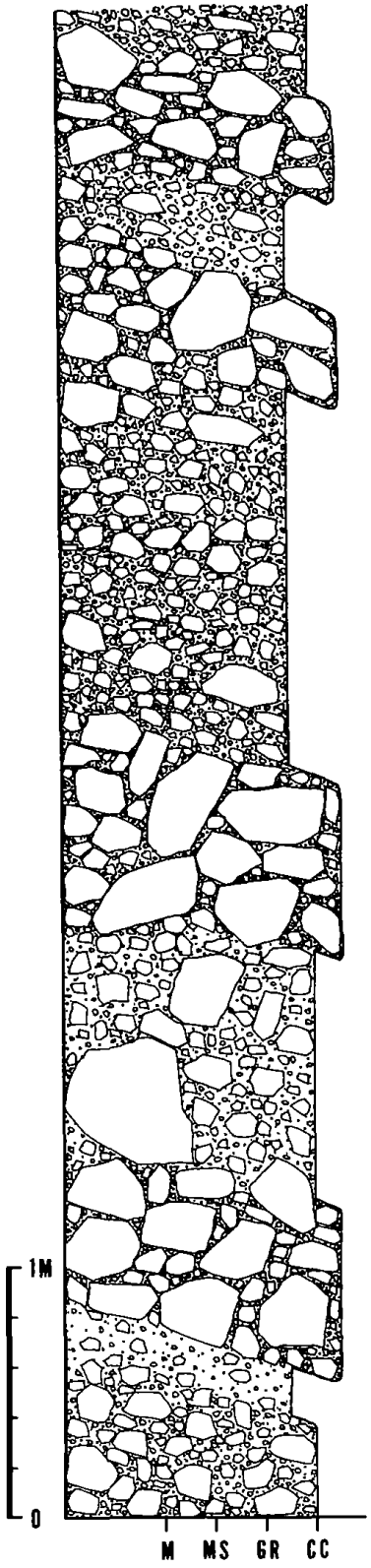

Disorganized gravelstone (G1-b); clast-supported; poorly-sorted sand matrix; clasts oriented parallel to bedding plane; partly imbricated [a(p), a(i)].

Disorganized gravelstone (G1-b); matrix-supported; poorly-sorted sand matrix; clasts oriented parallel to bedding plane; partly imbricated [a(p), a(i)].

Disorganized gravelstone (G1-b); clast-supported; poorly-sorted sand matrix; clasts oriented parallel to bedding plane; partly imbricated [a(p), a(i)]; downslope decrease in bed thickness and grain size.

Crudely-stratified gravelstone (G2-b); downslope decrease in grain size; clast- or matrix-supported; poorly-sorted sand matrix; laterally discontinuous large clast layers; clasts oriented parallel to bedding plane; imbricated [a(p), a(i)].

Disorganized gravelstone (G1-b); downslope decrease in bed thickness and grain size; clast-supported; poorly-sorted sand matrix; clasts oriented parallel to bedding plane; imbricated [a(p), a(i)].

Disorganized gravelstone (G1-b); outsized gravels; matrix-supported; clasts oriented parallel to bedding plane; imbricated [a(p), a(i)].

Disorganized gravelstone (G1-b); clast-supported; poorly-sorted sand matrix; clasts oriented parallel to bedding plane; imbricated [a(p), a(i)]; sharp lower and diffuse upper boundaries.

Fig. 4-6. Columnar section and description of subsection MG-3. For location, see Fig. 4-1.

villages about 150 m east of subsection MG-3 (near the Dalbat village) (Fig. 4-1). Stratigraphically, this section overlies subsection MG-3 with a general trend of N48°E/32°SE (Fig. 4-2). The sequence is characterized by thick homogeneous muddy sandstone (Facies M1-b) in which thin units of disorganized gravelstone (Facies G1-b), graded gravelstone (Facies G4), inverse-to-normally graded gravelstone (Facies G5-a) and massive sandstone (Facies S1-b) are partly intercalated (Fig. 4-7). The clasts are angular to subangular and are largely composed of felsite (Eocene). They are either matrix- or clast-supported in poorly-sorted sand matrix. Sandstone units are generally thin (< 10 cm) and laterally discontinuous. The lower and upper boundaries are generally irregular with flame structures, load structures and pseudonodules (Fig. 4-7). The sands are poorly-sorted. Granule-size gravels are widely dispersed. In the upper part of the exposure, a small-scale basalt body intruded the sedimentary sequence (Fig. 4-8).

Subsection MG-5

This section occurs near the Dalbat village, about 100 m east of subsection MG-4 (Fig. 4-1). Stratigraphically, this section overlies subsection MG-4 with a general trend of N24°W/6°NE (Fig. 4-2). The sequence is characterized by thick homogeneous muddy sandstone (Facies M1-b), containing abundant microfossils and plant debris as well as laterally

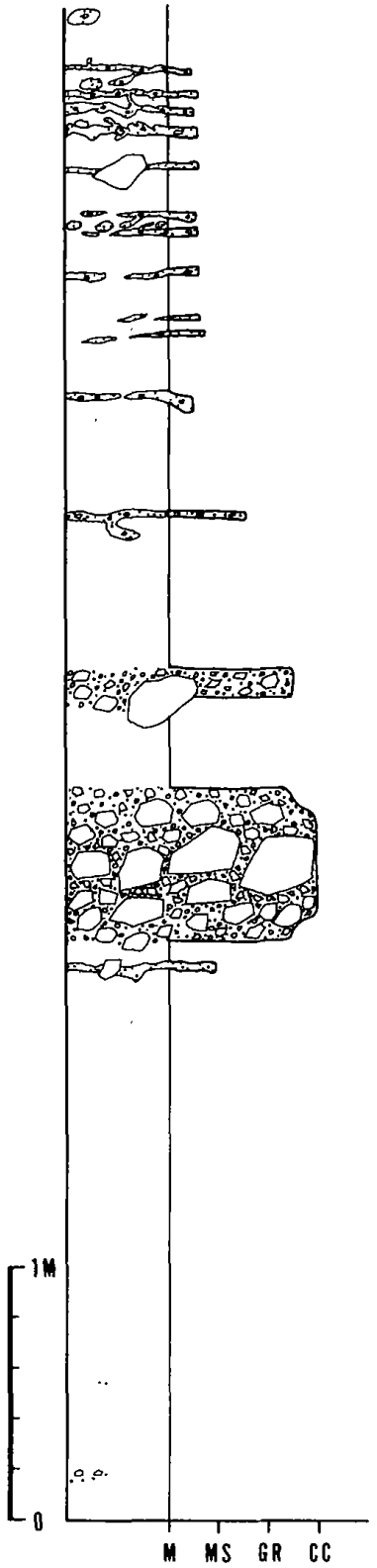

Massive sandstone layers (S1-b); load structures, pseudonodules and flame structures; widely dispersed angular gravels.

Laterally discontinuous massive sandstone layers (S1-b); load structures, pseudonodules and flame structures; widely dispersed angular gravels.

Disorganized gravelly sandstone (G1-b); load structure.

Homogeneous muddy sandstone (M1-b).

Disorganized gravelstone (G1-b); matrix-supported; sand matrix; outsized gravels.

Inverse-to-normally graded gravelstone (G5-a); matrix- or clast-supported; poorly-sorted sand matrix.

Homogeneous muddy sandstone (M1-b); laterally discontinuous thin sandstone layers; pebble pockets.

Fig. 4-7. Columnar section and description of subsection MG-4. For location see Fig. 4-1.

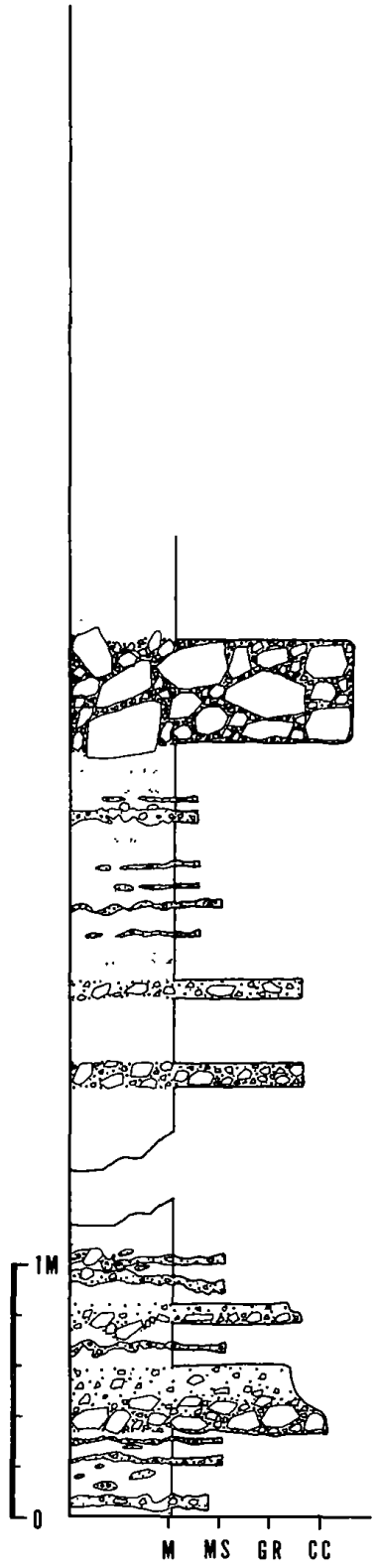

Homogeneous muddy sandstone (M1-b).

Disorganized gravelstone (G1-b); clast-supported; sand matrix.

Laterally discontinuous massive sandstone layers (S1-b); load structures, pseudonodules and flame structures; widely dispersed granule-size gravels; angular.

Disorganized gravelstone (G1-b); matrix-supported; sand matrix.

Disorganized gravelstone (G1-b); matrix-supported; sand matrix.

Basalt intrusion.

Massive sandstone layers (S1-b).

Graded gravelly sandstone (G4); load structures.

Graded gravelstone (G4) vertically grades into graded sandstone (S4); sharp lower and diffuse upper boundaries.
Massive sandstone layers (S1-b); load structures, pseudonodules and flame structures.

Fig. 4-7 (continued)

Fig. 4-8. Photograph of upper part of subsection MG-4. Note a basalt body which intruded the Miocene sedimentary sequence (arrows). Scale arrow is 20 cm long.

discontinuous thin sandstone layers (Fig. 4-9). In the lower part, thin, laterally discontinuous disorganized gravelstone (Facies G1-b) and graded gravelstone (Facies G4) layers are partly intercalated (Fig. 4-9). Upper boundaries of the gravelstones are generally diffuse and irregular with flame structures (Fig. 4-9). In the upper part of the exposure, parts of the muddy sandstone unit are cemented with calcite, ranging in size from 1 m to several meters in long diameter (Fig. 4-9). Sandstone units are generally thin (< 10 cm) and laterally discontinuous with irregular lower and upper boundaries (Fig. 4-9). The sandstones commonly contain angular, granule-size gravels.

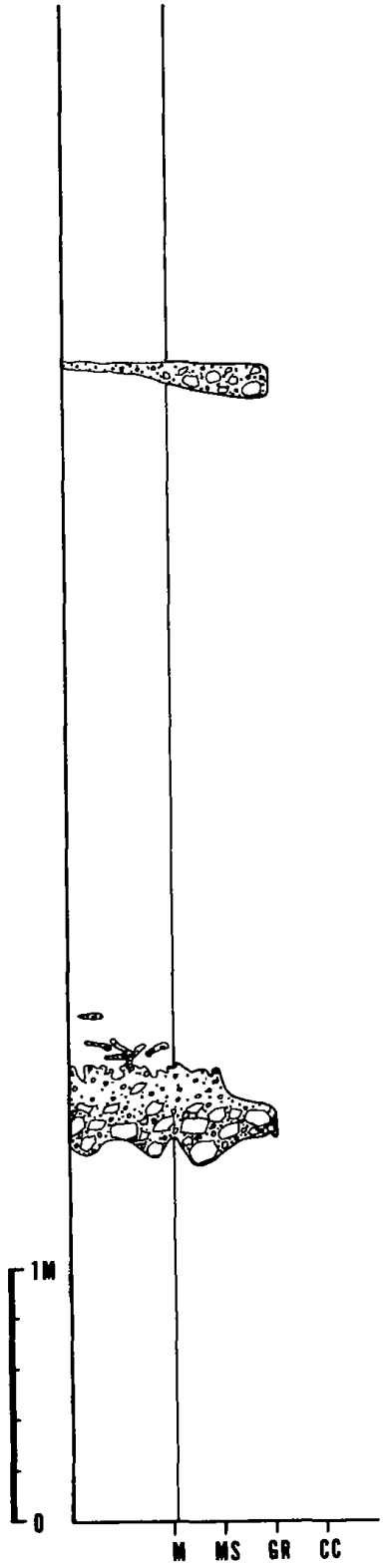

Homogeneous muddy sandstone (M1-b).

Disorganized gravelstone (G1-b) laterally grades into massive sandstone (S1-b); lateral decrease in bed thickness and grain size; widely dispersed granule size gravels; angular.

Homogeneous muddy sandstone (M1-b).

Graded gravelstone (G4) vertically grades into graded sandstone (S4); scour, load and flame structures.

Homogeneous muddy sandstone (M1-b).

Fig. 4-9. Columnar section and description of subsection MG-5. For location see Fig. 4-1.

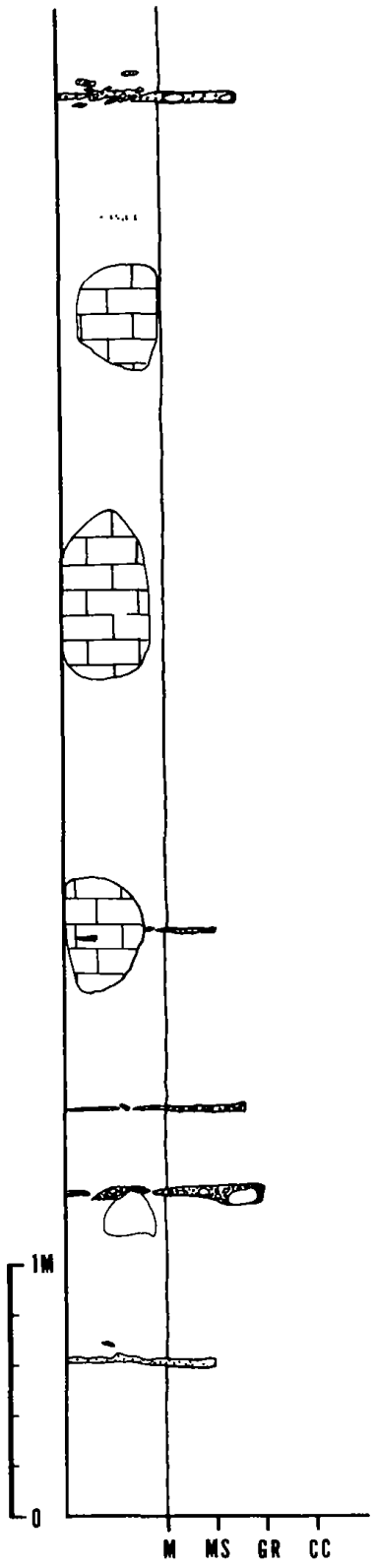

Homogeneous muddy sandstone (M1-b).

Massive sandstone (S1-b); load structures, pseudonodules and flame structures; widely dispersed granule-size gravels.

Homogeneous muddy sandstone (M1-b); thin, laterally discontinuous sandstone layers; partly cemented with calcite (several meters in long diameter).

Thin sandstone layer; partly cemented with calcite; lignite fragments.

Thin laterally discontinuous gravelly sandstone.

Thin laterally discontinuous disorganized gravelstone (G1-b); angular clasts; matrix-supported; sand matrix.

Thin massive sandstone layer (S1-b); flame structures.

Fig. 4-9 (continued)

4.2. Gwangbang Section (GB)

This section lies along the gullies between Ankye Reservoir and Gwangbang village (Fig. 4-1). Here, the Miocene sedimentary sequence unconformably overlies felsite (Eocene) (Fig. 4-10). Approximately 30 m west of the sequence boundary lies sedimentary rock (Cretaceous) (Fig. 4-10). In this section, four subsections (about 24 m thick) were measured in detail. The sequence represents deposition in a transitional zone between the subaerial and subaqueous parts (subsection GB-1), submarine scree apron (subsection GB-2), slope apron (subsection GB-3) and basin plain (subsection GB-4) environments (Hwang, 1993).

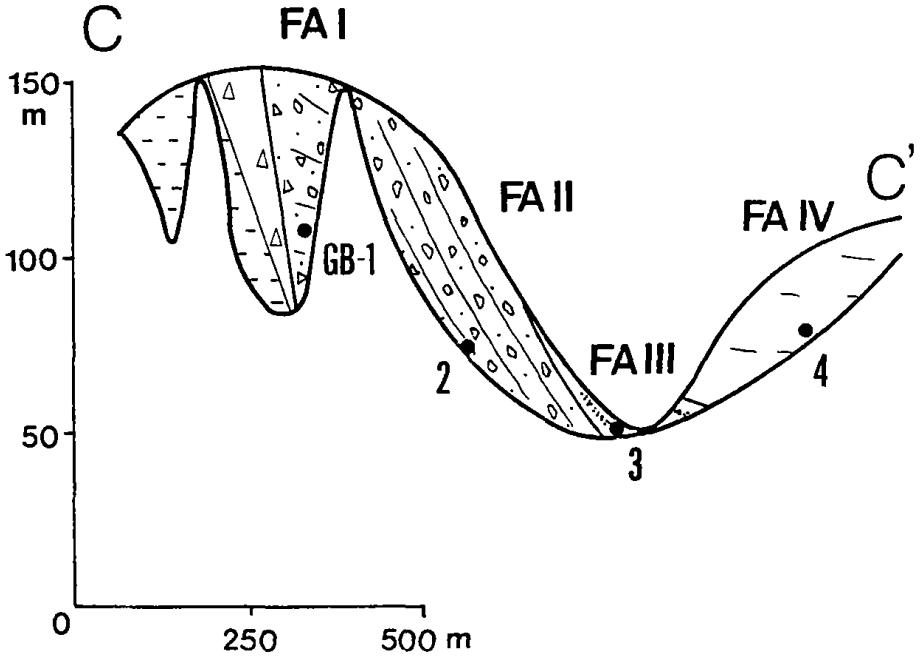

Fig. 4-10. Simplified cross-section of the Gwangbang section (GB). Note stratigraphic positions of measured sections. For location, see Fig. 4-1.

Subsection GB-1

This section lies along the small gully which runs from the mountain western part of the basin to the Ankye Reservoir, approximately 500 m northeast of the Ankye Reservoir and 600 m southwest of the Gwangbang village (Fig. 4-1). The sequence is represented by alternating units of disorganized gravelstone (Facies G1-a), crudely-stratified gravelstone (Facies G2-a) and massive sandstone (Facies S1-a) with a general trend of N8°E/-12°NE (Fig. 4-11). In this section, clast composition varies from bed to bed; it is largely composed of subangular to subrounded clasts of sedimentary rock (Cretaceous) (approximately 70%) and felsite (Eocene) (approximately 25%) with small amounts of volcanic rocks (Eocene).

The lower part of the sequence is represented by gravelstone and sandstone units which show a coarsening-upward trend (Fig. 4-11). The thick massive sandstone (Facies S1-a) in the lower part of the sequence is largely composed of poorly-sorted brownish sands with abundant lithic fragments of sedimentary rocks (Cretaceous). In this unit, thin (< 10 cm), laterally continuous disorganized gravelstone layers (Facies G1-a) are intercalated (Fig. 4-11). The lower and upper boundaries of the gravelstone layers are generally diffuse. The gravel clasts are matrix-supported in poorly-sorted sand matrix. It is overlain by thick (> 340 cm), disorganized gravelstone (Facies G1-a) with a diffuse unit boundary (Fig. 4-11). In this unit, the clasts

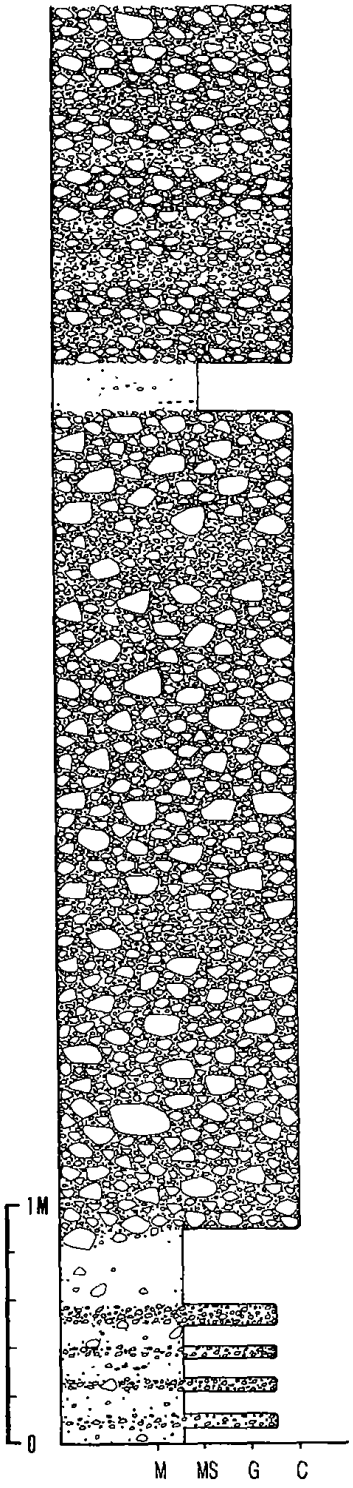

Crudely-stratified gravelstone (G2-a); clast- or matrix-supported; poorly-sorted sand matrix; sharp, erosional lower boundary.

Massive sandstone (S1-a); pebble trains; sharp lower and upper boundaries.

Crudely-stratified gravelstone (G2-a); clast- or matrix-supported; poorly-sorted sand matrix; diffuse lower and sharp upper boundaries.

Massive sandstone (S1-a); widely dispersed gravels; thin, laterally discontinuous gravelly sandstone layers; matrix-supported; sand matrix; diffuse lower and upper boundaries.

Fig. 4-11. Columnar section and description of subsection GB-1. For location, see Fig. 4-1.

are either clast- or matrix-supported with poorly-sorted sand matrix. It is overlain by massive sandstone (Facies S1-a) with a sharp unit boundary. The sandstone unit contains thin, laterally discontinuous gravel trains. It is overlain by a crudely-stratified gravelstone unit (Facies G2-a) with a sharp, erosional boundary (Fig. 4-11).

Subsection GB-2

This section occurs approximately 150 m east of subsection GB-1 (Fig. 4-1). Stratigraphically, this section overlies subsection GB-1 with a general trend of N8°W/20°SE (Fig. 4-10). The sequence is represented by steeply-inclined (> 20°) beds of disorganized gravelstone (Facies G1-b) and crudely-stratified gravelstone (Facies G2-b) with sheet-like bed geometry (Fig. 4-12). Clasts are angular to subrounded and are largely composed of sedimentary rock (Cretaceous) (approximately 65%) and felsite (Eocene) (30%). The clast composition is largely similar to that of subsection GB-1. Most clasts are aligned parallel to bedding plane (> 20°); some are imbricated [a(p), a(i)]. Data on clast orientations (measurement of 39 clasts) revealed southeastward (110°) paleocurrent direction. The clasts are either matrix- or clast-supported with poorly-sorted sand or muddy sand matrices.

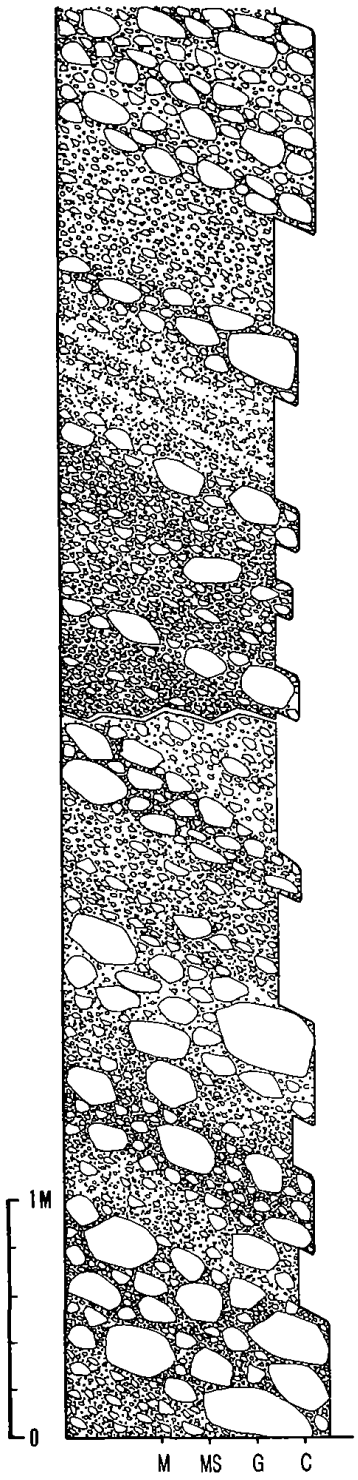

Crudely-stratified gravelstone (G2-b); matrix- or clast-supported; poorly-sorted sand matrix; clasts oriented parallel to bedding plane; partly imbricated [a(p), a(i)].

Disorganized gravelstone (G1-b); matrix-supported; poorly-sorted sand matrix; clasts oriented parallel to bedding plane; partly imbricated [a(p), a(i)].

Laterally discontinuous cobble-size gravel layer; downslope increase in bed thickness and grain size.

Crudely-stratified gravelstone (G2-b); matrix-supported; poorly-sorted sand matrix; thin sandstone layers; sharp lower and upper boundaries; clasts oriented parallel to bedding plane; partly imbricated [a(p), a(i)].

Crudely-stratified gravelstone (G2-b); laterally discontinuous large clast trains; matrix- or clast-supported; poorly-sorted sand matrix; clasts oriented parallel to bedding plane; imbricated [a(p), a(i)].

Laterally discontinuous disorganized gravelstone (G1-b); downslope decrease in bed thickness and grain size; clast- or matrix-supported; poorly-sorted sand matrix; clasts oriented parallel to bedding plane; imbricated [a(p), a(i)].

Disorganized gravelstone (G1-b); cobble- to boulder-size clasts; matrix-supported; well-sorted sand matrix; clasts oriented parallel to bedding plane; partly imbricated [a(p), a(i)].

Disorganized gravelstone (G1-b); matrix-supported; poorly-sorted sand matrix.

Disorganized gravelstone (G1-b); clast-supported; well-sorted sand matrix.

Disorganized gravelstone (G1-b); matrix-supported; poorly-sorted sand matrix.

Disorganized gravelstone (G1-b); clast-supported; well-sorted sand matrix; clasts oriented parallel to bedding plane; imbricated [a(p), a(i)].

Fig. 4-12. Columnar section and description of subsection GB-2. For location, see Fig. 4-1.

Subsection GB-3

This section occurs approximately 50 m southeast of subsection GB-2 (Fig. 4-1). This section stratigraphically overlies subsection GB-2 with a general trend of N4°W/12°NE (Fig. 4-10). The sequence is represented by thick homogeneous muddy sandstone (Facies M1-b) which contains thin, laterally discontinuous sandstone and lignite layers (Fig. 4-13). Parts of the muddy sandstone units are cemented with calcite (Fig. 4-13, arrow 1). In the middle part of the sequence, a thick graded gravelstone unit (Facies G4) is intercalated (Fig. 4-13, arrow 2). The lower boundary of the gravelstone unit is sharp and erosional; some outsized gravels are loaded into the underlying muddy sandstone. The upper boundary is generally sharp and planar. The grading is represented by an upward decrease in size and content of gravels (coarse-tail and distribution grading). Clasts are either matrix- or clast-supported with muddy sand matrix. Elongated clasts are aligned parallel to bedding plane; some are imbricated [a(p), a(i)].

Subsection GB-4

This section occurs approximately 50 m east of subsection GB-2 (Fig. 4-1). Stratigraphically, this section overlies subsections GB-2 and -3, occurring in topographically high areas (Fig. 4-10). The sequence is represented by thick homogeneous muddy sandstone (Facies M1-b). It varies in color from olive

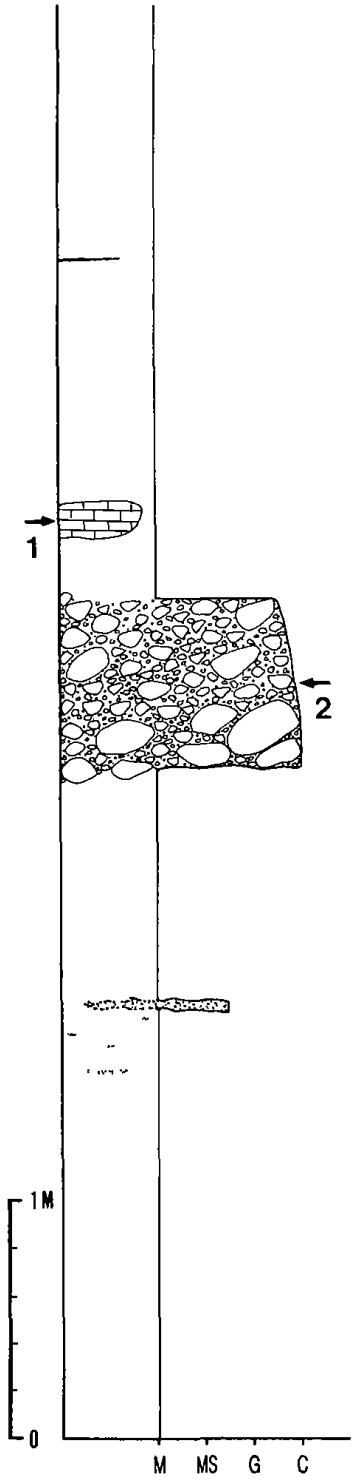

Thick, homogeneous muddy sandstone (M1-b); laterally discontinuous lignite laminae; partly cemented with calcite.

Graded gravelstone (G4); clast- or matrix-supported; poorly-sorted muddy sand matrix; clasts oriented parallel to bedding plane; imbricated [a(p), a(i)]; sharp, erosional lower and sharp, planar upper boundaries.

Thick, homogeneous muddy sandstone (M1-b).

Thin, laterally discontinuous massive sandstone (S1-b); diffuse lower and upper boundaries.

Thick, homogeneous muddy sandstone (M1-b).

Fig. 4-13. Columnar section and description of subsection GB-3. Arrowed features are described in the text. For location, see Fig. 4-1.

gray (5Y 3/2) to light yellowish gray (5Y 7/2) according to organic content.

4.3. Maebong Section (MB)

This section occurs along the gully which runs from the northern part of the Maebong mountain pass to the main valley which runs to the Kukurim village (Fig. 4-1). In the western boundary, the Miocene sedimentary sequence is overlain by volcanic rock (Eocene), representing a thrust-bounded basin margin (Fig. 4-14). Part of the sequence is bounded by left-lateral strike-slip fault system (Fig. 4-14). In this section, three subsections were measured. The sequence represents deposition in slope apron environment of Malgol system (subsections MB-1 and -2) and Gilbert-type foreset environment of the Doumsan system (subsections MB-2 and -3) (Fig. 4-14).

Subsection MB-1

This section occurs in the upper part of the gully, about 500 m north of the Maebong mountain pass and 1 km northwest of the Kukurim village (Fig. 4-1). Approximately 20 m west of the outcrop lies volcanic basement rock (Eocene), which overlies the Miocene sedimentary rock, representing a thrust-bounded basin margin (Fig. 4-14). The sequence is represented by thick, dark gray homogeneous muddy sandstone (Facies M1-b) with an outsized gravel (Fig. 4-15). The gravel clast is angular and is composed of volcanic rock

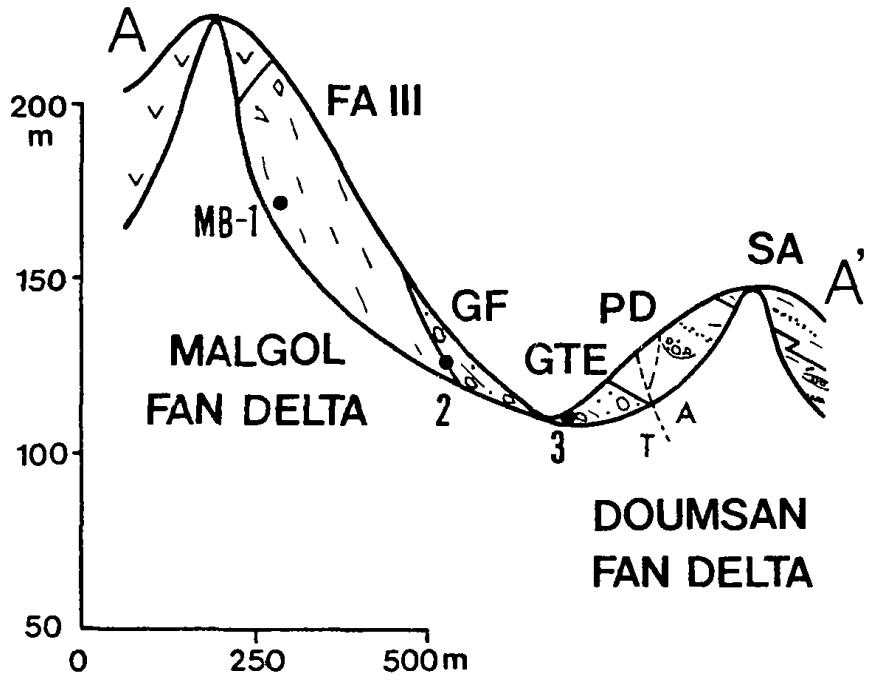

Fig. 4-14. Simplified cross-section of the Maebong section (MB). Note stratigraphic positions of measured sections. For location, see Fig. 4-1.

(Eocene), similar to the basement rock. The muddy sandstone also contains abundant lignite fragments and plant debris. The sequence is steeply inclined with a general trend of N40°E/24°SE.

Subsection MB-2

This section occurs along the gully approximately 100 m southeast of subsection MB-1 (Fig. 4-1). This section stratigraphically overlies subsection MB-1 with a general trend of N60°E/30°SE (Fig. 4-14). The lower part of the sequence is represented by thick homogeneous muddy sandstone (Facies M1-b) in which thin layers of lignite fragments are present (Fig. 4-16). It is

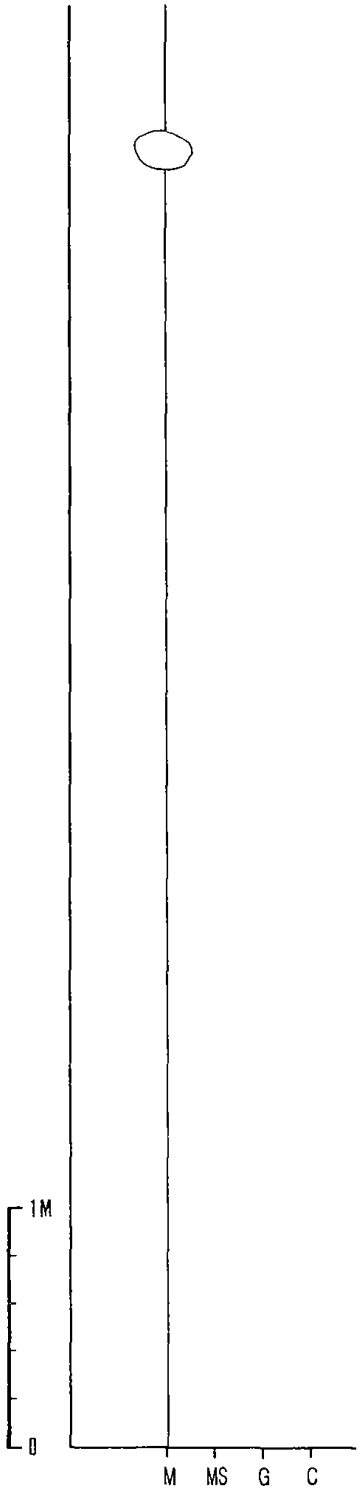

Thick, homogeneous muddy sandstone (M1-b); laterally discontinuous lignite laminae; outsized gravels.

Fig. 4-15. Columnar section and description of subsection MB-1. For location, see Fig. 4-1.

overlain by alternating units of disorganized gravelstone (Facies G1-a) and crudely-stratified gravelstone (Facies G2-b) (Fig. 4-16). Here, gravel clasts are generally subrounded to rounded and are largely composed of sedimentary rocks (Cretaceous) (58%), volcanic rocks (Eocene) (25%) and granitic rocks (Eocene) (17%), largely similar to those of the Doumsan fan-delta system (see Chapter 5). Flute casts in the lower part of the gravelstone unit suggest southeastward (120°) paleocurrent direction. Sedimentary facies and clast composition as well as paleocurrent direction suggest that the overlying gravelstone units are part of the Gilbert-type foreset sequences of the Doumsan fan-delta system.

Subsection MB-3

This section occurs approximately 50 m northeast of subsection MB-1, along the valley which runs from the Doumsan mountain to the Kukurim village (Fig. 4-1). This section stratigraphically overlies subsection MB-2 with a general trend of N50°E/24°SE (Fig. 4-14). The sequence is represented by steeply-inclined (> 20°) beds of disorganized gravelstone (Facies G1-b), crudely-stratified gravelstone (Facies G2-b) and stratified gravelstone (Facies G3) (Fig. 4-17). The clasts are generally subrounded to rounded and are largely composed of sedimentary rocks (Cretaceous) (58%), volcanic rocks (Eocene) (25%) and granitic rocks (Eocene) (17%) which are largely similar

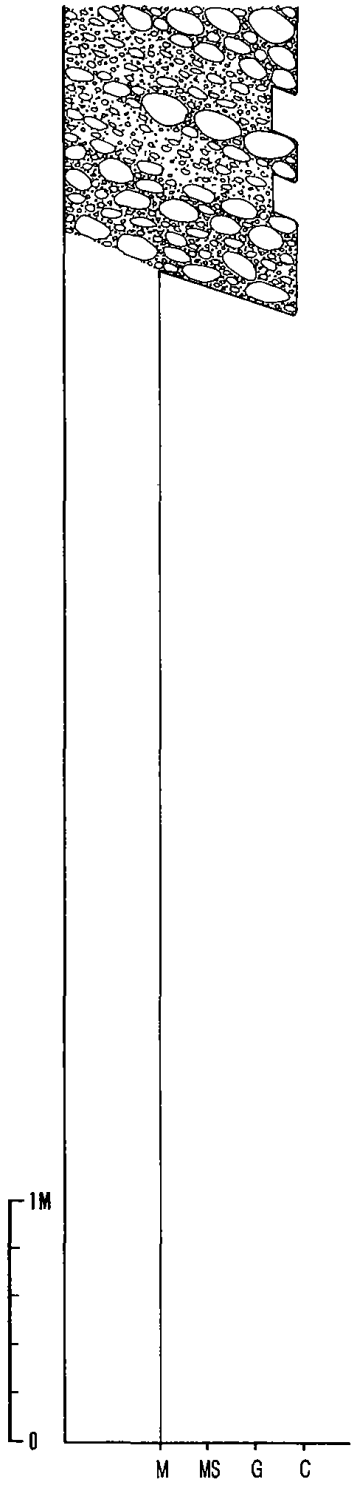

Crudely-stratified gravelstone (Gl-b); laterally discontinuous large clast trains; clast- or matrix-supported; sand matrix; clasts oriented parallel to bedding plane; imbricated [a(p), a(i)]; diffuse lower and upper boundaries.

Disorganized gravelstone (Gl-b); clast- or matrix-supported; sand matrix; clasts oriented parallel to bedding plane; imbricated [a(p), a(i)]; sharp erosional lower boundary; flute casts suggest southeastward (120°) paleocurrent direction; diffuse upper boundary.

Thick, homogeneous muddy sandstone (Ml-b).

Fig. 4-16. Columnar section and description of subsection MB-2. For location, see Fig. 4-1.

to those of the Doumsan fan-delta system.

In this unit, some outsized boulders (upto 1 m in long diameter) are partly intercalated (Fig. 4-17, arrows). The outsized boulders are composed of volcanic rocks (Eocene), largely similar to the basement rock approximately 150 m east of the outcrop. These gravels are absent in the northeastern part of the valley, forming the major foreset units of the Doumsan fan-delta system. The clast composition and their distributional pattern indicate that the outsized gravels originated from the east, a sediment source for the Malgol fan-delta system.

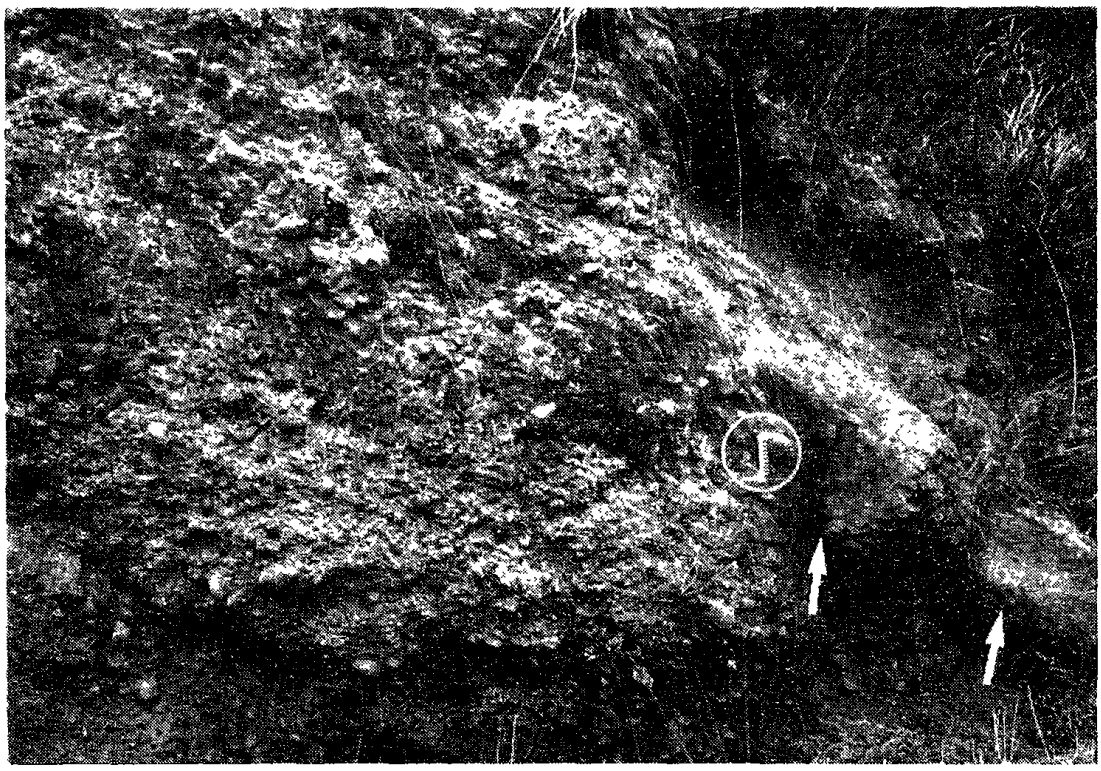

Fig. 4-17. Photograph of subsection MB-3. Note outsized boulders (arrows) For location, see Fig. 4-1. Scale arrow is 20 cm long.

4.4. Daljun Reservoir Section (DR)

This section occurs along the roadcut in the eastern part of the Daljun Reservoir (Fig. 4-1). Southern part of this section lies a volcanic rock (Eocene) which was intruded by Miocene basalt (21.8 Ma; Jin et al., 1989). The Yeonil Group sequence unconformably overlies the Miocene basalt basement (Fig. 4-18). In this section, three subsections (about 20 m thick) were measured. These sections represent deposition in submarine scree apron (subsections DR-1 and DR-2) and basin plain (subsection DR-3) environments.

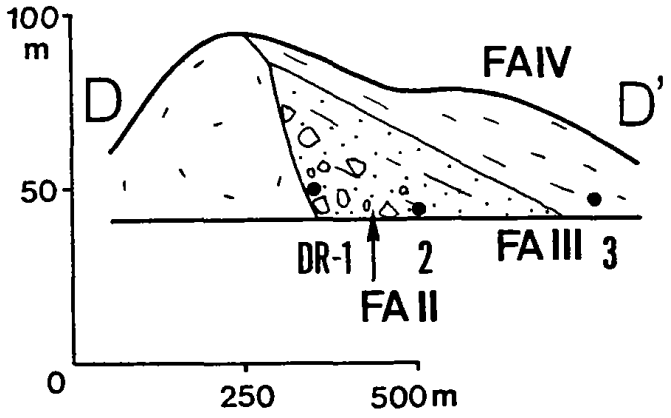

Fig. 4-18. Simplified cross-section of the Daljun Reservoir section (DR). Note stratigraphic positions of measured sections. For location, see Fig. 4-1.

Subsection DR-1

This section occurs approximately 300 m northeast of Gwangbang village, about 150 m north of Daljun Reservoir (Fig. 4-1). The lower right part of the exposure is represented by weathered basalt basement showing columnar joints (Fig. 4-19, arrow 1). It is unconformably overlain by disorganized

gravelstone (Facies G1-b) and crudely-stratified gravelstone (Facies G2-b) (Fig. 4-19, arrow 2). The clasts range in size from cobble to boulder, in which most clasts are composed of basalt (Miocene) (100%), similar to the directly underlying basement rock. The clasts are either matrix- or clast-supported with poorly-sorted sand matrix. The sand matrix is represented by rock fragments of basalt. In the upper part of the gravelstone unit, a homogeneous muddy sandstone unit (Facies M1-b) is partly intercalated (Fig. 4-19, arrow 3). It is overlain by massive sandstone (Facies S1-b) which contains pockets of cobble-size gravels (Fig. 4-19, arrow 4).

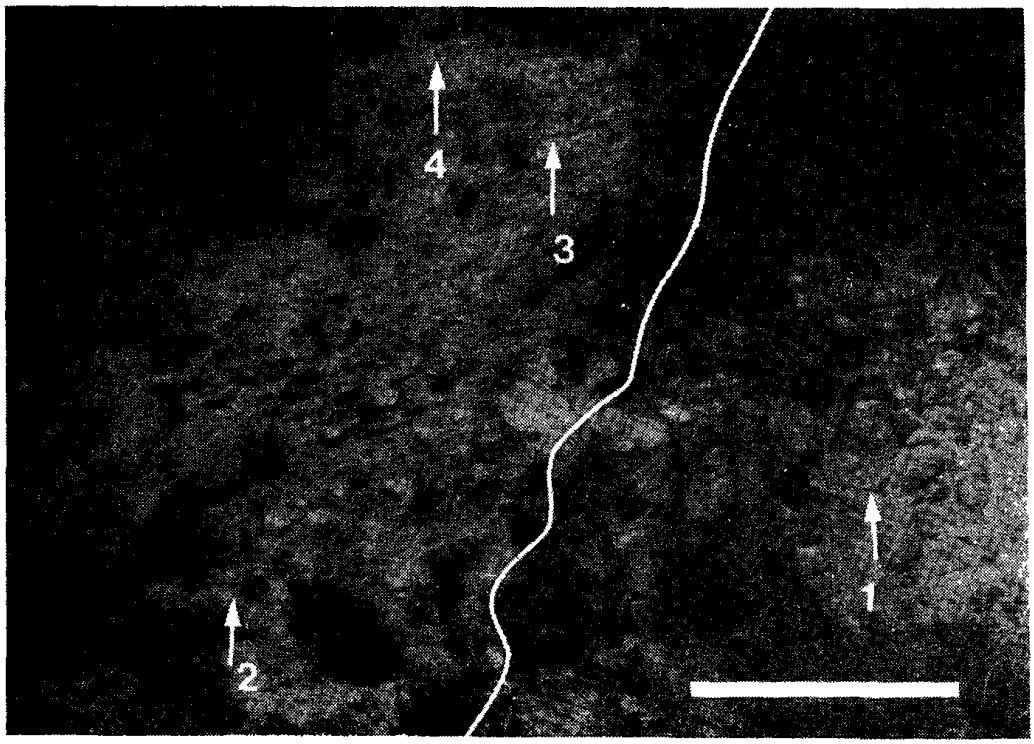

Fig. 4-19. Photograph of subsection DR-1. Note a sequence boundary between Miocene basalt and Yeonil Group sequence. Arrowed features are described in the text. For location, see Fig. 4-1. Scale bar is 2 m long.

Subsection DR-2

This section occurs along the roadcut approximately 80 m north of subsection DR-2 (Fig. 4-1). This section stratigraphically overlies subsection DR-1 (Fig. 4-18). The lower part of the sequence is represented by disorganized gravelstone (Facies G1-b) in which cobble- to boulder-size gravels are either clast- or matrix-supported with poorly-sorted sand matrix (Fig. 4-20). The clasts are angular to rounded and are mostly composed of basalt fragment (Miocene) (100%). The matrix is also represented by rock fragments of basalt. The gravelstone units are overlain by thick massive sandstone (Facies S1-b). In this unit, pockets of cobble- to boulder-size clasts are abundant (Fig. 4-20). The gravel pockets show vertical decrease in number and grain size (Fig. 4-20). In the upper part, thin (< 1 cm), laterally discontinuous homogeneous muddy sandstone (Facies M1-b) layers are partly intercalated (Fig. 4-20).

Subsection DR-3

This section occurs approximately 50 m north of subsection DR-2 (Fig. 4-1) and stratigraphically overlies subsection DR-2 (Fig. 4-18). The sequence is represented by thick, light yellowish gray, homogeneous sandy mudstone (Facies M1-b), similar to the subsection GB-4. In this unit, lignite fragments and plant debris are abundant.

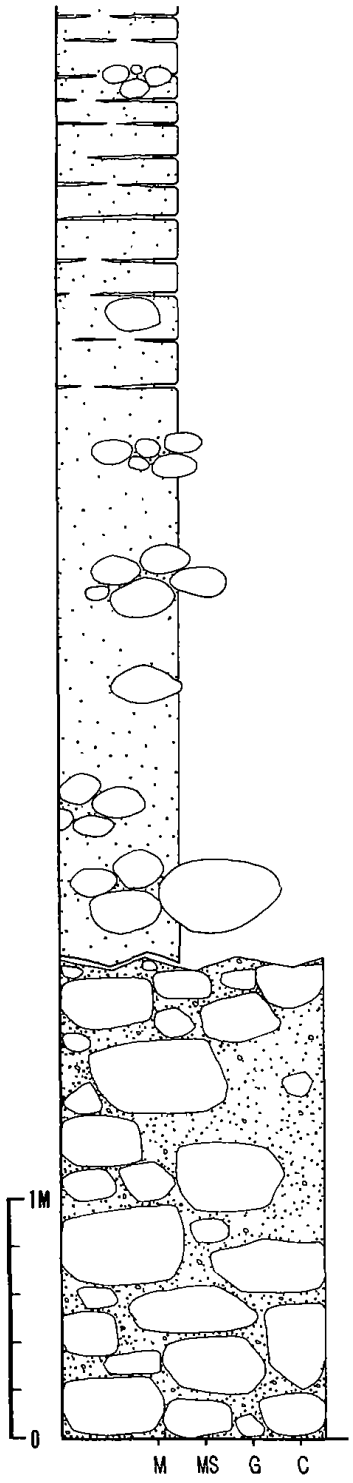

Massive sandstones (S1-b); thin, laterally discontinuous muddy sandstone layers; gravel pockets; subrounded to rounded basalt clasts.

Thick, amalgamated units of massive sandstone (S1-b); gravel pockets; subrounded to rounded basalt clasts.

Thick, disorganized gravelstone (G1-b); angular to subangular basalt clasts; matrix- or clast-supported; poorly-sorted sand matrix; clasts oriented parallel to bedding plane.

Fig. 4-20. Columnar section and description of subsection DR-2. For location, see Fig. 4-1.

5. DESCRIPTIONS AND INTERPRETATIONS OF SEDIMENTARY FACIES

The Malgol fan-delta system is largely composed of gravelstone and muddy sandstone units with thin layers of sandstone. Based on detailed measurements (1:20 scale) of outcrop sections, 15 major sedimentary facies are established (Fig. 5-1, Table 5-1). The classification scheme is based on a two-tier system of grain size and sedimentary structures, supplemented by grain fabric. Descriptions and interpretations of individual sedimentary facies are given in the following section.

5.1. Class B : Breccia

The breccia comprises angular to subangular rock fragments that are cemented with poorly-sorted, brownish muddy sand matrix. Clasts range in size from granule to outsized boulders (up to 1 m long in long diameter). They are largely composed of felsite (Eocene) (approximately 65%), sedimentary rocks (Cretaceous) (25%) with small amounts of volcanic rocks (Eocene) and granitic rocks (Eocene) (approximately 10%), with local variations depending on the basement rock. Some sections show bed-by-bed variations in clast composition.

Facies B1-a: Disorganized Breccia (clast-supported)

Description

This facies is characterized by a clast-supported fabric albeit with a brownish muddy sand matrix (Fig. 5-1, Table 5-1). Clasts range in size from

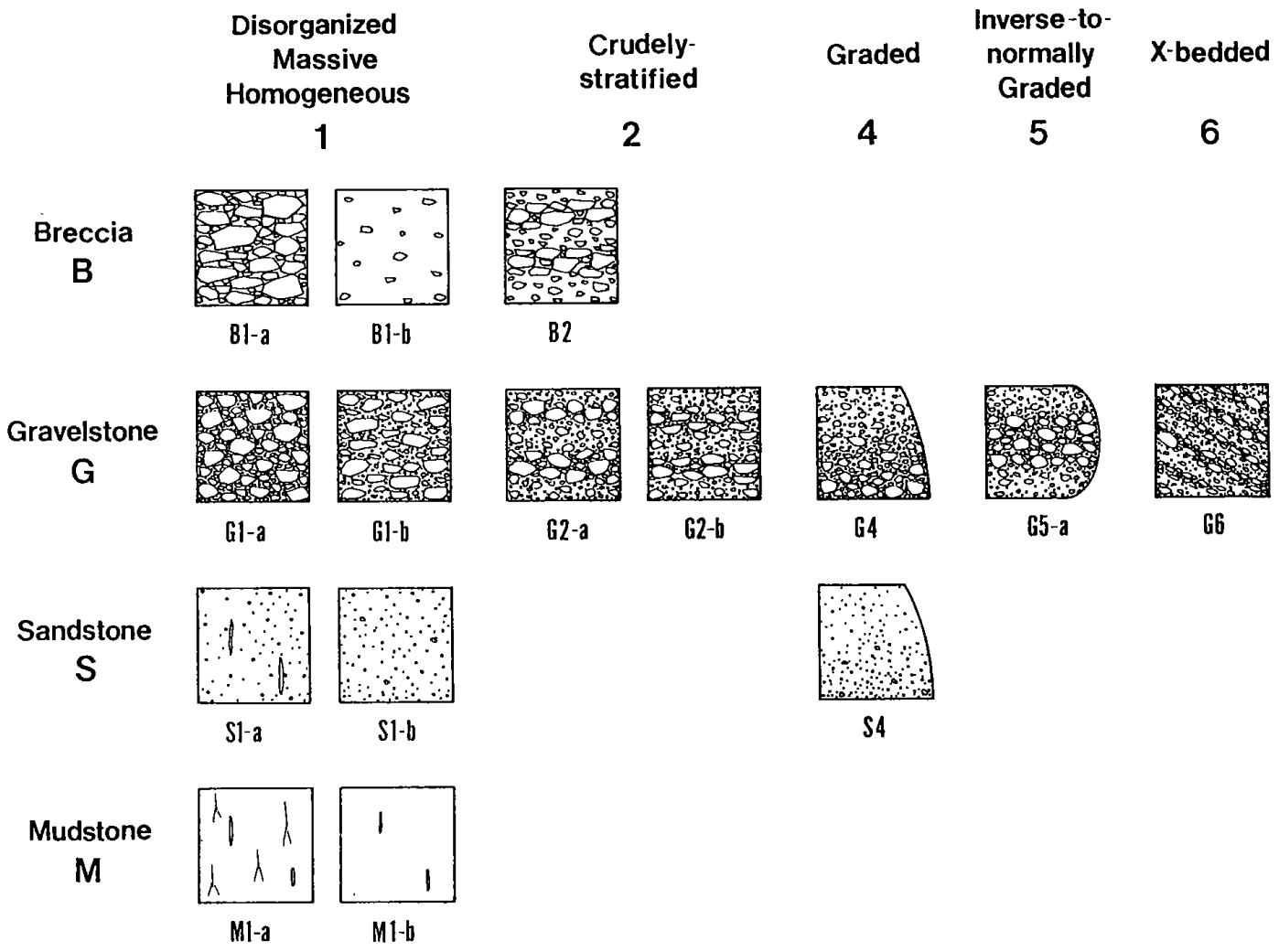

Fig. 5-1. Facies classification scheme and symbolic summary of the Malgol fan-delta sequence

Table 5-1. Description and inferred depositional processes of sedimentary facies in the Malgol fan-delta sequence.

Facies Type	Description	Occurrence	Interpretation
Disorganized Breccia (clast-supported) (Bl-a)	One or two clasts to several meters thick; poorly-sorted; angular to subangular granule- to boulder-size clasts; [a(p) a(i)] imbricated; partly crudely stratified; poorly-sorted sandy mud matrix; brownish; non-channellized, sheet-like geometry.	MG-1	Turbulent subaerial debris flow (Pierson 1981; Nemec & Steel 1984; Shultz 1984) or sheetflood (Bull 1972)
Disorganized Breccia (matrix-supported) (Bl-b)	Generally thin (< 50 cm); poorly-sorted; angular to subangular granule- to pebble-size clasts; random orientation; partly crudely stratified; poorly-sorted muddy sand matrix; brownish; plant debris	MG-1	Slurry subaerial debris flow or mud flow (Shultz 1984)
Crudely-stratified Breccia (B2)	Variable in thickness (30 - 100 cm); poorly-sorted; angular to subangular granule- to boulder size clasts; [a(p) a(i)] imbricated; poorly-sorted muddy sand matrix; brownish; partly cross-bedded.	MG-1	Turbulent subaerial debris flow (Pierson 1981; Nemec & Steel 1984; Shultz 1984; Blair 1987), sheetflood (Bull 1972) or traction in braided stream (Miall 1977)
Disorganized Gravelstone [a(t) b(i)] (Gl-a)	Variable in thickness (10 cm to several meters); poorly-sorted; subangular granule- to boulder-size clasts; [a(t) b(i)] imbricated; partly crudely stratified; poorly sorted sand matrix.	MG-1, GB-1	Traction in braided stream (Smith 1970, 1972; Rust 1972, 1977; Gustavson 1984; Miall 1977, 1978)
Disorganized Gravelstone [a(p) a(i)] (Gl-b)	Variable in thickness (20 - 100 cm); poorly-sorted; angular to subangular granule- to boulder size clasts; [a(p) a(i)] imbricated; poorly-sorted sand matrix; partly crudely stratified; thin layers of inversely-graded gravelly sandstone and sandstone.	MG-2, MG-3, MG 4, MG 5, GB-2, DR-1, DR-2	Cohesionless debris flow or density-modified grain flow (Curry 1966; Winn & Dott 1977; Lowe 1979; Postma 1986; Nemec 1990), debris fall or grain fall (Nemec 1990), or high-density turbidity current (e.g. Lowe 1982)
Crudely-stratified Gravelstone [a(t) b(i)] (G2-a)	Generally thick (upto 50 cm); random, partly [a(t) b(i)] imbricated; subangular granule- to boulder-size clasts; clast- or matrix-supported; partly openwork; sand matrix; alternation of thin units of gravelstone gravelly sandstone and sandstone with sharp or diffuse layer boundaries.	MG-1, GB-1	Multiple deposition and erosion of tractional flows (Collinson 1970; Smith 1974; Fraser & Cobb 1982); aggradation on a longitudinal bar during high flow stage (Smith 1970, 1974; Rust 1972; Gustavson 1974; Miall 1977, 1978)
Crudely-stratified Gravelstone [a(p) a(i)] (G2-b)	Generally thick (upto 50 cm); [a(p) a(i)] imbricated; angular to subangular granule- to boulder-size clasts; clast- or matrix-supported; poorly-sorted sand matrix; laterally discontinuous large clast-trains; partly graded and inversely graded gravelstone, gravelly sandstone and sandstone layers.	MG-2, MG-3, GB-2, DR-1, DR-2	Cohesionless debris flow or density-modified grain flow (e.g. Nemec 1990), debris fall or grain fall (e.g. Nemec 1990), or amalgamated units of high-density turbidity currents (e.g. Lowe 1982)

Table 5-1 (continued)

Facies Type	Description	Occurrence	Interpretation
Graded Gravelstone (G4)	Generally thin (< 50 cm); angular to subangular granule- to cobble-size clasts; matrix- or clast-supported; poorly-sorted sand matrix; [a(p) a(i)] imbricated; sharp, erosional lower boundary; commonly overlain by graded sandstone with diffuse facies boundary.	MG-4, MG-5, GB-3	Gravelly high-density turbidity current (Lowe 1982; Surlyk 1984; Postma 1986, 1988)
Inverse-to-normally Graded gravelstone (G5-a)	Generally thin (< 50 cm); angular to subangular granule- to cobble-size clasts; matrix- or clast-supported; poorly-sorted sand matrix; [a(p) a(i)] imbricated;	MG-4	Cohesionless debris flow (Curry 1966; Winn & Dott 1977; Lowe 1982; Nemec & Steel 1984)
Cross-bedded Gravelstone (G6)	Generally thin (< 50 cm); subangular granule- to pebble-size clasts; normally or inversely graded foreset laminae, partly openwork; planar or trough cross-bed; commonly amalgamated with facies G1-a.	MG-1	Migrating gravel bars and secondary channel fills (Miall 1977, 1978; Rust 1978)
Massive Sandstone (partly bioturbated) (S1-a)	Variable in thickness (20 cm to 1 m); poorly- to well-sorted fine to coarse sand; gravel pockets and trains; lignite fragments, partly bioturbated, commonly overlain by Facies G1-a and G2-a, diffuse unit boundary.	GB-1	Tractional processes; slow or rapid suspension fall out (Martinsen 1990)
Massive Sandstone (partly graded) (S1-b)	Generally thin (< 30 cm), poorly-sorted fine to coarse sand; widely dispersed granule-size gravels; grading in basal or topmost parts; sharp erosional lower boundary; *loading and pseudonodules*, diffuse upper boundary; flame structures.	MG-4, MG-5, GB-3, DR-1, DR-2	High- or low-density turbidity current (Bouma 1962; Middleton & Hampton 1976, Lowe 1982)
Graded Sandstone (S4)	Generally th[illegible] (< 20 cm); poorly-sorted fine to coarse sand; widely dispersed granule-size gravels; sharp, erosion[illegible] lower boundary; loading and pseudonodules; diffuse upper boundary, flame structures.	MG-4, MG-5	High- or low-density turbidity current (Bouma 1962; Middleton & Hampton 1976; Lowe 1982)
Homogeneous Muddy Sandstone (partly bioturbated) (M1-a)	Generally thin (< 50 cm); gravel pockets and trains; plant debris and lignite fragments; burrows, rootlets; brownish to dark gray according to organic content; commonly scoured by G1-a, G2-a and G6.	MG-1, GB-1	Suspension settling on floodplain or inter-channel areas
Homogeneous Muddy Sandstone (microfossils) (M1-b)	Thin to very thick (few cm to several tens of meters); *random distribution of clastic grain and biogenic* remains (distoms and foraminifers etc.); laterally discontinuous sandstone layers; partly cemented with calcite (up to 3 m long in long diameter).	MG-4, MG-5, GB-3, GB-4, MB-1, MB-2, DR-1, DR-2, DR-3	Hemipelagic settling (Pickering et al, 1986)

granule to boulder (more than 1 m in long diameter). Elongated clasts are aligned parallel to bedding plane. Each unit is laterally continuous and ranges in thickness from three or four clasts to several meters. Some units are partly inversely graded. This unit alternates with the matrix-supported disorganized breccia (Facies B1-b). Some units laterally grade into crudely-stratified breccia (Facies B2). It occurs in sections of MG-1, which form the lowermost part of the Chunbuk Formation (Fig. 4-1).

Interpretation

Although this facies is clast-supported, the abundant mud content indicates that cohesive strength played an important role. Orientation of clasts that are parallel to bedding plane indicates that clast collision occurred during transport. In addition, the partly inversely graded units are suggestive of dispersive pressure resulted from clast collision (Bagnold, 1954). These characters collectively suggest that this facies was deposited by highly turbulent fluidal debris flows in which the cohesive strength of mud matrix, clast collision and fluid turbulence played important roles during transport (e.g. Pierson, 1981; Nemec & Steel, 1984; Shultz, 1984). It is similar to the Facies Dcm (massive, clast-supported diamictite) of Shultz (1984) deposited by pseudoplastic debris flow.

Facies B1-b: Disorganized Breccia (matrix-supported)

Description

This facies shows a disorganized, matrix-supported fabric (Fig. 5-1). The

clasts comprise granule- to pebble-size breccias with small amounts of cobble- to boulder-size breccias. The clasts are widely dispersed in brownish mud matrix and show random orientation. Some units are inversely graded. Each unit is laterally continuous and ranges in thickness from a few centimeters to several meters. This facies is interlayered with disorganized, clast-supported breccias (Facies B1-a); some units are scoured by the latter.

Interpretation

The matrix-supported disorganized breccia is interpreted as subaerial debris flow deposit based on poor-sorting, randomly oriented clasts and brownish mud matrix. In this facies, abundant mud content suggests that cohesive strength was dominant, whereas dispersive pressure and fluid turbulence played less important role. The lack of grading as well as non-erosional lower bounding surface also suggest deposition from slurry debris flows (mudflows). Random clast orientation is commonly developed where the sediment contains abundant mud matrix (e.g. Cook, 1979) suggesting that clast collision was limited during flow (Lewis et al., 1980; Gravenor, 1986). Alternatively, random orientation may also reflect either short transport (e.g. Lindsay, 1968), non-sheared (high strength) plug flow or only weakly sheared (high viscosity) flow (Lewis et al., 1980; Nemec & Steel, 1984).

Facies B2: Crudely-stratified Breccia

Description

The disorganized clast-supported breccia (Facies B1-a) laterally grades

into crudely-stratified breccia (Facies B2). The stratification is characterized by alternation of laterally discontinuous, thin units of both clast- and matrix-supported breccias with diffuse lower and upper boundaries (Fig. 5-1). Trains of large clasts and elongated large clasts that are oriented parallel to bedding plane also show crude stratification (Fig. 5-1). The clasts range in size from granule- to cobble-size breccias with small amounts of boulder-size breccias. Some units are partly cross-bedded.

Interpretation

In this facies, relatively small amounts of mud matrix suggest limited influence of cohesive strength. The crude stratification and partly cross-bedded nature suggest that the breccia clasts were transported as bed load. However, the poorly-sorted nature and relatively less well organized fabric than that of the common fluidal flow deposits suggest that the breccias were transported by hyperconcentrated flows (Smith, 1986; Costa, 1988). According to Costa (1988), the hyperconcentrated flows have intermediate sediment concentration between the debris flow and common fluidal flow (or water flood), in which viscous drag of the sediment laden water plays an important role in transporting the coarse-grained sediment as a bed load. In this flow, the sediment and water mixture results in higher shear strength than that of the water flood (Costa, 1988). Buoyancy of the sediment-water mixture and dispersive pressure resulted from clast collision as well as fluid turbulence may also play important roles (Costa, 1988).

5.2. Class G: Gravelstone

The gravelstone class can be subdivided into two types based on clast and matrix compositions as well as the shape of clasts. The first type is largely composed of sedimentary (Cretaceous) rock (approximately 65 %) and felsite (Eocene) (approximately 25 %) with small amounts of granitic (Eocene) and volcanic (Eocene) rocks which commonly show local variations, depending on the underlying basement rocks. These gravels are generally subangular to subrounded and are either clast- or matrix-supported with poorly-sorted, brownish sand matrix, forming disorganized gravelstone (Facies G1-a), crudely-stratified gravelstone (Facies G2-a) and cross-bedded gravelstone (Facies G6). The second type is largely composed of felsite (Eocene) (> 50 %) and sedimentary (Cretaceous) rocks (approximately 30 %) which also show local variation in clast composition. Clasts are generally angular to subangular and are either clast- or matrix-supported with pale greenish yellow sand matrix. These units are represented by steeply-inclined beds of disorganized gravelstone (Facies G1-b), crudely-stratified gravelstone (Facies G2-b), graded gravelstone (Facies G4) and inverse-to-normally graded gravelstone (Facies G5-a).

Facies G1-a: Disorganized Gravelstone [a(t), b(i)]

Description

This facies has a clast-supported and partly openwork fabric with poorly- to well-sorted sand matrix (Fig. 5-1, Table 5-1). Clasts range in size from granule to cobble with occasional outsized boulders. Most clasts show

random orientation; some are oriented transverse to the flow direction [a(t), b(i)]. Trains of large clasts show crude-stratification. Individual facies unit is generally thick (> 1 m) and is commonly interbedded with crudely-stratified gravelstone (Facies G2-a) and cross-bedded gravelstone (Facies G6). The lower boundary is generally sharp and erosional, whereas the upper boundary is diffuse. This facies unit commonly occurs in subsections of MG-1 and GB-1.

Interpretation

The clast orientation and imbrication [a(t), b(i)] as well as the partly openwork fabric collectively suggest that the gravels were transported as bedload (Harms et al., 1975; Harms et al., 1982). The mechanics of gravel bedload transport and the origin of the disorganized gravelstone are still less well understood. Smith (1970, 1972), Rust (1972) and Gustavson (1974) pointed out that migrating longitudinal bars would tend to form poorly defined horizontal beds, possibly indicating transportation in planar sheets under high-flow energy. This facies is similar to the massive or crudely stratified gravelstone (Facies Gm) of Miall (1977, 1978) and Rust (1978).

Facies G1-b: Disorganized Gravelstone [a(p), a(i)]

Description

This facies is characterized by disorganized gravelstone in which the clasts are commonly oriented parallel to the local slope; some are imbricated [a(p), a(i)] (Fig. 5-1). Clasts range in size from granule to boulder and are either

clast- or matrix-supported in poorly- to well-sorted sand matrix with clay content less than 1 %. Each unit ranges in thickness from three or four clasts to several meters. This facies is interlayered with crudely-stratified gravelstone (Facies G2-b) and graded gravelstone (Facies G4) with diffuse lower and upper boundaries. This facies occurs in subsections of MG-2, -3, -4, -5, GB-2, DR-1, -2, probably deposited in submarine scree apron and slope apron environments (Fig. 4-1).

Interpretation

In this facies, the lack of clay suggests cohesionless flow. The relatively high content of clast reflects that dispersive pressure played an important role in maintaining the clasts in a dispersed state. Furthermore, the relatively well developed clast orientation indicates that grain collisions were important during the last stage of flow (Allen, 1982, Gravenor, 1986). This facies is similar to the density-modified grain flow deposits of Middleton & Hampton (1976) and Lowe (1982). It is also similar to deposits of cohesionless debris flow transitional to density-modified grain flow (Facies 4, non-graded, clast-supported, imbricated facies) of Surlyk (1984), and cohesionless debris flow deposits of Postma (1986) and Nemec (1990b).

Facies G2-a: Crudely-stratified Gravelstone [a(t), b(i)]

Description

This facies is characterized by laterally discontinuous disorganized gravel bands, trains and stringers as well as thin, laterally discontinuous sandstone

(Fig. 5-1, Table 5-1). Most clasts are randomly oriented; some elongate clasts are oriented transverse to the flow direction [a(t), b(i)]. The gravel unit has a clast-supported and partly openwork fabric with diffuse lower and upper boundaries. Intercalated sandstone layers gradually overlie the gravelstone units which are, in turn, scoured by the overlying gravelstone bands with sharp erosional upper boundary. The matrix is largely composed of poorly- to well-sorted sands with clay content less than 1 %. Individual facies unit is generally thick (> 1 m). Some units are low-angle cross-bedded. This facies unit is interlayered with disorganized gravelstone (Facies G1-a) and cross-bedded gravelstone (Facies G6) with diffuse lower and upper boundaries. This facies commonly occurs in sections of MG-1 and GB-1 (Fig. 4-1).

Interpretation

The clast orientation, imbrication [a(t), b(i)] and the partly openwork fabric collectively suggest that the gravels were transported as bedload (Harms et al., 1975; Harms et al., 1982). Vague stratification with erosional lower boundary and changes in grain size and sorting reflect variable discharge rate and discontinuous deposition. Insignificant variation in flow velocity also result in the deposition of gravelstone and sandstone, as there is little differences in velocity between the flows suspending sand grains and the flows transporting gravels as bed load (Walker, 1975). Smith (1970, 1972), Rust (1972) and Gustavson (1974) pointed out that migrating gravel bars tend to form poorly-defined horizontal beds possibly indicating transportation in planar sheets under high-flow energy. Because the longitudinal bar is of low

amplitude, avalanching in the slip face is rare and large clasts that lie oblique to the bedding planes are common (Miall, 1977, 1978). In this facies, the sharp erosional boundary in the upper part of the intercalated sandstone unit suggests multiple erosion and deposition induced by fluctuation in water discharge rate (e.g. Collinson, 1970; Smith 1974; Smith & Ashley, 1985). This facies is similar to the massive or crudely-stratified gravelstone (Facies Gm) of Miall (1977, 1978) and Rust (1978), deposited either on longitudinal bars or as channel lags.

Facies G2-b: Crudely-stratified Gravelstone [a(p), a(i)]

Description

This facies is characterized by crudely-stratified gravelstone which occurs in steeply-inclined beds (> 20°) (subsections MG-2, -3, GB-2, DR-1, -2) (Fig. 5-1, Table 5-1). The stratification is represented by laterally discontinuous, large-clast trains with diffuse lower and upper boundaries. Clasts range in size from granule to boulder, and are either clast- or matrix-supported in poorly- to well-sorted sand matrix with clay content less than 1 %. Some units show partly openwork fabric. Most clasts are aligned parallel to the local slope; some are imbricated [a(p), a(i)]. This facies alternates with the disorganized gravelstone (Facies G1-b) and graded gravelstone (Facies G4) with diffuse lower and upper boundaries.

Interpretation

In this facies, the well developed clast orientation and the abundant clast

content suggest that clast collision played an important role, whereas the cohesive strength was less important, probably indicating deposition either by cohesionless debris flows or density-modified grain flows (Curry, 1966; Middleton & Hampton, 1976; Winn & Dott, 1977; Lowe, 1979; Postma, 1986; Nemec, 1990b). Their occurrence on steeply-inclined slope suggests that the flows were triggered by avalanching of gravels and sands, which transformed into various sediment gravity flows such as debris fall (or grain flow) or cohesionless debris flows (or density-modified grain flows) (Nemec, 1990b). This facies is also similar to the gravity slide or flow slide deposit (Colella et al., 1987; Postma, 1986).

Facies G4: Graded Gravelstone

Description

The facies G4 is represented by normally graded gravelstone in which the grading is represented by an upward decrease in both concentration and size of clasts and matrix (Fig. 5-1, Table 5-1). Clasts are either matrix- or clast-supported in poorly- to well-sorted sand matrix with clay contents less than 1 %. Each facies unit ranges in thickness from a few tens of centimeters to several meters. Sometimes the facies unit is wedged or laterally grades into a sandstone unit. This facies occurs in subsections of MG-4, -5, and GB-3.

Interpretation

Various depositional mechanisms have been suggested for graded gravelstones with sand matrix: gravelly high-density turbidity currents of Walker &

Mutti (1973), Aalto (1976), Walker (1978), Lowe (1982), Massari (1984), Surlyk (1984), Postma et al. (1988) and Ineson (1989); density-modified grain flows of Middleton & Hampton (1976), Lowe (1979); and cohesionless debris flows of Curry (1966), Winn & Dott (1977), Lowe (1982) and Postma (1986). This facies can be attributed to deposits of gravelly high-density turbidity currents based on the sharp, erosional lower boundary and rip-up mud clasts.

Facies G5-a: Inversely or Inverse-to-normally Graded Gravelstone

Description

The facies G5-a is represented by inversely or inverse-to-normally graded gravelstones in which the inverse grading is represented by large clasts that occur in the middle and upper parts of the bed (Fig. 5-1). Most clasts are clast-supported. Elongated clasts are aligned parallel to bedding plane; some are imbricated [a(p), a(i)]. The matrix is composed of poorly- to well-sorted sands with clay content less than 1 %. The facies unit ranges in thickness from 30 cm to 1 m. This facies is commonly encased in homogeneous muddy sandstone (Facies M1-b). It occurs in subsections of MG-4 (Fig. 4-1).

Interpretation

The facies G5-a is interpreted as density-modified grain flow or cohesionless debris flow deposits based on the inversely graded nature and lack of mud matrix (Walker, 1975, 1977; Middleton & Hampton, 1976; Lowe, 1976a, 1976b, 1979; Mullins & van Buren, 1979; Hiscott & Middleton, 1980; Nemec, 1990b). Inverse grading can be formed either by dispersive pressure that

resulted from clast collision (Bagnold, 1954; Carter, 1975; Lowe, 1976a, 1976b) or kinetic sieving effect in which smaller grains percolate through the interstices between the large grains (Middleton, 1970; Scott & Bridgwater, 1975; Savage & Lun, 1988). In this facies, the clast-supported fabric and the parallel oriented clasts suggest that clast collisions which result in dispersive pressures may have played an important role during the last stage of the flow (Bagnold, 1954, 1956; Carter, 1975; Lowe, 1976, 1982).

Facies G6: Cross-bedded Gravelstone

Description

The facies G6 includes planar, tangential and trough cross-bedded gravelstones. The foreset angle is variable (10°-35°) and the foreset laminae consist of alternating units of gravelstone, gravelly sandstone and sandstone as well as thin mudstone (Fig. 5-1). Gravel layers are commonly openwork and some are graded. The trough cross-bedded unit commonly shows scoop-shaped, lower bounding surface (channel geometry). In the lower boundary of the scour surface, clasts are slightly larger than those in the cross-bedded units (channel lag deposits). Bed thickness ranges from tens of centimeters to several meters. This facies alternates with disorganized gravelstone (Facies G1-a) and crudely-stratified gravelstone (Facies G2-a) with diffuse lower and upper boundaries. It occurs in subsections of MG-1 (Fig. 4-1).

Interpretation

This facies was most probably deposited by migration of various gravel

bars and dunes, and by small-scale secondary channel fills in a braided stream. Remnants of gravel bar geometry commonly occurs in some planar and tangential cross-bedded units, whereas channel geometry is common in trough cross-bedded gravelstone units. This facies is similar to planar cross-bedded gravelstone facies (Facies Gp) and trough cross-bedded gravelstone facies (Facies Gt) of Miall (1977, 1978) and Rust (1977).

5.3. Class S : Sandstone

The class S contains more than 70% of sands with minor amounts of gravels and muds. It is commonly pale greenish yellow in color and is largely composed of angular rock fragments of felsite (Eocene) and sedimentary rock (Cretaceous) with small amounts of quartz and feldspar grains.

Facies S1-a: Massive Sandstone (partly bioturbated)

Description

This facies is represented by massive sandstone, largely composed of fine to coarse sands (Fig. 5-1, Table 5-1). Some units contain plant debris and lignite fragments. Parts of the sandstones are cemented with calcite and contain abundant brackish- to shallow-marine-type mollusc fossil fragments (Yoon, 1975, 1976a, 1976b). Burrows with a diameter of about 1 cm and length of several centimeters are common (Fig. 5-1). It is commonly scoured by the overlying disorganized gravelstone (Facies G1-a), crudely-stratified gravelstone (Facies G2-b) and cross-bedded gravelstone (Facies G6).

Interpretation

Massive sandstones can be formed either by rapid settling from suspension, penecontemporaneous deformation or by bioturbation. In this facies, the presence of lignite fragments and bioturbations suggest slow rate of suspension settling. Lack of fluid escape structures also suggests slow sedimentation rate. Brackish- to shallow-marine-type mollusc fossils indicate that deposition occurred near the river mouth draining shallow marine environments (e.g. lagoons or salt marshes).

Some sandstone units with trains of gravels and erosive lower boundary suggest powerful tractive flow. Lack of bioturbation, lignite fragments and wave ripples also suggest rapid suspension sedimentation. The brackish- to shallow-marine-type mollusc fossils are indicative of deposition in a transitional environment. It may have been deposited by sediment laden river water which entered into shallow marine water. Rapid deceleration of the flow at the river mouth resulted in rapid settling of the suspended loads, forming thick massive sandstones (van der Meulen, 1983; Martinsen, 1990; Mastalertz, 1990). Trains of gravels are indicative of tractional processes, probably representing inertia-dominated effluent diffusion (Wright & Coleman, 1974).

Facies S1-b: Massive Sandstone (partly graded)

Description

The facies S1-b consists of generally thin (< 30 cm) units of poorly- to well-sorted, coarse to fine sands. Some units contain widely dispersed gravels

ranging in size from granule to outsized boulder (upto 50 cm in long diameter). This unit rarely contains laterally discontinuous trains of very coarse sands and granules. Rip-up mud clasts and lignite fragments are common. Some units are partly graded in the basal and upper parts of the bed. The sandstone generally overlies the homogeneous mudstone (Facies M1-b) with a sharp and erosional lower boundary (partly channellized). Some sandstone units which overlie the mudstone units are partly irregular due to soft sediment deformation represented by microloads and pseudonodules of sands and flames of muds. This facies is commonly overlain by homogeneous mudstone (Facies M1-b) with a diffuse upper boundary. Some of the upper boundaries are irregular with fluid escape structures. This facies commonly occurs in sections of MG-4, -5, GB-2, DR-1 and DR-2 (Fig. 4-1).

Interpretation

This facies is interpreted as sandy turbidite based on its massive nature, presence of rip-up clasts, erosive lower boundary, indications of rapid sedimentation such as load structures, pseudonodules, flame structures (Walker, 1978; Lowe, 1982; Massari, 1984; Surlyk, 1984; Postma et al., 1988). This facies mimics T_a division of Bouma (1962), Facies V of Aalto (1976), S3 division of Lowe (1982) and S2 division of Massari (1984), deposited by high- or low-density turbidity currents. Massive sandstones can be formed by rapid settling from turbulent suspension in which rapid fall out of suspended load inhibits tractive transport, reducing lateral segregation of grains (Middleton, 1970; Collinson & Thompson, 1982; Allen & Leeder, 1980; Allen, 1984; Lowe,

1988).

Facies S4: Graded Sandstone

Description

This facies is represented by normally graded units of coarse to fine sands (Fig. 5-1, Table 5-1). Each facies unit is generally thin (< 20 cm) and is composed of moderately- to well-sorted fine to coarse sands. Gravels commonly occur in the lower part of the bed; outsized clasts (more than 50 cm in long diameter) are also contained. Rip-up mud clasts and lignite fragments are common in the upper parts of the bed; some occur as trains and pockets in the middle and upper parts of the bed (Fig. 5-1). This facies commonly overlies the mudstone with a sharp and erosional lower boundary; some are partly irregular due to soft sediment deformation including microloads and pseudonodules of sands as well as mud flames. Fluid escape structures are also common. This facies occurs in sections of MG-4 and MG-5.

Interpretation

Normally graded sandstones are generally deposited from turbulent suspension, from which coarse grains can be segregated and settle faster than the finer ones. It is similar to the T_a division of classical turbidite (Bouma, 1962) and represents deposition from turbulent suspension of high- and low-density turbidity currents (Lowe, 1982; Surlyk, 1984; Postma, 1986; Eyles et al., 1987; Postma et al., 1988).

5.4. Class M : Mudstone

The class M includes muddy sandstone and sandy mudstone as well as mudstone, containing more than 30% of muds with small amounts of gravel-size clasts (< 5%).

Facies M1-a: Homogeneous Muddy Sandstone (partly bioturbated)

Description

This facies is generally thin (< 50 cm) and is either brownish or dark gray in color depending on organic content. Granule- to pebble-size clasts are widely dispersed; some occur as trains. Otherwise, this facies is extensively bioturbated with vertical burrows and rootlets (Fig. 5-1). Some units contain rhizolith. Individual facies unit is commonly scoured by the disorganized gravelstone (Facies G1-a), crudely-stratified gravelstone (Facies G2-a) and cross-bedded gravelstone (Facies G6) with channel geometry. This facies occurs in subsections of MG-1.

Interpretation

The existence of plant debris and the brownish to dark gray color as well as the presence of rootlets and rhizolith suggest that this facies was deposited in subaerial environment. The channellized gravelstone units which scour this facies indicate that this facies was deposited on an interchannel area (floodplain). Muds can be deposited from suspension fallout due to overbank flooding. Original sedimentary structures may have been obliterated by extensive bioturbation. It is similar to the Facies Fl of Miall (1977, 1978) and

Rust (1978), deposited by vertical accretion in an overbank area or in a floodplain environment.

Facies M1-b: Homogeneous Mudstone (microfossils)

Description

This facies is represented by light olive gray and dark gray homogeneous mudstone, ranging in thickness from a few centimeters to several meters (Fig. 5-1, Table 5-1). Gravel clasts are widely dispersed with small amounts of biogenic sediments such as plant debris, lignites, shell fragments and microfossils. Some units contain calcareous siltstone blocks. Thin, laterally discontinuous fine to very fine sand layers are partly intercalated. Some units are extensively bioturbated.

Interpretation

The homogeneous nature and the co-occurrence of terrigenous materials with biogenic grains indicate deposition by hemipelagic settling. At the river mouth, sediment segregation is caused by the density difference between the inflowing water and the reservoir water (Bates, 1953). If the inflowing water and the reservoir water have the same density (homopycnal flow) or the inflowing water is less dense than the reservoir water (hypopycnal flow), the inflowing water will result in plane jet flow, transporting the sediments more basinward, while the coarse-grained bed loads will be deposited at the river mouth to form Gilbert-type deltas (Bates, 1953). Continuous supply of terrigenous sediments from the fluvial system will cause rapid sedimentation

which may be responsible for the thick, homogeneous muddy sandstones.

Some mudstone beds contain abundant biogenic grains with small amounts of terrigenous material. It is generally light olive gray in color and commonly occurs in the Duho Formation. According to Garrison et al (1985) and Issiacs (personal communication), this mudstone resembles 'porcelanites' in the Monterey Formation of California. It may have been deposited by pelagic settling of biogenic grains (diatoms) with small amounts of terrigenous materials.

Chapter 6. FACIES ORGANIZATION AND ARCHITECTURE

The Malgol fan delta sequence can be grouped into 4 facies organizations (or facies associations) based on sedimentary facies and bed geometry. Individual facies associations represent specific depositional environments: alluvial fan (or subaerial scree apron; Facies Association I), submarine scree apron (Facies Association II), slope apron (Facies Association III) and basin plain (Facies Association IV).

6.1. Facies Association I: Alluvial Fan (or Subaerial Scree Apron or Transitional Zone between Subaerial and Subaqueous Parts)

Occurrence

This association is represented by sheet-like beds of disorganized breccias (Facies B1-a and B1-b), crudely-stratified breccia (Facies B2), disorganized gravelstone (Facies G1-a), crudely-stratified gravelstone (Facies G2-a), cross-bedded gravelstone (Facies G6), massive sandstone (Facies S1-a) and homogeneous muddy sandstone (Facies M1-a) (Fig. 6-1). The breccia units commonly form the lower and proximal parts of the sequence which unconformably overlie the Cretaceous and Eocene basement rocks. The breccia units laterally and vertically grade into gravelstone units, forming the upper and distal parts of the sequence. The breccia units are either matrix- or clast-supported in poorly-sorted, brownish muddy sand matrix, whereas the gravelstone units contain poorly-sorted sand matrix. The homogeneous muddy sandstone (Facies M1-a) ranges in color from light brown to dark gray according to organic content. The muddy sandstone units are commonly

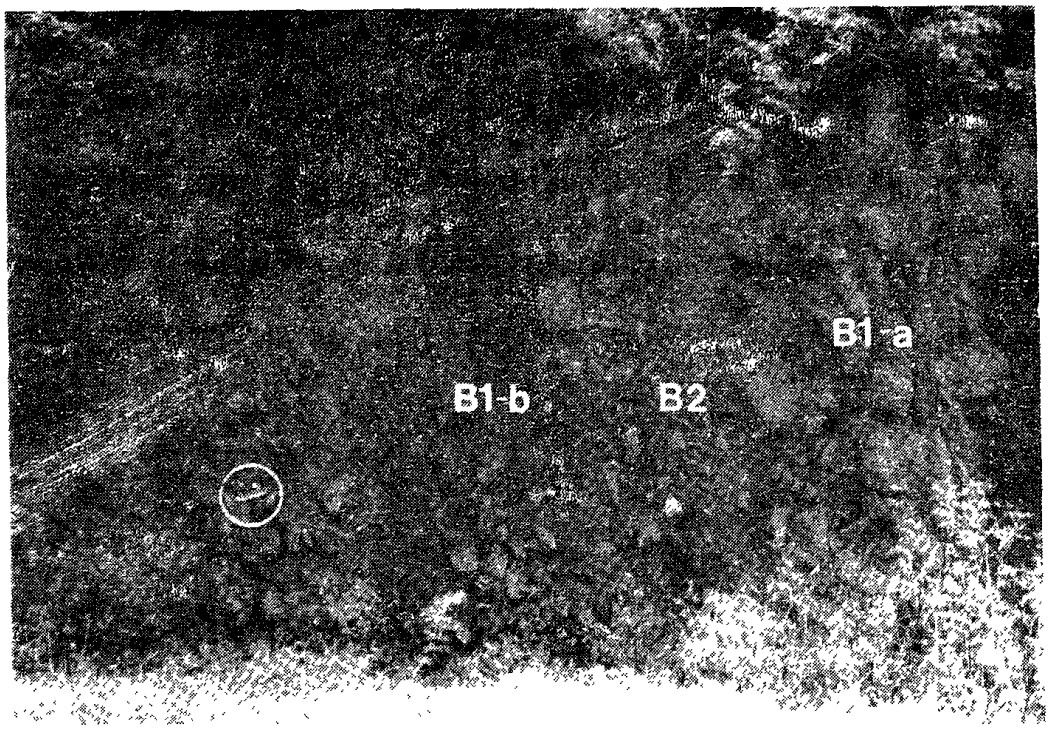

Fig. 6-1. Photograph of alluvial fan deposits (Facies Association I; subsection MG-1; Fig. 4-1). Note overturned beds of breccia and gravelstone units. Scale arrow is 20 cm long. Top to the left.

scoured by the overlying gravelstone units. The massive sandstone units (Facies S1-a) are, however, commonly overlain by gravelstone beds with diffuse unit boundary, showing a coarsening-upward trend. This association occurs as a narrow belt (< 100 m in width) along the faulted basin margin, occurring in subsections of MG-1 and GB-1 (Fig. 4-1).

Clast composition shows a regional variation along the basin margin, depending on the adjacent basement rocks. It also depends on the sedimentary facies. In Gwangbang section (GB), this association is bounded by felsite basement rock (Eocene) (Fig. 4-11). Approximately 10 m west of the sequence boundary lies sedimentary rock (Cretaceous) (Fig. 4-11). Here, the

gravelstone units comprise subangular to subrounded clasts of sedimentary rocks (approximately 65%), whereas the breccia units are dominated by angular to subangular clasts of felsite (> 80%). In the Malgol section, the Miocene sedimentary rocks are overlain by felsite basement rock (Eocene), representing a thrust fault. Approximately 50 m north of the outcrop, however, the sequence is overlain by sedimentary rock (Cretaceous). In this section, the breccia units are dominated by angular clasts of felsite (> 80%); some beds are entirely composed of felsite clasts (nearly 100%). The gravelstone units, however, comprise subangular to subrounded clasts of sedimentary rock (Cretaceous) (65%) and felsite (Eocene) (25%) with small amounts of volcanic rocks (Eocene). In the Gwangbang section, the sequence generally trends N8°W/12°NE (Fig. 4-10). In the northern part (e.g. Malgol section), however, the alluvial fan sequence is overturned, showing a general trend of N18°E/75°NW-85°SE (Fig. 4-2).

Interpretation

The disorganized breccias (Facies B1-a and B1-b) were most probably deposited by subaerial debris flows, whereas the crudely-stratified breccias (Facies B2) were formed either by sheetfloods or hyperconcentrated flows in alluvial fan environments (e.g. Bull, 1972; Costa, 1988). Angular clasts and their clast compositions which are largely similar to the adjacent basement rocks suggest short transport distance from the sediment sources, probably originated from the screes on the fault-bounded drainage basin. The gravelstone units may represent deposition in braided streams in which

migration of gravel bars and secondary channel fills are responsible for the disorganized gravelstone (Facies G1-a), crudely-stratified gravelstone (Facies G2-a) and cross-bedded gravelstone (Facies G6) (Miall, 1977, 1978; Rust, 1978). The relatively well-organized fabric than that of the breccia unit suggests that the gravelstone units experienced longer transport than the breccia units. Subangular to subrounded clasts as well as the lack of mud matrix also suggest longer transportation than the breccia units, probably transported through torrential streams in the fault-bounded drainage basin (or consequent hangingwall drainage; Leeder et al., 1988). Thin units of homogeneous muddy sandstone (Facies M1-a) may represent deposition by slow suspension settling on a floodplain environment. Although most of the sequence was deposited in subaerial environment, lignite fragments in some homogeneous muddy sandstone beds (Facies M1-b) indicate that the alluvial fan was deposited near the transitional zone between the subaerial and subaqueous parts. Furthermore, some coarsening-upward trends of gravelstone and sandstone units may represent progradation of alluvial fan to a shallow marine setting, largely similar to the major Gilbert-type topset units of the Doumsan and Duksung fan-delta systems (for further discussion, see Hwang, 1993).

This association occurs as a narrow belt (< 100 m in width) along the basin margin, suggesting that sediments were derived from a line source (or multi-point sources) and deposited at the base of the mountain, forming a small-scale coalescing alluvial fans (or bajada, pediments or subaerial scree aprons). The local variation in clast composition along the basin margin also

represents multi-point sediment sources. The long, narrow alluvial systems imply that the drainage basin was very narrow and steeply inclined, probably bounded by fault scarp (Gloppen & Steel, 1981; Mann et al., 1983; Dunne & Hempton, 1984; Nilsen & McLaughlin, 1985; Alexander & Leeder, 1987; Leeder et al., 1988; Gawthorpe & Colella, 1990).

The overturned units of alluvial fan sequence in the Malgol section area and the thrust faults in the basin margin suggest tectonic movement of the basin during and after the deposition (for further discussion, see Chapter 7).

6.2. Facies Association II: Submarine Scree Apron

Occurrence

This association is represented by steeply-inclined beds (> 25°) of disorganized gravelstone (Facies G1-b) and crudely-stratified gravelstone (Facies G2-b) with sheet-like bed geometry (Fig. 6-2). Clasts are generally angular to subangular and are largely composed of felsite (Eocene), volcanic rock (Eocene) and sedimentary rock (Cretaceous) which varies along the basin margin, depending on the adjacent basement rocks. The clasts range in size from granule to boulder in which some units contain extraordinary large clasts (more than 10 m in long diameter). Most clasts are aligned parallel to local slope; some are imbricated [a(p), a(i)]. Clast orientations suggest an eastward paleoflow. This association also occurs as a narrow belt along the basin margin (< 300 m in width).

This association overlies the Facies Association I (alluvial fan) with an abrupt vertical variation in sedimentary facies, architecture, clast composition

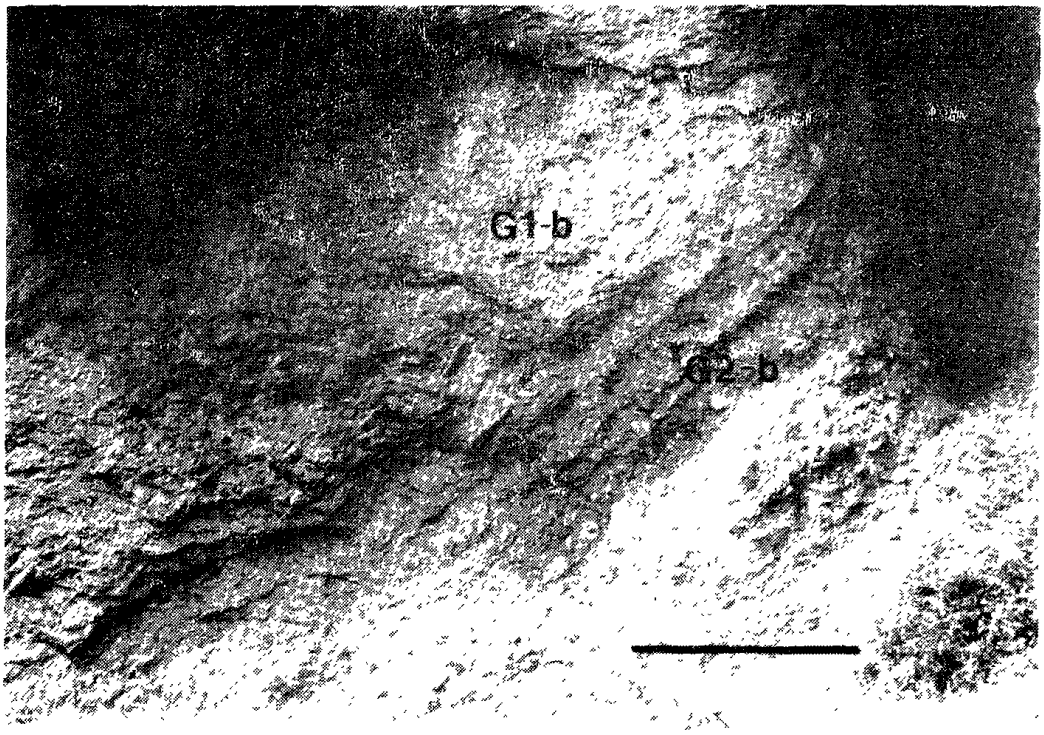

Fig. 6-2. Photograph of submarine scree apron deposits (Facies Association II; subsection MG-2; Fig. 4-1). Note steeply-inclined beds of gravelstone units. Scale bar is 2 m long.

and bed attitude. In the Malgol (MG) section, clasts of the underlying alluvial fan sequence (Facies Association I) is largely composed of sedimentary rocks (Cretaceous) (> 65%) and felsite (Eocene) (25%), whereas those of the overlying sequence (Facies Association II) is dominated by felsite (52%) and sedimentary rocks (38%). The underlying sequence is overturned (N18°E/75°NW-85°SE), whereas this association is steeply inclined (15°E/45°-25°SE). In the Gwangbang (GB) section, however, clast composition of the underlying alluvial fan sequence is largely similar to that of the overlying submarine scree apron deposits, containing angular to subrounded clasts of sedimentary rocks (Cretaceous) (approximately 70%) and felsite (Eocene)

(approximately 20%). Here, the underlying sequence shows a general trend of N8°W/12°NE, whereas the overlying sequence is steeply inclined (N18°W/-28°NE). This association laterally and vertically grades into Facies Association III (slope apron) with a gradual decrease in number and bed thickness of gravelstone units.

Interpretation

The disorganized gravelstone (Facies G1-b) and crudely-stratified gravelstone (Facies G2-b) units are interpreted as debris fall (or grain fall, gravity slide) and cohesionless debris flow (or grain flow, density-modified grain flow) deposits, as evidenced by the disorganized and crudely-stratified nature, thin units of graded and inversely graded gravelstone and sandstone layers, parallel oriented clasts as well as their occurrence in steeply-inclined beds (> 25°) (Postma, 1983, 1984a, 1984b; Postma & Roep, 1985; Colella et al., 1987; Colella, 1988a; Chough et al., 1989, 1990; Hwang & Chough, 1990; Nemec, 1990b). According to Nemec (1990b), these flows commonly occur in steeply-inclined slope environments, probably originated from avalanching of gravels and sands which transforms into various sediment gravity flows. Angular clasts suggest that the drainage basin was very narrow and steeply inclined, probably bounded by fault scarp. The coarse-grained sediments were supplied to the basin mainly by rock fall and debris flow as well as through small-scale torrential streams, forming a scree apron at the base of the fault scarp. Avalanching of the screes which transformed into various sediment gravity flows may be responsible for the progradation of submarine

scree aprons on the tectonic slope. Their occurrence as a narrow belt (< 300 m in width) along the faulted basin margin and their clast composition which depends on the adjacent basement rocks suggest that the sediments originated from multi-point sources (or a line source).

Vertical variation in clast composition and bed attitude as well as sedimentary facies between the Facies Association I and II suggest syn-depositional tectonic movement, probably related to the thrust faults in the western margin of the basin (for further discussion, see Chapter 8).

6.3. Facies Association III: Slope Apron

Occurrence

This association is represented by thick homogeneous muddy sandstone (Facies M1-b) in which thin units of disorganized gravelstone (Facies G1-b), graded gravelstone (Facies G4), inverse-to-normally graded gravelstone (Facies G5-a), massive sandstone (Facies S1-b) and graded sandstone (Facies S4) are partly intercalated (Fig. 6-3). The muddy sandstone units contain lignite fragments and mollusc fossil fragments. Part of the muddy sandstone units are cemented with calcite. Isolated outsized clasts also occur, ranging in size from granule to boulder (max.: > 10 m in long diameter). The gravelstone and sandstone units commonly show sheet-like bed geometries; some thin (< 10 cm) sandstone units are laterally discontinuous. The sandstone units commonly contain angular, granule-size clasts. Outsized gravels are also common.

The sequence shows an upward fining trend, represented by vertical

Fig. 6-3. Photograph of slope apron deposits (Facies Association III; subsection GB-3; Fig. 4-1). Note thick homogeneous muddy sandstone (Facies M1-b) with a graded gravelstone unit (Facies G4). Measuring bar is 2 m long.

decrease in number and bed thickness of gravelstone and sandstone units, which is, in turn, overlain by thick muddy sandstone unit (Facies Association IV; basin plain). In the northern part, however, this association is overlain by Gilbert-type foreset, toeset, prodelta and slope apron deposits of the Doumsan fan-delta system (e.g. Maebong section; Fig. 4-15). Here, some of the sequence is overlain by volcanic rocks (Eocene), representing a thrust fault (Fig. 4-15). In the Malgol section, a small-scale basalt body intruded the sedimentary sequence (Fig. 4-8).

Interpretation

The thick muddy sandstone units with thin layers of sandstone and gravelstone are envisaged to represent slope apron environment off the fan delta (e.g. Choe & Chough, 1988). The thick muddy sandstones were most probably deposited by particle-by-particle settling of fine-grained sediments (e.g. Pickering et al., 1986), whereas the sandstone and gravelstone units indicate intermittent sediment gravity flows such as high- or low-density turbidity currents and cohesive or cohesionless debris flows (e.g. Lowe, 1982). Outsized gravels may have rolled and slid along the steeply-inclined slope and deposited at the base of the slope (or slope apron).

The general upward fining sequence represents that sediment supply rate from the alluvial feeder systems gradually decreased during the deposition. In the Maebong (MB) section, the overlying volcanic rocks (Eocene) suggest extensive movement of the thrust faults after the deposition of the slope apron sequences (for further discussion, see Chapter 8).

6.4. Facies Association IV: Basin Plain

Occurrence

The Facies Association III (slope apron) is overlain by thick homogeneous mudstone (Facies Association IV) with light yellowish green color. The mudstone contains abundant microfossils such as diatoms and foraminifers. Mollusc fossil fragments and plant debris also occur. Part of the mudstone unit is cemented with calcite. In this association, thin (< 10 cm) units of sandstone are partly intercalated.

Interpretation

This association is interpreted as basin plain deposits in which the mudstone was deposited by particle-by-particle settling of fine-grained clastic materials and biogenic grains (hemipelagic settling; Pickering et al., 1986). Intermittent turbidity currents formed the thin units of sandstone. Their stratigraphic position suggests that this association was deposited during the last stage of the fan-delta progradation. The dominance of hemipelagic muds indicates that sediment supply from the alluvial feeder system was terminated.

Chapter 7. DEPOSITIONAL SYSTEMS

The facies organizations and bed geometries suggest that the Malgol fan-delta system was deposited in four depositional environments: alluvial fan, submarine scree apron, slope apron and basin plain (Fig. 7-1). This fan delta occurs as a long, narrow (< 500 m wide) belt along the faulted basin margin (Fig. 7-1). Sediments were derived from the multi-point sources along the upthrusted basement rock and deposited at the base of the fault scarp, both in subaerial and subaqueous environments, forming a scree-apron-type fan-delta system (Fig. 7-1). The sequence shows a general fining- and thinning-away trend from the fault bounded basin margin. Clast orientations suggest a general eastward paleocurrent direction.

The alluvial fan deposits are characterized by sheet-like beds of disorganized breccias (Facies B1-a and B1-b), crudely-stratified breccia (Facies B2), disorganized gravelstone (Facies G1-a), crudely-stratified gravelstone (Facies G2-a) and cross-bedded gravelstone (Facies G6) in which thin units of homogeneous muddy sandstone (Facies M1-a) and massive sandstone (Facies S1-a) beds are partly intercalated. The breccia units were deposited either by subaerial debris flows, hyperconcentrated flows or sheetfloods (Bull, 1972; Lewis et al., 1980; Nemec & Steel, 1984; Costa, 1988). Angular clasts and their clast composition which are similar to the adjacent basement rocks suggest that the breccia units experienced short transport distance, probably originated from the upthrusted basement rock and deposited at the base of the fault scarps. The gravelstone units were deposited by migration of gravel bars and secondary channel fills in subaerial

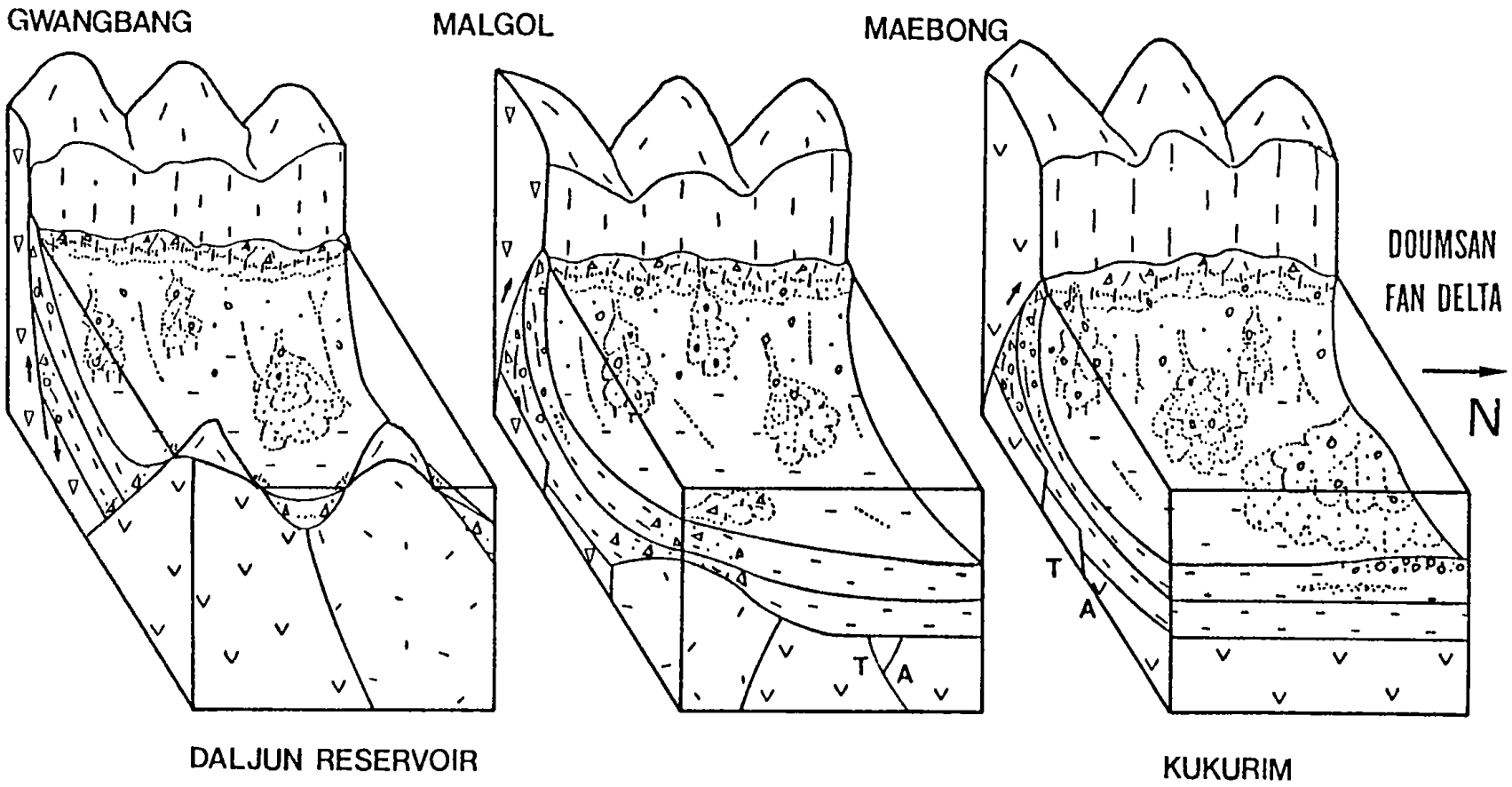

Fig. 7-1. Simplified depositional model for Malgol fan-delta system. The Malgol fan delta was deposited in alluvial fan (or subaerial scree apron), submarine scree apron, slope apron and basin plain environments.

and subaqueous braided streams (e.g. Miall, 1977, 1978). The muddy sandstone units represent deposition in a floodplain environment (e.g. Miall, 1977, 1978; Rust, 1978), whereas the sandstone units were deposited by rapid suspension settling in shallow marine setting (e.g. Martinsen, 1990). This association occurs as a long narrow belt (< 100 m in width) along the faulted basin margin. Their clast composition shows a regional variation along the basin margin depending on the adjacent basement rocks, suggesting that the sediments originated from a line source (or multi-point sources). The sediments were most probably deposited at the base of the fault scarps, forming a small-scale coalescing alluvial fan (or scree apron) (Fig. 7-1).

Coarse-grained sediments were also deposited on the subaqueous fault scarp, forming submarine scree-apron (Fig. 7-1). Here, the sequence is represented by steeply-inclined (> 20°) beds of disorganized gravelstone (Facies G1-b) and crudely-stratified gravelstone (Facies G2-b) (Facies Association II). The gravelstones were deposited by debris fall (or grain fall) and cohesionless debris flows (or grain flows, density-modified grain flows) (Postma, 1983, 1984a, 1984b; Postma & Roep, 1985; Colella et al., 1987; Colella, 1988a; Chough et al., 1989, 1990; Hwang & Chough, 1990; Nemec, 1990b). At the base of slope (or slope apron; Facies Association III), slow suspension settling of fine-grained materials formed thick homogeneous muddy sandstone (Facies M1-b) (Fig. 7-1). Thin units of gravelstone and sandstone are partly intercalated, probably deposited by intermittent turbidity currents and debris flows. Outsized gravels were rolled and slid along the steep slope and deposited at the base of the slope (or slope apron).

The basin plain environment is represented by thick, light yellowish gray mudstone (Facies Association IV), probably deposited by particle-by-particle settling of fine-grained clastic sediments and biogenic grains (hemipelagic settling) (Pickering et al., 1986).

The volcanic ridges in the eastern part of the basin acted as a minor sediment source (e.g. Daljun Reservoir section) (Fig. 7-1). Here, the Yeonil Group sequence (Miocene) unconformably overlies the volcanic (Eocene) and basaltic (Miocene, 21.8 Ma; Jin et al., 1989) basement rock. The clasts are entirely composed of basalt fragment, suggesting that the weathered Miocene basalt clasts were directly deposited at the base of the volcanic ridges. Limited development of the drainage system in the volcanic ridges probably resulted in the monomictic clast composition of the gravelstone and sandstone units (100% of Miocene basalt clasts).

Chapter 8. DEPOSITIONAL HISTORY

Based on the facies distribution, clast composition and the architecture, the sedimentary sequence in the Malgol fan-delta system can be grouped into three units, representing three stages of fan-delta progradation: 1) progradation of coastal alluvial fans (Stage M-1), 2) progradation of scree-apron-type fan-delta system (Stage M-2), and 3) deposition of hemipelagic muds (Stage M-3) (Figs. 8-1 and -2).

8.1. Stage M-1: Deposition of Coastal Alluvial Fans

Distribution

The sequence deposited during the Stage M-1 is represented by alluvial fan (Facies Association I) deposits in which probable subaqueous deposits are partly exposed in the southern part (Fig. 8-1). The alluvial fan sequence unconformably overlies the Cretaceous and Eocene basement rocks (sedimentary, granitic and volcanic rocks) (Fig. 8-1). The sequence is represented by disorganized breccias (Facies B1-a and B1-b), crudely-stratified breccia (Facies B2), disorganized gravelstone (Facies G1-a), crudely-stratified gravelstone (Facies G2-a), cross-bedded gravelstone (Facies G6), massive sandstone (Facies S1-a) and homogeneous muddy sandstones (Facies M1-a). The muddy sandstone unit varies in color from light brown to dark gray. Some units show coarsening-upward trends, in which the massive sandstone unit (Facies S1-a) is overlain either by disorganized gravelstone (Facies G1-b) or crudely-stratified gravelstone (Facies G2-b) units with diffuse unit boundary.

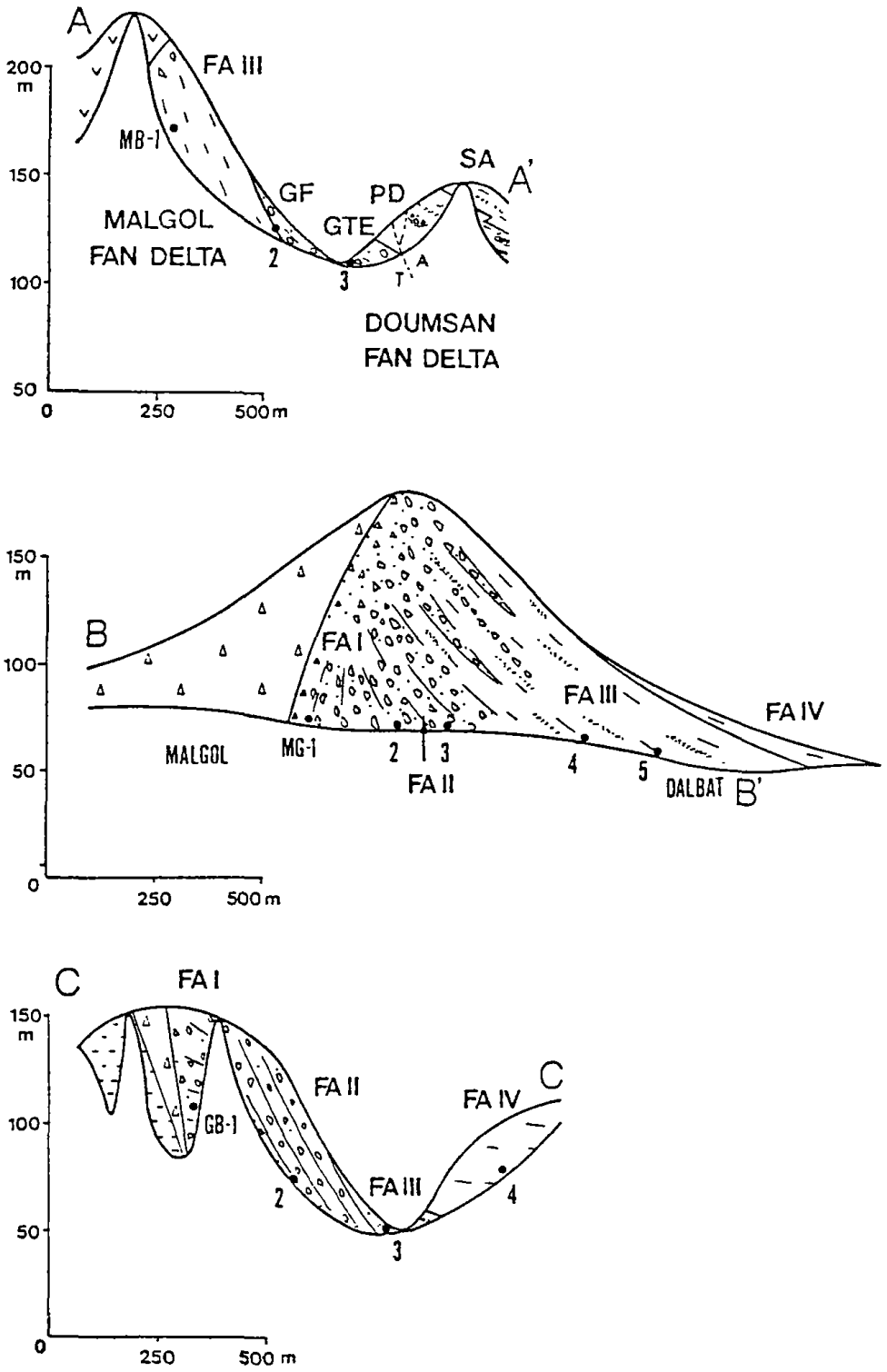

Fig. 8-1. Simplified cross-sections of the Malgol fan-delta system: A) Maebong (MB), B) Malgol (MG) and C) Gwangbang (GB) sections. Note stratigraphic positions and bed attitude of depositional sequences. For location, see Fig. 6-2-1.

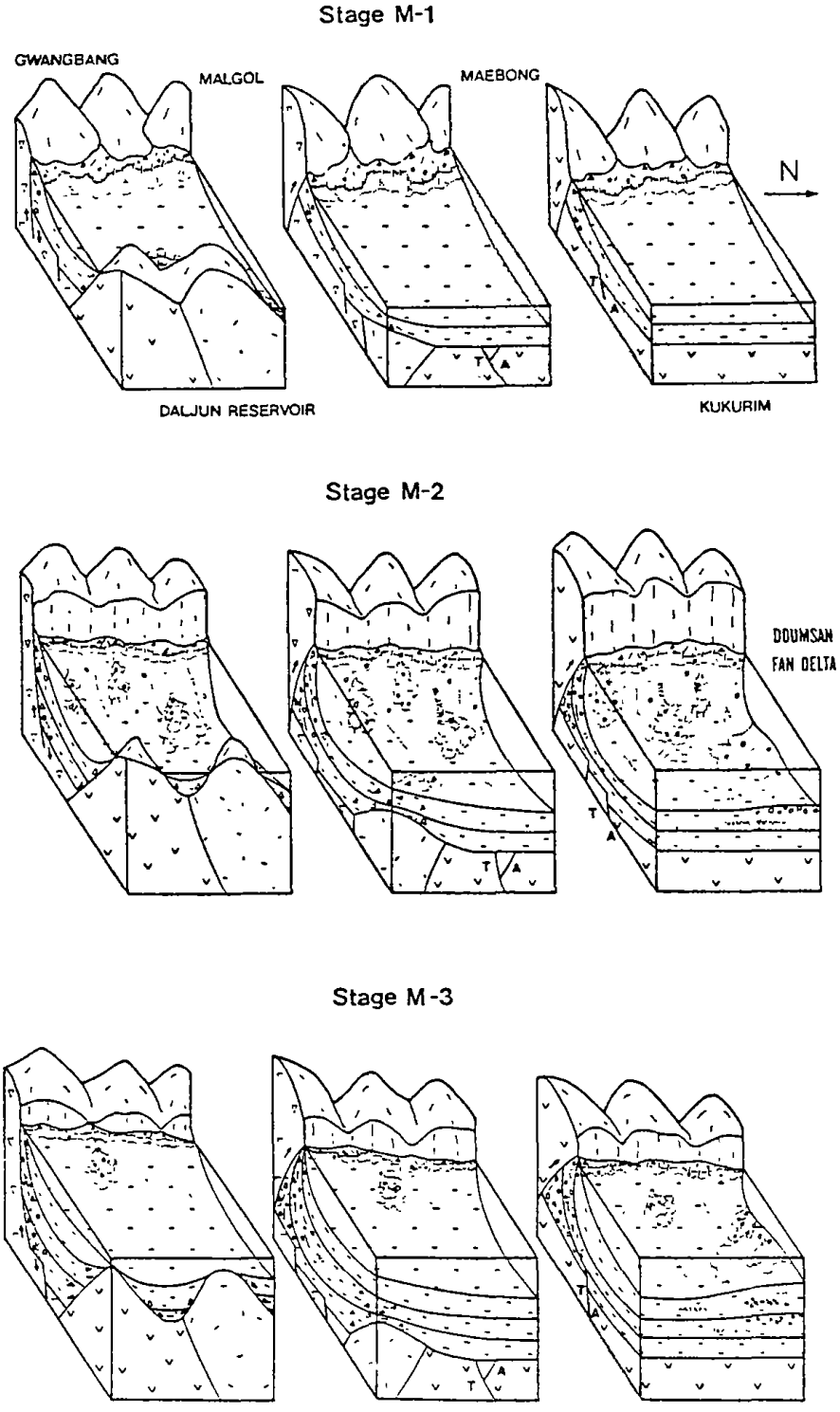

Fig. 8-2. Simplified depositional model for the Malgol fan-delta system: 1) deposition of coastal alluvial fan (Stage M-1), 2) deposition of scree-apron type fan delta (Stage M-2), and 3) deposition of hemipelagic muds (Stage M-3).

The alluvial fan sequence occurs as a narrow belt (< 100 m in width) along the basin margin. Along the basin margin, clast composition shows regional variation depending on the adjacent basement rocks (Cretaceous or Eocene). The sequence also shows local variation in bed attitude. In the Gwangbang (GB) section, the alluvial fan sequence is bounded by felsite basement rock (Eocene). Approximately 10 m west of the sequence boundary lies sedimentary rock (Cretaceous) (Fig. 8-1C). Gravel clasts are generally angular to subrounded and are largely composed of sedimentary rocks (Cretaceous) (approximately 70%) and felsites (Eocene) (25%). The sequence shows a general trend of N8°E/12°SE. In the Malgol section (e.g. subsection MG-1), the alluvial fan sequence is overlain by felsite (Eocene), representing a thrust fault. Lower part of the sequence is overturned with a general trend of N18°E/75°NW. In the middle part, the sequence is nearly vertical, whereas it is steeply inclined in the upper part of the sequence with a general trend of N18°E/85°SE. Gravel clasts are largely composed of sedimentary rock (Cretaceous) (65%) and felsite (Eocene) (25%). In the northern part of the fan delta (e.g. Maebong section), alluvial fan sequences is absent (Fig. 8-1A).

Interpretation

The narrow alluvial fan sequences suggest that the drainage basin was very narrow and steeply inclined, occurring along the fault-bounded basin margin (Gloppen & Steel, 1981; Mann et al., 1983; Dunne & Hempton, 1984; Nilsen & McLaughlin, 1985; Alexander & Leeder, 1987). The thrust faults in

the northern part of the fan delta are also indicative of the existence of fault-bounded alluvial fan systems. The variation in clast composition along the basin margin suggests that sediments originated from a line source (or multi-point sources), forming a coalescing alluvial fan or scree apron at the base of the fault scarp. Thin units of dark gray muddy sandstones containing abundant lignite fragments suggest that the alluvial fan was deposited near the transitional zone between the subaerial and subaqueous parts. The coarsening-upward trends of gravelstone and sandstone units may represent progradation of alluvial fan to shallow marine setting. Approximately 200 m east of subsection MG-5, an exploratory well (H-well) penetrated the Yeonil group sequence and underlying volcanic basement rock (Eocene) (Fig. 4-1). In the lower part of the H-well section (310 m - 290 m), shallow-marine-type dynocysts such as *Cribroperidinium* and *Tasmanites* are abundant (Kim, 1987). These also indicate that the alluvial fan prograded into shallow marine environments during the early stage of the fan-delta progradation, probably representing progradation of coastal alluvial fans (e.g. Ethridge & Wescott, 1984) (Fig. 8-2).

Bed attitudes of the alluvial fan sequence suggest syndepositional tectonic movement, probably related to the thrust fault in the basin margin. In the Malgol section (e.g. subsection MG-1), the lower part of the sequence is overturned with a general trend of N18°E/75°NW. In the middle part, the sequence is nearly vertical, whereas it is steeply inclined in the upper part of the sequence with a general trend of N18°E/85°SE (Fig. 8-1B). The sequence is overlain by felsite basement rock (Eocene), representing a thrust-bounded

basin margin (Fig. 8-1B). If the thrust fault was inactive during the deposition of the alluvial fan sequence, gradual subsidence of the hanging-wall and high-rate of sediment supply from the alluvial feeder system would result in the deposition of a thick wedge of alluvial fan sequence which shows downfan decrease in bed thickness and grain size (Fig. 8-3A). In case of postdepositional movement of the thrust fault, the overlying alluvial fan sequence would be more extensively overturned than that of the underlying sequence, because the alluvial fan sequence shows downslope decrease in bed thickness (Fig. 8-3A). The entire outcrop section, thus, will show downward convergence in bed attitude (Fig. 8-3A). In the Malgol section example (e.g. subsection MG-1), however, the underlying sequence is more extensively overturned than that of the overlying sequence, showing downward divergence in bed attitude (Fig. 8-1). These may indicate downslope increase in bed thickness of the alluvial fan sequence during the deposition (Fig. 8-3B). It may largely be due to the gradual uplift of the basin margin during the deposition, probably dragged by the upward

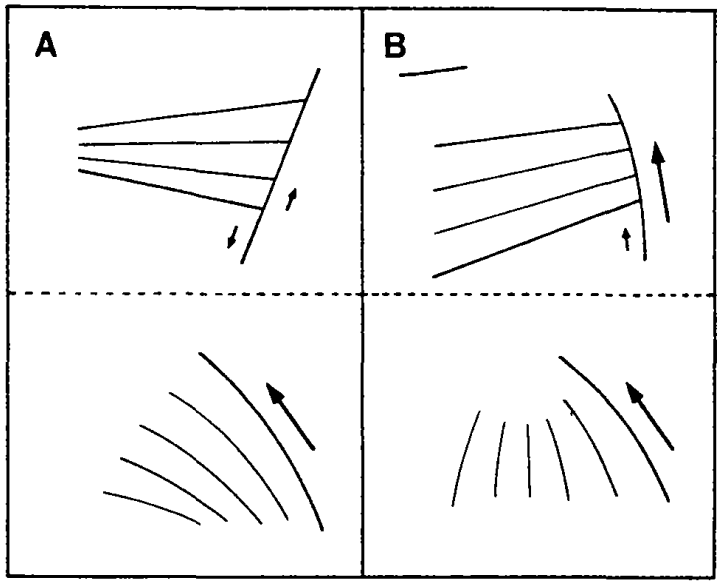

Fig. 8-3. Schematic bed attitude patterns of alluvial fan sequence in which the thrust fault experienced postdepositional (A) and syn-depositional (B) movement.

movement of the thrust fault (Fig. 8-3B). Continued movement of the thrust fault after the deposition of the alluvial fan sequence resulted in the overturning of the underlying sequences (N18°E/75°NW). The overlying sequence was also deformed with less extensively overturned bed attitude (N18°E/85°SE) (Figs. 8-1 and -3B).

In the Gwangbang section, however, the relative plane beds (N8°E/12°SE) of the alluvial fan sequence suggest limited influence of the thrust fault. Furthermore, the Yeonil Group sequence is bounded by the felsite basement (Eocene) with a normal fault (Fig. 8-1), indicating gradual subsidence of the hangingwall and uplift of the footwall during and after the deposition of the alluvial fan sequence (Fig. 8-2).

8.2. Stage M-2: Deposition of Scree-apron-type Fan-delta System

Distribution

The sequence deposited during the Stage M-2 is represented by alluvial fan (or subaerial scree apron; Facies Association I), submarine scree apron (Facies Association II) and slope apron (Facies Association III) deposits (Fig. 8-1). These units also occur as a narrow (< 300 m in width) belt along the faulted basin margin (Fig. 4-1). The sequence boundary between the Stage M-1 and M-2 is represented by an abrupt vertical change in clast composition and shape, sedimentary facies and architectures as well as an abrupt variation in bed attitude. In the Malgol section, the underlying alluvial fan sequence is dominated by subangular to subrounded clasts of sedimentary rock (Cretaceous) (65%), whereas the overlying submarine scree-apron sequence

is represented by angular to subangular clasts of felsite (Eocene) (52%). The underlying sequence is overturned with a general trend of N18°E/75°NW-85°SE. It is overlain by steeply-inclined (N15°E/45°-25°SE) units of gravelstone, deposited during the Stage M-2 (Fig. 8-1). In the Gwangbang section, however, clast composition and shape of the overlying submarine scree apron deposits are largely similar to those of the underlying alluvial fan sequence. In this section, the underlying sequence generally trends N8°E/12°SE, whereas the overlying sequence is steeply inclined (N8°E/20°SE).

The alluvial fan (or subaerial scree apron; Facies Association I) is represented by disorganized breccias (Facies B1-a and B1-b) and crudely-stratified breccia (Facies B2). This association laterally grades into submarine scree apron deposits (Facies Association II) containing steeply-inclined (25°-40°) beds of disorganized gravelstone (Facies G1-b) and crudely-stratified gravelstone (Facies G2-b) with sheet-like bed geometry. This association laterally and vertically grades into Facies Association III (slope apron) with gradual decrease in number and bed thickness of gravelstone units (Fig. 8-1). The sequence is represented by thick homogeneous muddy sandstone (Facies M1-b) with intercalated gravelstone (Facies G1-b, G4 and G5-a) and sandstone (Facies S1-b and S4) units. The sequence varies in thickness along the basin margin (from 100 to 300 m).

The sequence is overlain by thick mudstone unit (Facies Association IV) deposited during the last stage of the fan-delta progradation (Stage M-3). In the northern part (e.g. Maebong section), the sequence is overlain by sedimentary and volcanic basement rocks (Cretaceous and Eocene), represent-

ing a thrust-bounded basin margin (Fig. 8-1). Some units are overlain by Gilbert-type foreset units of the Doumsan fan-delta system, probably deposited during the Stage D-2 of the Doumsan system (for further discussion, refer to Hwang, 1993).

Interpretation

During this stage (Stage M-2), the sequence was deposited in alluvial fan (or subaerial scree apron), submarine scree apron and slope apron environments, forming a scree-apron-type fan-delta system (Fig. 8-2). The coarse-grained sediments were derived from the fault-bounded basin margin and deposited at the base of the fault scarp both in subaerial and subaqueous environments (Fig. 8-2). These units may have been deposited by rock fall (or debris fall) and debris flow, probably initiated by avalanching of screes in the upper part of the fault scarp (Fig. 8-2). The fine-grained sediments were transported by small-scale torrential streams and deposited in the slope apron environment (Fig. 8-2). Intermittent sediment gravity flows such as high- or low-density turbidity currents and cohesive or cohesionless debris flows formed the thin gravelstone and sandstone units in the slope apron environment. The overall sequence shows an upward fining trend, representing gradual decrease in sediment supply rate from the alluvial feeder system.

Abrupt vertical change in clast composition and shape, sedimentary facies as well as the variation in bed attitude in the sequence boundary between the Stage M-1 and M-2 deposits probably resulted from the syndepositional tectonic movement of the basin margin, related to the thrust fault. In the

Malgol section, the dominance of sedimentary rock clasts (65%) in the underlying alluvial fan sequence suggests that most of the gravelstones originated from the Cretaceous sedimentary rocks which occur approximately 50 m north of the outcrop (Fig. 4-2). These units were deposited by small-scale stream flows. In the overlying sequence (submarine scree apron; Facies Association II), the dominance of angular to subangular clasts of felsite (52%) suggests that the felsite basement may have acted as a major sediment source, during the second stage of the fan delta progradation (Stage M-2). The clasts in the overlying submarine scree apron deposits are more angular than those of the underlying alluvial fan deposits, suggesting that the drainage basin was more steeply inclined than that of the previous stage (Stage M-1). The overturned beds in the underlying alluvial fan sequence suggest syn-depositional movement of the thrust along the basin margin (for further discussion, see Chapter 6). These movements may also have resulted in the upthrusting of the felsite basement rocks in the Malgol area, which may be responsible for the dominance of angular clasts of felsite in the overlying submarine scree apron deposits (Facies Association II).

Bed attitude also suggests syndepositional tectonic movement. In the Malgol section, the underlying alluvial fan sequence (Facies Association I) is overturned with a general trend of N18°E/75°NW-85°SE. It is overlain by steeply-inclined (N15°E/45°-25°SE) units of submarine scree apron deposits (Facies Association II) (Fig. 8-1). Detailed analysis of sedimentary facies suggests that the submarine scree apron units were initially deposited in steeply-inclined (> 20°) tectonic slope, whereas the cross-bedded gravelstone and

crudely-stratified gravelstone units in the alluvial fan sequence (Facies Association I) suggest deposition on a rather flat (< 10°) basin (Fig. 8-4A). If the thrust fault was inactive during the deposition, the sequence may retain Gilbert-type profile, in which the rather planar bedded alluvial fan sequences are transitional to steeply-inclined beds of submarine scree apron sequence (Fig. 8-4A). Postdepositional movement of the thrust fault which results in overturning of the plane bedded alluvial fan sequence would result in more extensively deformed units of the scree apron deposits which were initially deposited in more steeply-inclined slopes (Fig. 8-4A). However, the submarine scree apron and slope apron deposits show a general trend of N12°E/20°-40°SE, representing that the sequence was less extensively deformed than that of the underlying alluvial fan sequence. These indicate that most deformation occurred prior to the deposition of submarine scree apron and slope apron sequences. However, the abnormally steeply-inclined beds of gravelstone units (> 40°) in the lower part of the submarine scree apron deposit (e.g. subsection MG-2) suggest that the thrust fault was still

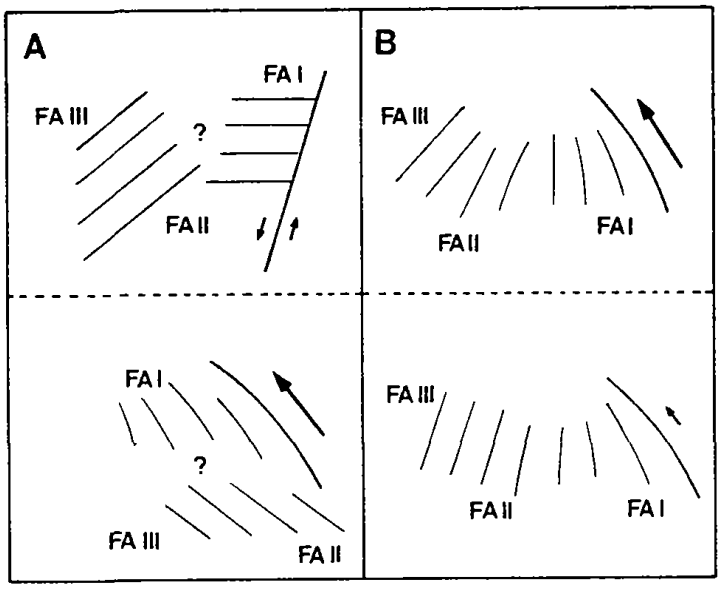

Fig. 8-4. Schematic bed attitude patterns of the alluvial fan (FA I), submarine scree apron (FA II) and slope apron (FA III) deposits in which active movement of the thrust fault occurred after (A) and during (B) the deposition.

active during the Stage M-2.

In the northern part (e.g. Maebong section), the sedimentary (Cretaceous) and volcanic (Eocene) rocks which overlie the submarine scree-apron (Facies Association II) and slope apron (Facies Association III) deposits suggest more extensive movement of the thrust fault than that of the Malgol area (Figs. 8-1 and -2). The abnormally steeply-inclined (> 30°) beds of muddy sandstone units (slope apron deposits) also suggest continued movement of the thrust in the northern part of the basin after the deposition of the slope apron sequences (or after the Stage M-2) (Figs. 8-1 and -2). In the southern part (e.g. Gwangbang section), however, the sequence is bounded by felsite basement (Eocene) with a normal fault. Here, clast composition and shape of the overlying submarine scree apron deposits (Stage M-2 deposit) are largely similar to those of the underlying alluvial fan sequence (Stage M-1 deposits), representing limited influence of the thrust movement. Bed attitude also suggests limited influence of the thrust fault in which the underlying sequence generally trends N8°E/12°SE, whereas the overlying scree apron sequence is steeply inclined (N8°E/20°SE).

In the northern part (e.g. Maebong section), the slope apron sequence deposited during this stage (Stage M-2) is overlain by Gilbert-type foreset of the Doumsan fan-delta system (Fig. 8-1). The Gilbert-type foreset sequences were deposited during the Stage D-2 of the Doumsan system, representing that the Stage M-2 sequences of the Malgol fan-delta system were deposited prior to the early Middle Miocene (for further discussion, see Hwang, 1993).

The volcanic ridges in the eastern part of the basin may have acted as a

minor sediment source, depositing disorganized gravelstone (Facies G1-b), crudely-stratified gravelstone (Facies G2-b) and massive sandstone (Facies S1-b). In the Daljun Reservoir section, the clasts of the gravelstone and sandstone units are entirely composed of basalt fragment, suggesting that the weathered Miocene basalt clasts (21.8 Ma; Jin et al., 1989) were directly deposited at the base of the volcanic ridges. Thin units of homogeneous muddy sandstone (Facies M1-b) were deposited by suspension settling. Limited development of the drainage system in the volcanic ridges probably resulted in the monomictic clast composition of the gravelstone and sandstone units (100% of Miocene basalt clasts).

8.3. Stage M-3: Deposition of Hemipelagic Muds

Distribution

The Stage M-2 sequence is overlain by thick, light yellowish gray mudstone (Facies Association IV; basin plain) (Fig. 8-1). The sequence boundary between the Stage M-2 and Stage M-3 is represented by an abrupt vertical decrease in clastic sediments, in which the overlying mudstone contains abundant biogenic grains (diatoms, foraminifers, silicoflagellates, palynomorphs, gastropods, plants and molluscs).

In the northern part (Maebong & Malgol sections), the sequence is overlain by Gilbert-type toeset (or fine-grained foreset), mass-flow-dominated prodelta (or Gilbert-type bottomset) and slope apron sequences of the Doumsan fan-delta system, deposited during the Stage D-3 of the Doumsan system (for further discussion, refer to Hwang, 1993). In the eastern part of

the basin, part of the volcanic ridges are unconformably overlain by thick mudstone (Fig. 4-19).

Interpretation

The abrupt vertical decrease in clastic sediments and increase in biogenic grains suggest that sediment supply from the alluvial feeder system was terminated during the last stage of the fan-delta progradation (Fig. 8-2). The mudstone units were deposited by particle-by-particle settling of fine-grained clastic grains and biogenic grains, representing (hemi)pelagic settling in a basin plain environment (e.g. Pickering et al., 1986). Intermittent low-density turbidity currents formed thin units of sandstone (e.g. Bouma, 1962). The mudstone is largely similar to 'porcelanites' of Monterey Formation in California and diatomaceous sediments in the East Sea, deposited during middle to late Miocene times (Garrison et al., 1979; Ingle et al., 1989).

The overlying Gilbert-type toeset (or fine-grained foreset), mass-flow-dominated prodelta (or Gilbert-type bottomset) and slope apron sequences of the Doumsan fan-delta system in the northern part of the Malgol fan delta suggest that the Stage M-3 sequences of the Malgol fan-delta system were deposited during the Middle Miocene (for further discussion, refer to Hwang, 1993). In the eastern part of the basin, part of the volcanic ridges are overlain by thick hemipelagic muds, suggesting that most of the volcanic ridges were submerged during this stage, probably related to the tectonic subsidence of the basin and/or eustatic rise in sea level (Fig. 8-2).

Chapter 9. CONCLUSIONS

The sedimentary sequence in the Malgol fan-delta system is represented by 15 sedimentary facies which can be organized into four facies organizations (or facies associations), representing deposition in alluvial fan (Facies Association I), submarine scree apron (Facies Association II), slope apron (Facies Association III) and basin plain (Facies Association IV) environments. Individual facies association occurs as a long, narrow belt along the faulted basin margin. Clast composition shows a regional variation along the basin margin, depending on the adjacent basement rocks.

The Facies Association I is represented by disorganized breccias (Facies B1-a and B1-b), crudely-stratified breccia (Facies B2), disorganized gravelstone (Facies G1-a), crudely-stratified gravelstone (Facies G2-a) and cross-bedded gravelstone (Facies G6) in which thin units of homogeneous muddy sandstones (Facies M1-a) and massive sandstone (Facies S1-a) are partly intercalated. The breccia units were deposited either by subaerial debris flows, hyperconcentrated flows or sheetfloods. The gravelstone units may represent deposition from migration of gravel bars and secondary channel fills in braided streams. The muddy sandstone units represent deposition in a floodplain environment, whereas the sandstone units were deposited by rapid suspension settling in shallow marine environment. This association occurs as a narrow belt (< 100 m in width) along the faulted basin margin, indicating that the sediments were derived from a line source (or multi-point sources). The sediments were deposited at the base of the fault scarp, forming a coalescing of small-scale alluvial fans (or alluvial apron, scree apron, bajada,

or piedmont). The alluvial fans may have been deposited near the transitional zone between the subaerial and subaqueous parts, representing progradation of a coastal alluvial fan.

The Facies Association II is characterized by steeply-inclined beds (> 25°) of disorganized gravelstone (Facies G1-b) and crudely-stratified gravelstone (Facies G2-b) with sheet-like bed geometry. The gravelstone units were deposited by debris fall (or grain fall, gravity slide) and cohesive or cohesionless debris flows (or density-modified grain flows) on a steeply-inclined slope (submarine scree apron) environments. The occurrence of this association as a long, narrow (< 300 m) belt along the basin margin and regional variation in clast composition depending on the adjacent basement rocks suggest that most sediments were derived from a line source (or multi-point sources), and deposited on the subaqueous tectonic slope (or submarine scree apron).

The Facies Association III is represented by thick homogeneous muddy sandstone (Facies M1-b) in which thin units of disorganized gravelstone (Facies G1-b), graded gravelstone (Facies G4), inverse-to-normally graded gravelstone (Facies G5-a), massive sandstone (Facies S1-b) and graded sandstone (Facies S4) are partly intercalated. The thick homogeneous muddy sandstones (Facies M1-b) were deposited by slow suspension settling of fine-grained materials, whereas the gravelstone and sandstone units represent intermittent sediment gravity flows such as high- or low-density turbidity currents and cohesive or cohesionless debris flows. The Facies Association IV is characterized by thick, light yellowish gray mudstone, deposited by particle-by-particle settling of fine-grained clastic sediments and biogenic

grains.

Based on facies distribution, architecture, grain size and clast composition, the sedimentary sequence in the Malgol system can be grouped into three units. These units represent three stages of fan-delta progradation: 1) deposition of coastal alluvial fan (Stage M-1), 2) deposition of scree-apron-type fan delta (Stage M-2), and 3) deposition of hemipelagic muds (Stage M-3).

The sequence deposited during the early stage (Stage M-1) is represented by alluvial fan deposits (Facies Association I) which unconformably overlie the Cretaceous and Eocene basement rocks (sedimentary, granitic, felsite and volcanic rocks). Coarsening-upward trend of the gravelstone and sandstone units in some outcrop sections and shallow-marine-type dynocysts in the lower part of the well-section (H-well) suggest that the alluvial fan may have prograded to the shallow marine environment, forming a coastal alluvial fan.

The sequence deposited during the Stage M-2 is represented by scree-apron-type fan-delta system, containing alluvial fan (or subaerial scree apron; Facies Association I), submarine scree apron (Facies Association II) and slope apron (Facies Association III) deposits. The lower boundary of the sequence is represented by an abrupt vertical change in clast composition, sedimentary facies and bed attitude. The variations may largely be due to the syn-depositional tectonic movement of the basement, probably related to thrust faults in the basin margin. During this stage, sediments were derived from the upthrusted basement rock and deposited at the base of the fault scarp, forming long, narrow coalescing alluvial fan systems (or subaerial scree

apron). Some coarse-grained sediments were deposited in subaqueous tectonic slope, forming submarine scree apron. Further downfan, the sequence is characterized by thick muddy sandstone in which thin units of gravelstone and sandstone are partly intercalated (Facies Association III), representing deposition in slope apron environment. The sequence generally shows an upward fining trend, suggesting that sediment supply rate from the adjacent fault-bounded drainage basin gradually decreased.

The sequence deposited during the last stage (Stage M-3) is represented by thick light yellowish gray mudstone, deposited by particle-by-particle settling of fine-grained clastic sediments and biogenic grains (hemipelagic settling). The sequence boundary between the Stage M-2 and Stage M-3 is represented by an abrupt vertical decrease in clastic grains, in which the overlying sequence contains abundant biogenic grains. It may indicate that the sediment supply from the alluvial feeder system was abruptly terminated during the last stage of the fan-delta progradation.

REFERENCES

Aalto, K.R., 1976. Sedimentology of a melange: Franciscan of Trinidad, California. *Jour. Sed. Petrol.*, v. 46, p. 913-929.

Allen, J.R.L., 1982. *Sedimentary Structures: Their Character and Physical Basis.* Vol. I, Amsterdam, Elsevier, 593pp.

Allen, J.R.L., 1984. Parallel lamination developed from upper-stage plane beds: a model based on the larger coherent structures of the turbulent boundary layer. *Sed. Geol.*, v. 39, p. 227-242.

Allen, J.R.L. & Leeder, M.R., 1980. Criteria for the instability of upper-stage plane beds. *Sedimentology*, v. 27, p. 209-217.

Alexander, J. & Leeder, M.R., 1987. Active tectonic control on alluvial architecture. In: Ethridge, F.G., Flores, R.M. & Harvey, M.D., Eds., *Recent Developments in Fluvial Sedimentology.* Soc. Econ. Petrol. Min. Spec. Publ., Tulsa, 39, p. 243-252.

Bagnold, R.A., 1954. Experiments on a gravity-free dispersion of large solid spheres in a Newtonian fluid under shear. *Proc. Royal Soc. London.*, v. 225, p. 49-63.

Bagnold, R.A., 1956. The flow of cohesionless grains in fluids. *Proc. Royal Soc. London*, v. 249, p. 235-297.

Barg, E., 1986. *Cenozoic geohistory of the southwestern margin of the Ulleung Basin, East Sea.* Unpubl. M.S. Thesis, Seoul Nat'l. Univ., 174pp.

Bates, C.C., 1953. Rational theory of delta formation. *Am. Ass. Petrol. Geol. Bull.*, v. 37, p. 2119-2162.

Bong, P.Y., 1982. Palynology and stratigraphy of Yeonil-Dongsanri area. *Rep. Geosci. and Mine. Resour., Korea Institute of Energy Resources*, v. 13, p. 19-24.

Bong, P.Y., 1985. *Palynology of the Neogene strata in the Pohang sedimentary Basin.* Unpubl. Ph.D. Thesis, Seoul Nat'l. Univ., 239pp.

Bouma, A.H., 1962. *Sedimentology of Some Flysch Deposits*, Amsterdam,

Elsevier, 166pp.

Bull, W.B., 1972. Recognition of alluvial-fan deposits in the stratigraphic record. In: Rigby, J.K. & Hamblin, W.K., Eds., *Recognition of Ancient Sedimentary Environments.* Soc. Econ. Paleont. Min., Spec. Publ., No. 16, p. 63-83.

Carter, R.M., 1975. A discussion and classification of subaqueous mass-transport with particular application to grain-flow, slurry-flow, and fluxoturbidites. *Earth Sci. Rev.*, v. 11, p. 145-177.

Chang, K.J., 1984. *Sedimentary environments of the Lower Tertiary Yeonil Group in the Pohang Basin.* Unpubl. M.S. Thesis, Korea Univ., 65pp.

Chang, K.H., Woo, B.G., Lee, J.H., Park, S.O. & Yao, A., 1990. Cretaceous and Early Cenozoic stratigraphy and history of eastern Kyongsang Basin, S. Korea, *J. Geol. Soc. Korea,* v. 26, p. 471-487.

Choe, M.Y., 1986. *The Hunghae Formation: Coalescing slope apron.* Unpubl. M.S. Thesis, Seoul Nat'l. Univ., 208pp.

Choe, M.Y., 1990. *Submarine Depositional Processes of the Doumsan Fan-delta System, Miocene Pohang Basin, Southeast Korea.* Unpubl. Ph.D. Thesis, Seoul Nat'l. Univ., 287pp.

Choe, M.Y. & Chough, S.K., 1988. The Hunghae Formation, SE Korea: Miocene debris aprons in a back-arc intraslope basin. *Sedimentology*, v. 35, p. 239-255.

Choi, H.I. & Park, K.S., 1985. Cretaceous/Neogene stratigraphic transition and post Gyeongsang tectonic evolution along and off the southeast coast, Korea, *J. Geol. Soc. Korea,* v. 21, p. 281-296.

Choi, H.W., 1983. *Paleontological study in the southern part of Pohang Basin (southern part of the Hyeongsan River), Korea.* Unpubl. M.S. thesis, Seoul Nat'l. Univ., 75pp.

Chough, S.K. & Barg, E., 1986. Comments of two modes of back- arc spreading. *Geology*, v. 14, p. 629-630.

Chough, S.K. & Barg, E., 1987. Tectonic history of Ulleung Basin Margin,

East Sea (Sea of Japan). *Geology,* v. 15, p. 45-48.

Chough, S.K., Choe, M.Y. & Hwang, I.G., 1993. *Fan Deltas in the Pohang Basin (Miocene), SE Korea.* Field Excursion Guidebook, Woongjin Publisher, 150pp.

Chough, S.K., Hwang, I.G. & Choe, M.Y., 1989. *The Doumsan Fan-delta System, Miocene Pohang Basin (SE Korea).* Field Excursion Guidebook, Woosung Publishing Co., 95pp.

Chough, S.K., Hwang, I.G. & Choe, M.Y., 1990. The Miocene Doumsan fan-delta, southeast Korea: a composite fan-delta system in back-arc margin. *Jour. Sed. Petrol.*, v. 60, p. 445-455.

Chun, H.Y., 1982. Plant fossils from the Tertiary Pohang sedimentary basin, Korea. *Rep. Geosci. and Mine, Resour., Korea Institute of Energy and Resources*, v. 14, p. 7-24.

Chun, H.Y., Lee, H.Y., Bong, P.Y. & Baek, I.S., 1983. Biostratigraphical study of Pohang Basin (northern part of the Hyeongsan river). *Rep. Geosci. and Mine, Resour., Korea Institute of Energy and Resources*, p.7-29.

Colella, A., 1988a. Pliocene-Holocene fan deltas and braid deltas in the Crati Basin, southern Italy: a consequence of tectonic conditions. In: Nemec, W. & Steel, R.J., Eds., *Fan Deltas: Sedimentology and Tectonic Settings.* Blackie and Son Ltd., p. 50-74

Colella, A., 1988b. Fault-controlled marine Gilbert-type fan deltas. *Geology*, v. 16, p. 1031-1034.

Colella, A., De Boer, P.L. & Nio, S.D., 1987. Sedimentology of a marine intermontane Pleistocene Gilbert-type Fan-delta complex in the Crati Basin, Calabria, southern Italy. *Sedimentology*, v. 34, p. 721-736.

Collinson, J.D., 1970. Bedforms of the Tana River, Norway. *Geogr. Ann.*, v. 52, p. 31-56.

Collinson, J.D. & Thompson, D.B., 1982. *Sedimentary Structures.* Boston, Allen & Unwin. 194pp.

Cook, H.E., 1979. Ancient continental slope sequences and their values in understanding modern slope development. In: Doyle, L.J. & Pilkey, O.H., Eds., *Geology of Continental Slopes.* Soc. Econ. Paleont. Min., Spec. Publ., No. 27, p. 287-306.

Costa, E.H., 1988. Rheologic, geomorphic, and sedimentologic differentiation of water floods, hyperconcentrated flows, and debris flows. In: Baker, R. et al., Eds., *Flood Geomorphology*, p. 113-121.

Crowell, J.C., 1975. Sedimentation along the San Andreas fault, California, In: Dott, R.H. Jr., & Shaver R.H., Eds., *Modern and Ancient Geosyncline Sedimentation,* Soc. Econ. Paleont. Min., Spec. Publ., No. 19, p. 292-203.

Curry, R.R., 1966. Observation of Alpine mudflows in the Tenmile Range, Central Colorado. *Geol. Soc. Am. Bull.*, v. 77, p. 771-776.

Dunne, L.A. & Hempton, M.R., 1984. Deltaic sedimentation in the Lake Hazar pull-apart basin, south-eastern Turkey. *Sedimentology,* v. 31, p. 401-412.

Ethridge, F.G. & Wescott, W.A., 1984. Tectonic setting, recognition and hydrocarbon potential of fan-delta deposits. In: Koster, E.H. & Steel, R.J., Eds., *Sedimentology of Gravels and Conglomerates.* Can. Soc. Petrol. Geologists, Mem. 10, p. 217-235.

Eyles, N., Clark, B.M. & Clague, J.J., 1987. Coarse-grained sediment gravity flow facies in a large superglacial lake. *Sedimentology*, v. 34, p. 193-216.

Fraser, G.S. & Cobb, J.C., 1982. Late Wisconsian proglacial sedimentation along the west Chicago moraine in northeastern Illinois. *Jour. Sed. Petrol.*, v. 52, p. 473-491.

Galloway, W.E., 1989a. Genetic stratigraphic sequences in basin analysis II: architecture and genesis of flooding-surface bounded depositional units. *Am. Ass. Petrol. Geol. Bull.*, v. 73, p. 125-142.

Galloway, W.E., 1989b. Genetic stratigraphic sequences in basin analysis II: application to Northwest Gulf of Mexico Cenozoic basin. *Am. Ass.*

Petrol. Geol. Bull., v. 73, p. 143-154.

Garrison, R.E., Mack, L.E., Lee, Y.G. & Chun, H.Y., 1979. Petrology, sedimentology and diagenesis of Miocene diatomaceous and opal-CT Mudstone in the Pohang Area, Korea. *J. Geol. Soc. Korea*, v. 15, p. 230-252.

Gawthorpe, R.L. & Collela, A., 1990. Tectonic controls on coarse-grained delta depositional systems in rift basins. In: Collela, A. & Prior, D.B., Eds., *Coarse-grained deltas.* Int. Ass. Sediment., Spec. Publ., No. 10, p. 113-127.

Gawthorpe, R.L., Hurst, J.M. & Sladen, C.P., 1990. Evolution of Miocene footwall-derived coarse-grained deltas, Gulf of Suez, Egypt: implications for exploration. *Am. Ass. Petrol. Geol. Bull.*, v. 74, p. 1077-1086.

Gloppen, T.G. & Steel, R.J., 1981. The deposits, internal structure and geometry in six alluvial fan-fan delta bodies (Devonian-Norway) - A study in the significance of bedding sequence in conglomerates. In: Ethridge, F.G. & Flores, R.M., Eds., *Recent and Ancient Nonmarine Depositional Environments: Models for Exploration,* Soc. Econ. Paleont. Min., Spec. Publ., No. 31, p. 49-69.

Gravenor, C.P., 1986. Magnetic and pebble fabrics in subaquatic debris-flow deposits. *J. Geology,* v. 94, p. 683-698.

Gustavson, T.C., 1974. Sedimentology on gravel outwash fans, Malaspina Glacier foreland, Alaska. *Jour. Sed. Petrol.*, v. 44, p. 374-389.

Han, J.H., Kwak, Y.H. & Son, J.D., 1986. *Tectonic evolution and depositional environments of the Tertiary sedimentary basin, southeastern part of Korea.* Res. Rep. KR-86-(B)-8, Korea Institute of Energy and Resources, 76pp.

Harms, J.C., Southard, J.B., Spearing, D.R. & Walker, R.G., 1975. *Depositional Environments as Interpreted from Primary Sedimentary Structures and Stratification Ssequences.* Soc. Econ. Paleont. Min., Short Course No. 2, 161pp.

Harms, J.C., Southard, J.B. & Walker, R.G., 1982. *Structures and Sequences in Clastic Rocks.* Soc. Econ. Paleont. Min., Short Course No. 9.

Hein, F.J., 1984. Deep-sea and fluvial braided channel conglomerates. In: Koster, E.H. & Steel, R.J., Eds., *Sedimentology of Gravels and Conglomerates.* Can. Soc. Petrol. Geologists, Mem. 10, p. 33-49.

Hiscott, R.N. & Middleton, G.V., 1980. Fabric of coarse deep-water sandstones Tourelle Formation, Quebec, Canada. *Jour. Sed. Petrol.*, v. 50, p. 703-722.

Hwang, I.G., 1989. *The Miocene Chunbuk Formation, Pohang Basin: Gilbert-type fan-delta system.* Unpubl. M.S. thesis, Seoul Nat'l. Univ., 244pp.

Hwang, I.G., 1993. *Fan-delta Systems in the Pohang Basin (Miocene), SE Korea.* Unpubl. Ph.D. thesis, Seoul Nat'l. Univ., 923pp.

Hwang, I.G. & Chough, S.K., 1990. The Miocene Chunbuk Formation, SE Korea: marine Gilbert-type fan-delta system. In: Colella, A. & Prior, D.B., Eds., *Coarse-Grained Deltas.* Int. Ass. Sediment., Spec. Publ., No. 10, p. 235-254.

Ineson, J.R., 1989. Coarse-grained submarine fan and slope apron deposits in a Cretaceous back-arc basin, Antarctica. *Sedimentology*, v. 36, p. 793-820.

Ingle, J., Suyehiro, K. & Breymann, M.T. von., 1989. Leg 128: Japan sea II site report. *JOIDES Journal* XVI(1), p. 3-8.

Jin, M.S., Kim, S.J., Shin, S.C. & Lee, J.Y., 1989. K/Ar fission track dating for granites and volcanic rocks in the southeastern part of Korean Peninsula. *Research on Isotope Geology,* Res. Rep. KR-88-6D, Korea Institute of Energy and Resources. p. 51-84.

Kanehara, K., 1935. For the Geological Age of Ennichi Series. *Jap. Jour. Geology*, v. 24, p. 496-507.

Kanehara, K., 1936a. Neogene shells from the South Chosen (Korea). *Jap. Jour. Geol. Geogr.*, v. 13, p. 31-37.

Kanehara, K., 1936b. Geological study of northern Yeongil Kun, N. Kyeong-

san Province, Korea. *Jap. Jour. Geol. Geogr.*, v. 13, p. 73-103.

Kim, B.K., 1965. The stratigraphic and paleontologic studies on the Tertiary (Miocene) of the Pohang area, Korea. *Jour. Seoul Nat'l. Univ., Sci. Tech. Ser.*, v. 15, p. 32-121.

Kim, B.K. & Yoon, S., 1982. Cenozoic sedimentary sequence. In: *Alumi of Yonsei Univ., Dept. of Geology, Geology and Mineral Resources of Korean Peninsula,* p. 133-153.

Kim, B.K. & Choi, D.K., 1977a. Preliminary biostratigraphy zonation by benthonic foraminifers in the Tertiary Pohang Basin, Korea. *Proc. Coll. Natural Sci., Seoul Nat'l. Univ.*, v. 2, p. 115-168.

Kim, B.K. & Choi, D.K., 1977b. Species diversity of benthic foraminifers in the Tertiary strata of Pohang Basin, Korea. *J. Geol. Soc. Korea,* v. 13, p. 111-120.

Kim, I.S., 1985a. Geologic structures and plate tectonics of Korea and East Asia (I): geologic structures and fault patterns. *Jour. Pusan Nat'l. Univ., Sci. Tech. Ser.,* v. 40, p. 297-310.

Kim, I.S., 1985a. Geologic structures and plate tectonics of Korea and East Asia (I): development of geologic structures and East Sea. *Jour. Pusan Nat'l. Univ., Sci. Tech. Ser.,* v. 40, p. 311-325.

Kim, K.J., 1987. *Organic-walled microfossils from the Neogene strata of H-well, Pohang, Korea.* Unpubl. M.S. Thesis, Seoul Nat'l. Univ., 69pp.

Kim, J.Y., 1988. *A study on the nature and movement history of the Yangsan fault.* Unpubl., Ph.D. thesis, Pusan Nat'l. Univ., 97pp.

Kim, J.Y. & Yoon, S., 1989. Geology and structure of the western marginal part of the Pohang Basin. *J. Sci. Pusan Nat,l. Univ.*, v. 47. p. 275-282.

Kim, W.H. 1990. Significance of Early to Middle Miocene planktonic foraminiferal biostratigraphy of the E-core in the Pohang Basin, Korea (submitted).

Koh, Y.K., 1986. *A micropaleontological study on silicoflagellates, ebridians, and nannofossils from the Pohang area, Pohang Basin and the Ulleung*

Basin. Unpubl. Ph.D. thesis, Seoul Nat'l. Univ., 210pp.

Lee, H.Y., 1982. Neogene foraminifera from southern part of Euichang area, Korea. *Rep. Geosci. and Mine. Resour., Korea Institute of Energy and Resources,* v. 13, p. 19-34.

Lee, J.H., 1989. *Cretaceous stratigraphy and sedimentation in Chongha-Ankang area, Kyongsangbukdo, Korea.* Unpubl. M.S. Thesis, Kyungpook Nat'l. Univ., 64pp.

Lee, K.H., Kim, Y.H. & Chang, T.W., 1986. Seismicity of Korean Peninsula (II): seismicity of the northern part of the Yangsan Fault. *J. Geol. Soc. Korea,* v. 22, p. 347-356.

Lee, S.M., 1974. The tectonic setting of Korea with relation to plate tectonics. *J. Geol. Soc. Korea,* v. 10, p. 25-36.

Lee, Y.G., 1975. Neogene diatoms of Pohang and Gampo area, Kyeongsang-bug-do, Korea. *J. Geol. Soc. Korea,* v. 11, p. 99-114.

Lee, Y.G., 1978a. Diatom flora of the middle part of the Yeonil Group, in the vicinity of the Cheongha, Kyeongsangbug-do, Korea. *Res. Rev. Kyungpook Nat'l. Univ.,* v. 25, p. 215-222.

Lee, Y.G., 1978b. Silicoflagellates and ebridians from Yeonil Group, Pohang area, Korea. *J. Geol. Soc. Korea,* v. 14, p. 30.

Lee, Y.G., 1979. Preliminary study of silicoflagellata and ebridian of Yeonil Group in Pohang area. *J. Geol. Soc. Korea,* v. 15, p. 102.

Lee, Y.G., 1983. Diatom zonation and biostratigraphy of Neogene strata of Pohang area, Korea. *Res. Rev. Kyungpook Nat'l. Univ.,* v. 35, p. 401-420.

Lee, Y.G., 1984. *Micropaleontological (Diatom) study of the Neogene deposits in Korea.* Unpubl. Ph.D. Thesis, Seoul Nat'l. Univ., 285pp.

Lee, Y.G., 1986. Micropaleontological study of Neogene strata of southeast-ern Korea and adjacent sea floor. *J. Paleont. Soc. Korea,* v. 2, p. 83-113.

Leeder, M.R. & Gawthorpe, R.L., 1987. Sedimentary models for extensional

tilt-block/half-graben basins. In: Coward, M.P., Dewey, J.F. & Hancock, P.L., Eds., *Continental Extensional Tectonics.* Geol. Soc. Spec. Publ., No. 28, p. 139-152.

Leeder, M.R., Ord, D.M. & Collier, R. 1988. Development of alluvial fans and fan deltas in neotectonic extensional settings: implications for the interpretation of basin fills. In: Nemec, W. & Steel, R.J., Eds., *Fan Deltas: Sedimentology and Tectonic Settings.* Blackie and Son Ltd., p. 173-185.

Lewis, D.W., Laird, M.G. & Powell, R.D., 1980. Debris flow deposits of early Miocene age, Deadman Stream, Marlborough, New Zealand. *Sed. Geol.*, v. 27, p. 83-118.

Lindsay, J.F., 1968. The development of clastic fabric in mudflows. *Jour. Sed. Petrol.*, v. 38, p. 1242-1253.

Ling, H.Y. & Kim, B.K., 1983. Miocene archaeomonards from Pohang area, Korea. *J. Geol. Soc. Korea,* v. 19, p. 247-251.

Link, M.H. & Osbourne, R.H., 1978. Lacustrine facies in the Pliocene Ridge Basin Group: Ridge Basin, California. In: Matter, A. & Tucker, M.E., Eds., *Modern and Ancient Lake Sediments.* Int. Ass. Sediment., Spec. Publ., No. 2, p. 169-187.

Lowe, D.R., 1976a. Grain flow and grain flow deposits. *Jour. Sed. Petrol.*, v. 46, p. 188-199.

Lowe, D.R., 1976b. Subaqueous liquefied and fluidized sediment flows and their deposits. *Sedimentology*, v. 23, p. 285-308.

Lowe, D.R., 1979. Sediment gravity flows: their classification and some problems of application to natural flows and deposits. In: Doyle, L.J. & Pilkey, O.H., Eds., *Geology of Continental Slopes.* Soc. Econ. Paleont. Mineral., Spec. Publ., No. 27, p. 75-82.

Lowe, D.R., 1982. Sediment gravity flows: II. Depositional models with special reference to the deposits of high-density turbidity currents. *Jour. Sed. Petrol.*, v. 52, p. 279-297.

tilt-block/half-graben basins. In: Coward, M.P., Dewey, J.F. & Hancock, P.L., Eds., *Continental Extensional Tectonics.* Geol. Soc. Spec. Publ., No. 28, p. 139-152.

Leeder, M.R., Ord, D.M. & Collier, R. 1988. Development of alluvial fans and fan deltas in neotectonic extensional settings: implications for the interpretation of basin fills. In: Nemec, W. & Steel, R.J., Eds., *Fan Deltas: Sedimentology and Tectonic Settings.* Blackie and Son Ltd., p. 173-185.

Lewis, D.W., Laird, M.G. & Powell, R.D., 1980. Debris flow deposits of early Miocene age, Deadman Stream, Marlborough, New Zealand. *Sed. Geol.*, v. 27, p. 83-118.

Lindsay, J.F., 1968. The development of clastic fabric in mudflows. *Jour. Sed. Petrol.*, v. 38, p. 1242-1253.

Ling, H.Y. & Kim, B.K., 1983. Miocene archaeomonards from Pohang area, Korea. *J. Geol. Soc. Korea,* v. 19, p. 247-251.

Link, M.H. & Osbourne, R.H., 1978. Lacustrine facies in the Pliocene Ridge Basin Group: Ridge Basin, California. In: Matter, A. & Tucker, M.E., Eds., *Modern and Ancient Lake Sediments.* Int. Ass. Sediment., Spec. Publ., No. 2, p. 169-187.

Lowe, D.R., 1976a. Grain flow and grain flow deposits. *Jour. Sed. Petrol.*, v. 46, p. 188-199.

Lowe, D.R., 1976b. Subaqueous liquefied and fluidized sediment flows and their deposits. *Sedimentology*, v. 23, p. 285-308.

Lowe, D.R., 1979. Sediment gravity flows: their classification and some problems of application to natural flows and deposits. In: Doyle, L.J. & Pilkey, O.H., Eds., *Geology of Continental Slopes.* Soc. Econ. Paleont. Mineral., Spec. Publ., No. 27, p. 75-82.

Lowe, D.R., 1982. Sediment gravity flows: II. Depositional models with special reference to the deposits of high-density turbidity currents. *Jour. Sed. Petrol.*, v. 52, p. 279-297.

Lowe, D.R., 1988. Suspended-load fallout rate as an independent variable in the analysis of current structures. *Sedimentology,* v. 35, p. 765-776.

Mann, P., Hempton, M.R., Bradley, D.C. & Burke, K., 1983. Development of pull-apart basins. *J. Geology,* v. 91, p. 529-554.

Martinsen, O.J., 1990. Fluvial, inertia-dominated deltaic deposition in the Namurian(Carboniferous) of northern England. *Sedimentology*, p. 37, v. 1099-1113.

Massari, F., 1984. Resedimented conglomerates of a Miocene fan-delta complex, southern Alps, Italy. In: Koster, E.H. & Steel, R.J., Eds., *Sedimentology of Gravels and Conglomerates.* Can. Soc. Petrol. Geologists, Mem. 10, p. 259-278.

Mastalerz, K., 1990. Diurnally and seasonally controlled sedimentation on a glaciolacustrine foreset slope: an example from the Pleistocene of eastern Poland. In: Colella, A. & Prior, D.B., Eds., *Coarse-Grained Deltas.* Int. Ass. Sediment., Spec. Publ., No. 10, p. 297-310.

Miall, A.D., 1977. A review of braided river depositional environments. *Earth Sci. Revs.*, v. 13, p. 1-62.

Miall, A.D., 1978. Lithofacies types and vertical profile models in braided river deposits: a summary. In: Miall, A.D., Ed., *Fluvial Sedimentology.* Can. Soc. Petrol. Geologists, Mem. 5, p. 597-604.

Middleton, G.V., 1970. Experimental studies related to problems of flysch sedimentation. *Geol. Assoc. Can. Spec. Paper,* No. 7, p. 253-272.

Middleton, G.V. & Hampton, M.A., 1976. Subaqueous sediment transport and deposition by sediment gravity flows. In: Stanley, D.J. & Swift, D.J.P., Eds., *Marine Sediment Transport and Environmental Management.* New York, Wiley, p. 197-218.

Mullins, H.T. & van Buren, H.M., 1979. Modern modified carbonate grain flow deposit. *Jour. Sed. Petrol.*, v. 49, p. 747-752.

Nemec, W., 1990b. Aspects of sediment movement on steep delta slopes. In: Collela, A. & Prior, D.B., Eds., *Coarse-grained Deltas.* Int. Ass.

Sediment. Spec. Publ., No. 10, p. 29-73.

Nemec, W. & Steel, R.J., 1984. Alluvial and coastal conglomerates: their significant features and some comments on gravelly mass-flow deposits. In: Koster, E.H. & Steel, R.J., Eds., *Sedimentology of Gravels and Conglomerates.* Can. Soc. Petrol. Geologists, Mem. 10, p. 1-32.

Nilsen, T.H. & McLaughlin, R.J., 1985. Comparison of tectonic framework and depositional patterns of the Hornelen strike-slip basin of Norway. In: Biddle, K.T. & Christie-Blick, N., Eds., *Strike-slip Deformation, Basin Formation, and Sedimentation,* Soc. Econ. Paleont. Min., Spec. Publ., No. 37, p. 79-104.

North American Commission on Stratigraphic Nomenclature, 1983. North American Stratigraphic Code. *Am. Ass. Petrol. Geol., Bull.,* v. 67, p. 841-875.

Pickering, K., Stow, D., Watson, M. & Hiscott, R., 1986. Deep-water facies, processes and models: a review and classification scheme for modern and ancient sediments. *Earth Sci. Rev.,* v. 23, p. 75-174.

Pierson, T.C., 1981. Dominant particle supporting mechanisms in debris flows at Mt. Thomas, New Zealand, and implications for flow mobility. *Sedimentology,* v. 28, p. 49-60.

Postma, G., 1983. Water-escape structures in the context of a depositional model of a mass-flow dominated conglomeratic fan delta, Abrioja Formation, Pliocene, Almeria Basin, SE Spain. *Sedimentology,* v. 30, p. 91-103.

Postma, G., 1984a. Mass-flow conglomerates in a submarine canyon: Abrioja fan-delta, Pliocene, SE Spain. In: Koster, E.H. & Steel, R.J., Eds., *Sedimentology of Gravels and Conglomerates.* Can. Soc. Petrol. Geologists, Mem. 10, p. 237-258.

Postma, G., 1984b. Slumps and their deposits in the delta-front and slopes. *Geology,* v. 12, p. 27-30.

Postma, G., 1986. Classification for sediment gravity-flow deposits based on flow conditions during sedimentation. *Geology,* v. 14, p. 291-294.

Postma, G. & Cruickshank, C., 1988. Sedimentology of a late Weichselian to Holocene terraced fan delta, Varangerfjord, northern Norway. In: Nemec, W. & Steel, R.J., Eds., *Fan deltas: Sedimentology and Tectonic Settings.* Blackie and Son Ltd., London, p. 144-157.

Postma, G. & Roep, T.B., 1985. Resedimented conglomerates in the bottomset of Gilbert-type gravel deltas. *Jour. Sed. Petrol.*, v. 55, p. 874-885.

Postma, G., Babic, L., Zupanic, J. & Roe, S.-L., 1988. Delta-front failure and associated bottomset deformation in a marine Gilbert-type fan-delta. In: Nemec, W. & Steel, R.J., Eds., *Fan Deltas: Sedimentology and Tectonic Settings.* Blackie and Son Ltd., London, p. 91-102.

Prior, D.B. & Bornhold, B.D., 1988. Submarine morphology and processes of fjord fan deltas and related high-gradient systems: modern examples from British Columbia. In: Nemec, W. & Steel, R.J., Eds., *Fan Deltas: Sedimentology and Tectonic Settings.* Blackie and Son Ltd., London, p. 125-143.

Prior, D.B. & Bornhold, B.D., 1989. Submarine sedimentation on a developing Holocene fan delta. *Sedimentology*, v. 36, p. 1053-1076.

Prior, D.B. & Bornhold, B.D., 1990. The underwater development of Holocene fan deltas. In: Collela, A. & Prior, D.B., Eds., *Coarse-grained deltas.* Int. Ass. Sediment., Spec. Publ., No. 10, p. 75-90.

Reedman, A.J. & Um, S.H., 1975. *The Geology of Korea.* Seoul, Korea. Geol. Min. Inst. Korea, 139pp.

Rust. B.R., 1972. Structure and processes in a braided river. *Sedimentology*, v. 18, p. 221-246.

Rust, B.R., 1978. Depositional models for braided alluvium. In: Miall, A.D., Ed., *Fluvial Sedimentology.* Can. Soc. Petrol. Geologists, Mem. 5, p. 605-626.

Savage, S.B. & Lun, C.K.K., 1988. Particle size segregation in inclined chute flow of dry cohesionless granular solids. *J. Fluid Mech.*, v. 189, p.

311-335.

Scott, A.M. & Bridgwater, J., 1975. Interparticle percolation: a fundamental solids mixing mechanism. *Ind. Eng. Chem. Fundam.* v. 14, p. 22-27.

Shin, I.C., 1981. *Foraminiferal studies on the Neogene Tertiary in the Pohang Basin, Korea.* Unpubl. M.S. Thesis, Seoul Nat'l. Univ., 76pp.

Shultz, A.W., 1984. Subaerial debris-flow deposition in the Upper Paleozoic Cutler Formation, western Colorado. *Jour. Sed. Petrol.,* v. 54, p. 759-772.

Sloss, L.L., 1988. Forty years of sequence stratigraphy. *Geol. Soc. Am. Bull.,* v. 100, p. 1661-1665.

Smith, G.A., 1986. Coarse-grained non-marine volcaniclastic sediment: Terminology and depositional process. *Geol. Soc. Am. Bull.,* v. 97, p. 1-10.

Smith, N.D., 1970. The braided stream depositional environment: comparison of the Platte River with some Silurian clastic rocks, north-central Appalachians. *Geol. Soc. Am. Bull.,* v. 81, p. 2993-3014.

Smith, N.D., 1972. Some sedimentological aspects of planar cross-stratification in a sandy braided river. *Jour. Sed. Petrol.,* v. 42, p. 624-634.

Smith, N.D. & Ashley, G., 1985. Proglacial lacustrine environments. In: Ashley, G.M., Shaw, J. & Smith, N.D., Eds., *Glacial Sedimentary Environments.* Soc. Econ. Paleont. Min., Short Course, No. 16, p. 135-216.

Surlyk, F., 1984. Fan-delta to submarine fan conglomerates of the Volgian--Valanginian Wollastone Foreland Group, East Greenland. In; Koster, E.H. & Steel, R.J., Eds., *Sedimentology of Gravels and Conglomerates.* Can. Soc. Petrol. Geologists, Mem. 10, p. 359-382.

Takahashi, K. & Kim, B.K., 1979. Palynology of the Miocene formations in the Yeonil Bay District, Korea. *Paleogeographica, Band 170, Abt. B,* p. 1-80.

Tateiwa, I., 1924. *Ennichi-Kyuryuho and Choyo Sheet.* Geol. Atlas Chosen,

No.2, Geol. Surv. Chosen.

Um, S.H., Lee, D.W. & Park, B.S., 1964. *Geological Map of Korea, Pohang Sheet (1:50,000).* Geol. Surv. Korea, 21pp.

van der Meulen, S., 1983. Internal structures and environmental reconstruction of Eocene transitional fan-delta deposits, Monllobat-Castigaleu Formations, southern Pyrenees, Spain. *Sed. Geol.*, v. 37, p. 85-112.

Walker, R.G., 1975. Generalized facies models for resedimented conglomerates of turbidite association. *Geol. Soc. Am. Bull.*, v. 86, p. 737-748.

Walker, R.G., 1977. Deposition of upper Mesozoic resedimented conglomerates and associated turbidites in southwestern Oregon. *Geol. Soc. Am. Bull.*, v. 88, p. 273-285.

Walker, R.G., 1978. Deep-water sandstone facies and ancient submarine fans: models for exploration for stratigraphic traps. *Am. Ass. Petrol. Geol. Bull.*, v. 62, p. 932-966.

Winn, R.D., Jr. & Dott, R.H., Jr., 1977. Large-scale traction-produced structures in deep-water fan-channel conglomerates in southern Chile. *Geology*, v. 5, p. 41-44.

Woo, B.G., 1989. *Cretaceous stratigraphy and sedimentation in Pyonghae-Yongduk area, Kongsangbuk-do, Korea.* Unpubl. M.S. thesis, Kyungpook Nat,l. Univ., 72pp.

Wright, L.D. & Coleman, J.M., 1974. Mississippi river mouth processes: Effluent dynamics and morphological development. *J. Geology*, v. 82, p. 751-778.

Yoo, E.K., 1969. Tertiary Foraminifera from the PY-1 well, Pohang basin, Korea. *J. Geol. Soc. Korea*, v. 5, p. 77-96.

Yoon, S., 1975. Geology and paleontology of the Tertiary Pohang Basin, Pohang district, Korea, Part 1. Geology. *J. Geol. Soc. Korea*, v. 11, p. 187-214.

Yoon, S., 1976a. Geology and paleontology of the Tertiary Pohang Basin, Pohang district, Korea, Part 2. paleontology (mollusca), No. 1.

systematic description of bivalvia. *J. Geol. Soc. Korea*, v. 12, p. 1-22.

Yoon, S., 1976b. Geology and paleontology of the Tertiary Pohang Basin, Pohang district, Korea, Part 2. paleontology (mollusca), No. 2. scaphopoda and gastropoda. *J. Geol. Soc. Korea*, v. 12, p. 63-72.

Yoon, S., 1978. Correlation of Tertiary deposits in southern Korea. *J. Geol. Soc. Korea*, v. 14, p. 30-31.

Yoon, S., 1979. Neogene molluscan fauna of Korea. *Mem. Geol. Soc. China*, No. 3, p. 125-130.

Yoon, S., 1986. Tectonic history of the Tertiary Pohang and Yangnam basins, In: Nakagawa, H., Tamio, K. & Takayanaga, Y., Eds., *Kitamura Commem. Essay Geol.*, p. 637-644.

You, H.S., 1983. *The biostratigraphy of the Neogene Tertiary deposits, Korea.* Unpubl. Ph. D. Thesis, Seoul Nat'l. Univ., 180pp.

You, H.S. & Koh, Y.G., 1984. Studies on the silicoflagellates and ebridians from Tertiary deposits in the northern area of the Pohang Basin, Korea. *J. Geol. Soc. Korea*, v. 20, p. 127-132.

You, H.S., Koh, Y.G. & Kim, 1986. A study on the nannoplankton from the Neogene formation, Pohang, Korea. *J. paleont. Soc. Korea*, v. 2, p. 137-154.

You, I.C., 1985. *Depositional environments of the Yeonil Group of the Pohang Basin.* Unpubl. M.S. Thesis, Korea Univ., 123pp.

Yun, H.S., 1981. Dinoflagellates from Pohang Tertiary Basin, Korea. *Rep. Geosci. and Mine. Resour., Korea Institute of Energy and Resources*, v. 11, p. 5-18.

Yun, H.S., 1986. Emended stratigraphy of the Miocene formations in the Pohang Basin, Part 1. *J. Paleont. Soc. Korea*, v. 2, p. 54-69.

Yun, H.S., Paik, K.H., Chang, S.K. & Yi, S.S., 1990. Microfossil assemblages from the Bomun area. *J. Paleont. Soc. Korea*, v. 6, p. 1-63.